DIPARTIMENTO DI SCIENZE AGRARIE E FORESTALI

Corso di Dottorato di Ricerca in
BIOTECNOLOGIE VEGETALI
XXVIII Ciclo

Pectin methyl-esterases (*PMEs*) in wheat: genome-wide characterization and their role in wheat-*Fusarium graminearum* interaction

s.s.d. BIO/04

Tesi di dottorato di:
Dott. Alessandra Zega

Coordinatore del corso
Prof.ssa Stefania Masci

Firma ……..

Tutore
Prof. Renato D'Ovidio

Firma ……

29-06-2016

AIMS AND STRUCTURE OF THE THESIS

The present thesis reports the results of the work carried out during my PhD project focused on the identification and characterization of the pectin methyl esterases (*PMEs*) gene family in wheat and the study of their involvement in wheat resistance against the Fusarium Head Blight (FHB) disease caused by the fungal pathogen *Fusarium graminearum*. The whole project has been conducted by following three different aims: 1) wheat *PMEs in silico* identification and structural analysis; 2) wheat *PMEs* functional characterization by analyzing their gene expression in different bread wheat tissues and following the infection with *F. graminearum*; 3) investigation of the role of *PMEs* in wheat-*F. graminearum* interaction by silencing specific *PME* genes.

The structure of the thesis is the following: an outline of the complete project (Abstract) and a general introduction (General introduction, pag. 2) about wheat and its genetics, the plant cell wall and enzymes related to its degradation and modification and, finally, a general introduction about PMEs. These parts precede two chapters about the obtained results. Chapter I (pag. 16) is addressed to the first and to the second aim and it includes a short specific introduction, a section regarding the experimental procedures, then the results and finally the discussion. Chapter II (pag. 47) is addressed to the third aim and its structure is as described for the previous chapter.

At the end (pag. 91), general conclusions are reported, highlighting the main results obtained during this work.

Results reported in the first chapter are included in the manuscript titled "Genome-wide characterization of pectin methyl esterase genes reveals members differentially expressed in tolerant and susceptible wheats in response to *Fusarium graminearum*" submitted to *Plant Physiology and Biochemistry* (March 25th 2016).

Abstract

Pectin methyl esterase (*PME*) genes code for enzymes that are involved in structural modifications of the plant cell wall, in plant development and they are also involved in plant-pathogen interaction. *PME* genes belong to a multigene family in plants, both in dicotyledonous and monocotyledonous species. So far there is a limited knowledge about *PMEs* in wheat, consequently in this work a genome-wide search was performed on the recently available wheat genome. Forty complete *PME* sequences and 4 incomplete sequences, 2 of which have been subsequently completed from the bread wheat cv. Bobwhite, were identified. Structural analysis revealed that exon-intron structure is conserved between homoeologous genes sharing a high sequence identity. Expression analysis of *PME* genes in different bread wheat tissues showed a diverse expression pattern in those tissues and developmental stages analyzed. Most of the members of this gene family underwent a down-regulation following the opening of the florets to perform infection with *Fusarium graminearum* by using the point inoculation method. Following infection, the expression behavior of specific *PME* genes was markedly different in the FHB-resistant wheat genotype Sumai3 in comparison to the susceptible cv. Bobwhite, being more strongly induced in the latter than in the former, thus suggesting a possible involvement of *PME* genes in FHB susceptibility. *TRI6* gene of *F. graminearum* was used to quantify the fungal biomass in three different portions of the spike: the central spikelets directly infected and the upper and lower spikelets respect to the central ones. These analysis showed the presence of the pathogens in the central and upper spikelets and its absence in the lower spikelets. The analysis of *PME* genes expression in the different parts of the spike showed that the presence of the pathogen in the upper spikelets is associated with an increase of the expression of specific *PMEs* at 48 hour post infection (hpi). Conversely, in the lower spikelets a down-regulation of *PME* genes was observed, possibly as result of the stress generated by the opening of the central spikelets for the infection. These preliminary analysis lead us to the identification of those *PMEs* that could be involved in the susceptibility or resistance in wheat. In order to validate our results and hypothesis, three selected *PMEs* (*PME13*, *PME21* and *PME28*) were silenced through RNA interference. Two transgenic lines each silenced for *PME13* or *PME28* were subjected to a preliminary infection experiment with *F. graminearum*, but no significant differences were found between the transgenics and the control plants, except between AZ4-11 transgenic line and Svevo plants at 2 days post infection (DPI) .

Silenced *PME* genes were also searched by a TILLING approach, by screening a durum wheat TILLING population of 4000 plants available at the University of Tuscia. However, the screening of 1920 samples for mutations in the *PME13* gene did not identify any silenced genotype. We screened also the recent available TILLING population database developed by the University of California, Davis. We found 28 mutated accessions for 12 different *PME* genes: STOP codons were found in 18 accessions and splicing sites mutations were found in the remaining 10 accessions.

In conclusion, this genome-wide study of wheat *PMEs* revealed structural and functional characteristics of this gene family and highlighted the possible involvement of specific *PME* in wheat-*F. graminearum* interaction. Silencing of *PME13* and *PME28* did not modify wheat resistance against *F. graminearum* in the preliminary infection experiment. However, the selected TILLING mutants for additional *PME* genes will represent the basis for further study to verify the involvement of PMEs in wheat-pathogen interaction.

Keywords

Triticum aestivum; *Triticum durum*; Cell wall; Pectin methyl esterase (PME); Wheat- *F. graminearum* interaction; Gene family; Gene expression; RNAi; TILLING; *F. graminearum*

Riassunto

Le pectin metil esterasi (*PME*) codificano enzimi coinvolti in molteplici funzioni, come modificazioni strutturali della parete cellulare, sviluppo della pianta, interazione pianta-patogeno. I geni *PME* appartengono ad una famiglia multigenica, sia in monocotiledoni che dicotiledoni. Data la mancanza di informazioni riguardo le *PME* in frumento, lo scopo di questo lavoro è stato quello di studiare e caratterizzare i geni appartenenti a questa famiglia genica utilizzando il recente database di sequenze del genoma di frumento. Sono state identificate 40 sequenze *PME* complete e 4 incomplete, 2 delle quali sono state sequenziate dalla cv. di frumento tenero Bobwhite. Le analisi strutturali rivelano che la struttura esoni-introni è conservata tra geni omeologhi con elevata identità di sequenza. Le analisi di espressione delle *PME* in diversi tessuti di frumento tenero rivelano un differente pattern di espressione nei tessuti e stadi di sviluppo analizzati. La maggior parte dei membri di questa famiglia genica mostra una repressione a seguito dell'apertura del fiore realizzata per effettuare l'infezione con *F. graminearum* impiegando il metodo del "point inoculation". A seguito dell'infezione, il comportamento di specifici geni *PME* è differente tra la cv. resistente Sumai3 e la cv. suscettibile Bobwhite, essendo più fortemente indotti in quest'ultima rispetto alla prima, suggerendo così un possible coinvolgimento degli stessi nella suscettibilità al patogeno. Il gene *TRI6* di *F. graminearum* è stato impiegato per la quantificazione della biomassa fungina in tre differenti porzioni della spiga: le spighette centrali direttamente inoculate e le spighette sopra e sotto il sito di infezione. Queste analisi hanno rilevato la presenza del patogeno nelle spighette centrali e superiori e la sua assenza in quelle inferiori. L'analisi di espressione dei geni *PME* nelle tre diverse porzioni della spiga ha mostrato che la presenza del patogeno nelle spighette superiori è associata a un aumento dei livelli di espressione di specifiche *PME* 48 ore dopo l'infezione. Al contrario, nelle spighette inferiori è stata osservata una repressione delle *PME*, probabilmente a causa dello stress dovuto all'apertura dei fiori delle spighette centrali. Queste analisi hanno permesso di identificare le *PME* potenzialmente coinvolte nella suscettibilità o resistenza. Per validare i risultati e le ipotesi, sono stati silenziati tre geni *PME* (*PME13, PME21* e *PME28*) mediante "RNA interference". Due linee transgeniche silenziate nel gene *PME13* o *PME28* sono state sottoposte ad un esperimento preliminare di infezione con *F. graminearum*, ma non sono state riscontrate differenze significative tra le linee transgeniche e quella controllo, ad eccezione della linea transgenica AZ4-11 e Svevo 2 giorni dopo l'infezione. Geni *PME* silenziati sono stati ricercati anche tramite approccio TILLING, analizzando una popolazione di 4000 piante disponibile presso l'Università della Tuscia. Tuttavia, l'analisi effettuata su 1920 individui per mutazioni nel gene *PME13* non ha identificato nessuna mutazione. Quindi, si è proceduto con lo screening di una popolazione TILLING completamente sequenziata recentemente messa a disposizione dall'Università della California, Davis. In questo caso, sono state identificate 28 accessioni mutate per 12 differenti geni *PME*: 18 accessioni recanti mutazioni per codoni di STOP e 10 accessioni con mutazioni nei siti di splicing. In conclusione, questo studio di caratterizzazione dei geni *PME* in frumento ha rivelato caratteristiche strutturali e funzionali della famiglia genica, sottolineando un possibile coinvolgimento di specifiche *PME* nell'interazione frumento-*F. graminearum*. La verifica di questo possibile coinvolgimento tramite le piante silenziate nel gene *PME13* o *PME28* non ha evidenziato alcuna differenza con le piante controllo, almeno nel primo esperimento d'infezione. La selezione dei mutanti TILLING per altri geni *PME* offre la possibilità di indagare più estesamente il coinvolgimento delle PME nell'interazione del frumento con microrganismi patogeni.

Parole-chiave

Triticum aestivum; *Triticum durum*; Parete cellulare; Pectin methyl esterase (PME); Interazione frumento- *F. graminearum*; Famiglia genica; Espressione genica; RNAi; TILLING; *F. graminearum*

Table of content

Abbreviations

4)-α-D-Gal*p*A-(1,2)-α-L-Rha*p*-(1: 4)-α-D-Galactopyranosyluronic acid-(1,2)-α-L-Rhamnopyranose-(1
β-D-Xyl*p*: β-D-Xylopyranose
β-D-Api*f* : β-D-Apiofuranose
β-D-Api*f*(1,3')- β-D-Api*f*-(1: β-D-Apiofuranose (1,3')-β-D-Apiofuranose-(1
IWGSC: International Wheat Genome Sequencing Consortium
CWDEs: cell wall degrading enzymes
HG: homogalacturonan
GHs: glycoside hydrolases
PGs: polygalacturonases
PL: pectin lyases
PAEs: pectin acetyl esterase
PMEs: pectin methyl esterases
SP: signal peptide
TM: transmembrane domain
PMEI: pectin methyl esterase inhibitor
DM: degree of methylesterification
OGs: oligogalacturonides
CBP: cellulose binding protein
FHB: Fusarium Head Blight
DON: deoxyvalenol
QTL: quantitative trait loci
RNAi: RNA interference
PM: processing motif
NT: nulli-tetrasomic
CDD: conserved domain database
EST: expression sequence tags
hpa: hours post anthesis
***PR1.1*:** pathogen related 1.1
***TRI6*:** trichothecene 6
DPI: days post infection

Figures

Figure 1. Production of wheat in 2013 (http://faostat3.fao.org/browse/Q/*/E).
Figure 2. Genetic base of wheat.
Figure 3. Structure of the plant cell wall.
Figure 4. General structure of plant cell wall pectins.
Figure 5. The egg-box structure formed between the negative charges of the de-esterified carboxyl groups of galacturonic acids and the positive charged calcium ions.
Figure 6. Schematic representation of a plant secondary cell wall, composed by cellulose, hemicelluloses and lignin polymer.

1. GENERAL INTRODUCTION

1.1 The wheat

Among crops wheat is the most worldwide cultivated plant (Fig. 1), being the third most produced cereal after maize and rice (FAOSTAT data, 2013). The centre of origin of wheat is supposed to be the Fertile Crescent after about 8000 BCE and then it spreads in other countries, like Turkey, Syria, Egypt and then Greece, India, Cyprus, Germany and Spain and finally wheat reached England and North Europe (Shewry, 2009).

Wheat is one of the most important protein source in human diet, having the higher protein content then other major cereals; besides it is an important source of carbohydrate, minerals and vitamins. This cereal is also commonly used in animal feed and in industrial processes, such as the production of paper additives or to make biodegradable plastics (Sarka et al., 2011).

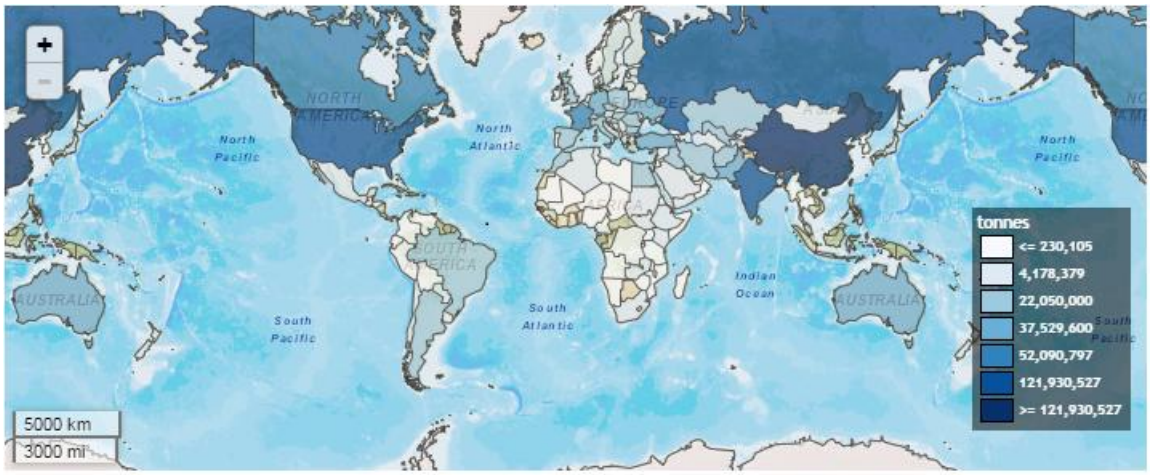

Figure 1. Production of wheat in 2013 (http://faostat3.fao.org/browse/Q/*/E).

Nowadays wheat cultivars that are mostly cultivated belong to two species, *Triticum turgidum* (durum wheat) and *Triticum aestivum* (bread wheat) with the latter one grown on over 95% of the wheat growing area. Moreover, durum wheat is mainly involved in pasta making whereas bread wheat is mainly involved in bread making industry.

1.2 Genetics of wheat

Wheat belong to *Graminaceae* family, tribe *Triticeae*, genus *Triticum*.

From a genomic point of view, *Triticum* includes several species that can be divided according to the somatic chromosome number in diploid, tetraploid and hexaploid

wheats (Fig. 2). An example of diploid wheat is the domesticated wheat *Triticum monococcum*, with two sets of seven chromosomes (2n= 14) belonging to the so called genome A. Most tetraploid wheats nowadays cultivated (e.g. *Triticum durum*) are derived from the wild emmer *Triticum dicoccoides* (genome AABB). The wild emmer is itself the result of a hybridization between two diploid species, *Triticum urartu* (genome AA) and *Aegilops speltoides* (genome BB).

Either domesticated emmer or durum wheat (*T. turgidum*, genome AABB) hybridized with the wild diploid wheat *Triticum tauschii* (genome DD) to make the hexaploid wheat *Triticum aestivum*, with the AABBDD genome (Hancock, 2004).

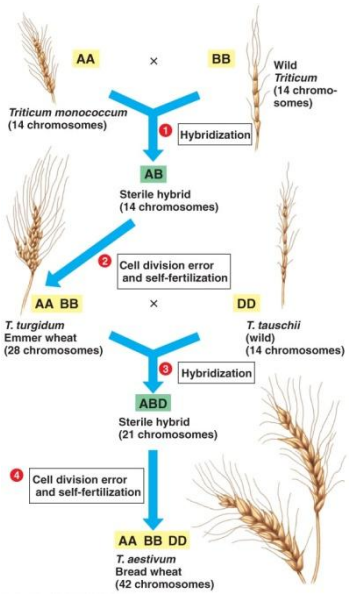

Figure 2. Genetic base of wheat.

Bread wheat with its 21 chromosomes pairs (A, B and D genome) and durum wheat with its 14 chromosomes pairs (A and B genome), are allopolyploid but they behave as diploids because of *Ph* gene prevents homeologous gene pairing (Martinez-Perez et al., 2001).

In 2005 was established the International Wheat Genome Sequencing Consortium (IWGSC), a collaborative consortium formed by 1100 members from 55 countries with the aim to create an high quality wheat genome sequencing database, accelerating wheat breeding and improving all aspects of wheat science. IWGSC is working on bread wheat 21 chromosomes pairs sequencing and physical maps developing. The first milestone was reached on July 2014 with the publication of the chromosome-based

draft sequence in the journal Science (The International Wheat Genome Sequencing Consortium, 2014).

1.3 Plant cell wall: structure and functions

The plant cell wall is a sophisticated and complicated structure that is involved in the determination of cells size and shape, plant growth and development, intercellular communication and interaction with the environment, as it is a barrier between the plant and the "outside world". Plant cell wall is formed by diverse elements, such as proteins, cellulose, hemicelluloses and pectins organized into a complex network (Fig. 3).

There are two type of cell wall that are called primary and secondary cell wall. The primary cell wall, a complex and dynamic structure, is generally a thin, flexible and extensible layer formed during cell growth and it is composed by structural proteins, enzymes and largely by polysaccharides as cellulose, hemicellulloses and pectins.

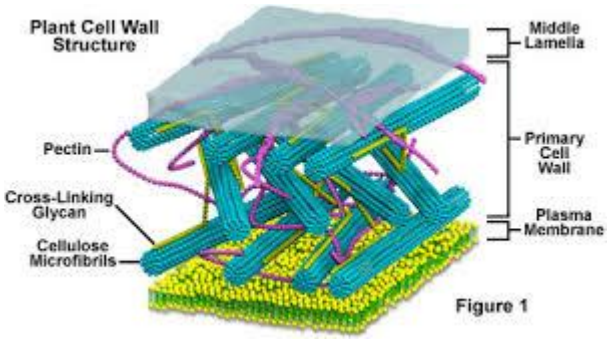

Figure 3. Structure of the plant cell wall.

1.3.1 Cellulose and hemicelluloses

Cellulose is an organic compound, a polysaccharide consisting of a linear chain of β (1→4) linked D-glucose units. Cellulose microfibrils are connected to hemicelluloses component via hydrogen bonds and most wall models identify this interaction as one of the main features of cell wall architecture.

Hemicelluloses are branched polysaccharides structurally similar to cellulose because they have a backbone composed of 1,4-linked β-D-hexosyl residues. The predominant hemicellulose in many primary walls is xyloglucan. Other hemicelluloses found in primary and secondary walls include glucuronoxylan, arabinoxylan, glucomannan, and galactomannan.

1.3.2 Pectins

The cellulose/hemicellulose network is embedded in a jelly-like matrix of pectins, that are the most complex class of cell wall polysaccharides (Fig. 4). Pectins are mostly found in the primary cell wall and in the middle lamella, being particularly abundant in the non-woody plant tissues. The amount, the structure and the chemical composition of pectins differ from plant to plant and, within the same plant, from tissue to tissue; they occupy about 35% of dicotyledonous cell wall and only about 5% of grasses cell wall (Mohnen, 2008). Pectins are important for plant growth and development, cell adhesion and extension, cellular structure integrity and also for the mediation of defence responses (Caffal and Mohnen, 2009).

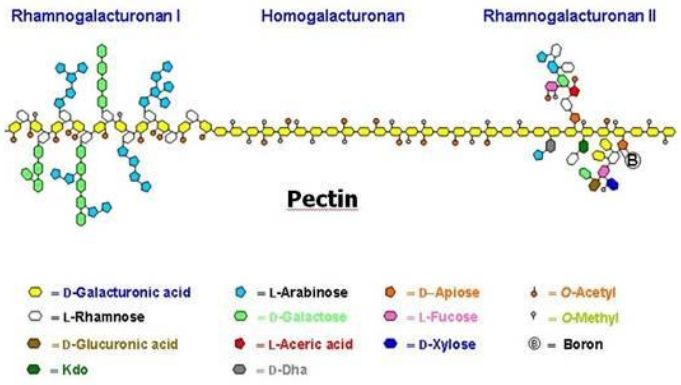

Figure 4. General structure of plant cell wall pectins.

Pectins are polysaccharide rich in galacturonic acid units linked together via α (1→4) bounds. So far four classes of pectic components have been characterized:

- Rhamnogalacturonans

Rhamnogalacturonans (RGs) are a group of polysaccharides that, depending on the repeated unit of the backbone, could be divided into rhamnogalacturonans type I and type II:

- RGsI contain a backbone of the repeating disaccharide 4)-α-D-Gal*p*A-(1,2)-α-L-Rha*p*-(1 from which branch off various neutral sugars, mainly D-galactose, L-arabinose or D-xylose, depending on the origin of pectin.
- RGsII are less frequent, but they are a complex and an highly branched polysaccharides, where the backbone is made exclusively of at least 8 D-galacturonic acid units; for this reason are sometimes classified within the

group of substituted galacturonan.

- Xylogalacturonans

Xylogalacturonan have β-D-Xyl*p* residues attached to C-3 of the galacturonan backbone; these polysaccharides are only present in reproductive tissues and they could prevent pathogen degrading enzymes (Jensen et al., 2008).

- Apiogalacturonans

Apiogalacturonans are present in the cell wall of some aquatic monocot plants. The backbone is substituted with β-D-Api*f* and β-D-Api*f*(1,3')- β-D-Api*f*-(1.

- Homogalacturonans

Homogalacturonans (HGs) are the most abundant polysaccharides within pectin, representing up to the 65% of the plant cell wall (Mohen, 2008). HGs are composed by 1,4-linked α-D-galacturonic acid residues, in which some of the carboxyl groups are methylesterified or acetylesterified. Together with other cell wall polysaccharides, HGs are involved in plant growth and development. Homogalacturonans are synthesized in an highly methylesterified form in the *cis* Golgi, exported into the cell wall, and de-methylesterified *in muro* by the action of enzymes called pectin methylesterase (PME; EC3.1.1.11), releasing acidic pectins and methanol.

Around 80% of carboxyl groups of galacturonic acid are esterified with methanol and, depending on the degree of de-esterification, pectins are classified in high- or low-pectins (HM or LM pectins) with more or less than half of all the galacturonic acids esterified, respectively. In LM pectins ionic bridges are formed between calcium ions and the ionised carboxyl groups of the galacturonic acid, forming the so called egg-box structure (Fig. 5) (Grant et al., 1973).

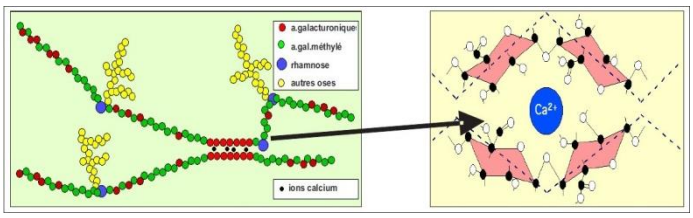

Figure 5. The egg-box structure formed between the negative charges of the de-esterified carboxyl groups of galacturonic acids and the positive charged calcium ions.

Unlike the primary cell wall, the secondary cell wall is not present in all type of cells. The secondary cell wall is a layer between the primary cell wall and the plasma membrane and is formed when primary wall is completely assembled and the cell ends to expand, giving it rigidity and an additional protection. As primary cell wall, also the secondary cell wall is formed by cellulose and hemicelluloses but pectins, structural proteins or enzymes are or may be absent; in the secondary plant cell wall is present the lignin, an heterogeneous organic polymer that is included into cellulose microfibrils, conferring an hydrophobic nature to plant tissues (Fig. 6).

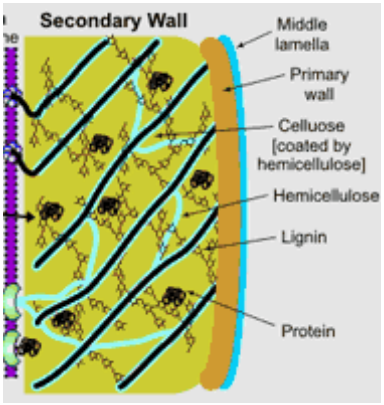

Figure 6. Schematic representation of a plant secondary cell wall, composed by cellulose, hemicelluloses and lignin polymer.

1.4 Cell wall as target for plant cell wall degrading enzymes (CWDEs)

The cell wall degrading enzymes (CWDEs; Kubicek et al., 2014) play a significant role in the life cycle of a fungal pathogen as they are used to prove the assimilation of nutrients and to overcome the plant cell wall. In fact, the degradation of the plant cell wall components, as cellulose, hemicelluloses and pectins, is required for fungal pathogens to penetrate and proliferate within host cells. The complexity of the plant cell wall is reflected by the high number of CWDEs secreted by pathogens, generally referred as glycoside hydrolases (GHs; http://www.afmb.cnrs-mrs.fr/CAZY/; Henrissat, 1991), enzymes able to cleave hydrolytically glycosidic bonds in polysaccharides. GHs are distributed among diverse gene families genetically and structurally different.

1.4.1 Cellulose and hemicelluloses-degrading enzymes

The hydrolysis of cellulose generally involve the synergic action of two different enzymes, one of them that acts in a endo-acting way (endoglucanase) and the other one that acts in a exo-acting way (exoglucanase). The activity of these enzymes are followed

by the activity of a β-glucosidase that hydrolyze the cellodextrin oligomers to glucose. Cellulases are found in GH5, GH6, GH7, GH12 and GH45 families whereas β-glucosidases belong to GH1 and GH3 families.

Hemicelluloses is a term used to describe the non-cellulosic components of the plant cell wall, as xyloglucans, xylans and galactomannans. In their main chain are present different kind of linkage and sugars, but their side-chain substituents often comprise the same sugar and the same linkage and for this reason the same enzymes could be involved in the depolymerisation. Xyloglucan is breakdown by the activity of endo-β-1,4- glucanases, enzymes belonging to GH5, GH12, GH16 and GH44 families. Xylan are depolymerised by the activity of endo-1,4-β-xylanases (EC 3.2.1.8) that cleave the glycosidic bond in the xylan backbone. Most fungal xylanases are classified into the GH10 and GH11 families. In particular, GH10 xylanases are found in a very high number in plant pathogenic fungi and some fungi have also hydrolytic enzymes belong to GH30 family showing a xylanase activity. Galactomannans are degraded by enzymes comprising β-mannanase (EC 3.2.1.78) and β-mannosidase (EC 3.2.1.25) (Moreira and Filho, 2008). β-mannanase are found in GH5 and GH26 families, whereas β-mannosidase belong to GH1 and GH2 families.

1.4.2 Pectin-degrading enzymes

The degradation of pectin requires the action of different enzymes that act both in a hydrolytic way (polygalacturonases, PGs, EC 3.2.1.15 and 3.2.1.67) and in a non-hydrolytic way, *via* a β-elimination (pectin lyases, EC 4.2.2.10 and pectate lyases, EC 4.2.2.2).

PGs have an endo- and an exo-activity and they belong to the GH28 family. They are present in all fungal genomes but in a variable number (Zhao et al., 2013). GH28 family contain also rhamnogalacturonan hydrolases that cleave the α-1,2-glycosidic bond between D-galacturonic acid and L-rhamnose residues within the pectin backbone (van den Brink J. and de Vries, 2011). The polysaccharide lyases (PLs, EC 4.2.2.-) cleave uronic acid–containing polysaccharide chains via a β-elimination mechanism to generate an unsaturated hexenuronic acid residue and a new reducing end. PLs are classified into 21 families (Lombard et al., 2010).

The homogalacturonan backbone of pectin varies in its degree of methylation from a highly methyl esterified form to a fully demethylated form, which are consequently called pectine and pectate, respectively. Enzymes attacking these structures are termed pectin lyase and pectate lyase, respectively, with this latter having a calcium ion

dependent activity. Up to now, all the characterized pectin lyases are found in PL1 family, whereas fungal pectate lyases are found in PL1 and PL3 families.

1.4.3 Role of CWDEs in plant pathogenesis

CWDEs and enzymes that destroy physical barrier as cutin, are the first components that pathogens use to overcome the obstacle represented by the cell wall. CWDEs are key factors for several pathogens: for instance, the CUT2 cutinase produced by the rice and barley fungal pathogen *Magnaporthe grisea*, plays its role by sensing the leaf surface area and by leading to the correct differentiation, penetration and virulence (Skamnioti et al., 2007); in pea, the disruption of a cutinase coding gene in *Fusarium solani* f. sp. *pisi* decreases its virulence (Rogers et al., 1994). Xylan and pectin degradation is required as well, as demonstrated by Wu et al. (2006) for *M. grisea*. Polygalacturonanases are characterized to be crucial virulence factors in *Botrytis cinerea*, *Claviceps purpurea* and *Aspergillus niger* (ten Have et al., 1998; Oeser et al., 2002; Shieh et al., 1997).

Depending on their lifestyle, pathogens are traditionally divided into three classes: biotrophs, necrotrophs and hemibiotrophs, secreting a diverse range of CWDEs. Biotrophic pathogens need to maintain plant cells alive, in order to take advantage from them. Because of this, this class of plant pathogens generally secretes a relatively little amount of lysis enzymes (Mendgen and Hahn, 2002). Contrarily, necrotrophic organisms produce a large variety and amount of CWDEs targeting multiple sites on plant cell wall and causing extensive damages. In most cases a redundancy in degrading enzymes was found in necrotrophs (Idnurm and Howlett, 2001). For example, *B. cinerea* has at least six PGs that hydrolize the partially de-methylesterified homogalacturonan of pectin (Wubben et al., 1999). Hemibiotrophs behave as biotrophs in the early stage of their lifecycle and as necrotrophs in the later part of their growth, consequently the production of CWDEs is related to their developmental stage (Zhao et al., 2013).

1.5 Pectin: an important component for plant defence

The plant cell wall represent an effective physical barrier against pathogens entry and several studies indicated that its composition is of great importance to play this crucial

defensive role. For example, several works report that the degree and pattern of methylesterification is an important feature for host defence (Lionetti et al., 2012).

1.5.1 Homogalacturonan modifying enzymes (HGMEs)

Homogalacturonan is one of the main component of pectin. It is a linear homopolymer of galacturonic acid residues and it can carry either acetyl groups at O2 or O3 (Gou et al., 2012) or be methyl esterified at the C6 carboxyl (Wolf et al., 2009). Acetylation and methylation are modifications carried out from enzymes named pectin acetylesterases (PAE; EC 3.1.1.6, CAZy class 12 of carbohydrate esterase) and pectin methylesterases (PME; EC 3.1.1.11, CAZy class 8 of carbohydrate esterase), respectively.

- *Pectin acetylesterases*

Pectin acetylesterases belong to a gene family that counts a similar number of members both in dicotyledonous and in monocotyledonous plants, despite the different amount of pectins found between them. For example, 12, 10, 7 and 11 ORFs were annotated as putative PAEs in *Arabidopsis thaliana*, *Populus trichocarpa*, *Brachypodium distachyon* and *Oryza sativa*, japonica group, respectively (Cao, 2012; Geisler-Lee et al., 2006; Tyler et al., 2010; Davidson et al., 2012). The degree of acetylation vary between 0.25 and 10% (Gou et al., 2012) depending on the species. In addition to homogalacturonan other plant cell components could be *O*-acetylated, as rhamnogalacturonans, xylogalacturonans and glucoronoarabinoxylans, being present in a large amount in the grass cell wall and representing possible targets for PAEs activity (Vogel, 2008). The presence of acetyl groups could affect plant cell wall viscosity (Orfila et al., 2012) and impairs the formation of Ca^{2+} bonds between homogalacturonan chains (Turquois et al., 1999). Acetylation can also affect the degradation of homogalacturonan by some endo- or exo-polygalacturonases (Bonnin et al., 2003). PAEs enzymes have been found in plants (Williamson, 1991; Christensen et al., 1996), bacteria (Shevchik and Hugouvieux-Cotte-Pattat, 1997) and fungi (Kauppinen et al., 1995; Bonnin et al., 2008). Generally they act specifically on homogalacturonan and rhamnogalacrutonan-I and seem to be inactive against other classes of pectins. Moreover, PAEs activity is increased when the substrate has previously been demethylesterified (Williamson, 1991; Bordenave et al., 1995; Oosterveld et al., 2000), suggesting a synergistic effect between PAEs and PMEs in the formation or degradation of the egg-box within the cell wall. The 3D crystallographic structure of PAEs has not yet been resolved.

.

- *Pectin methylesterases*

Pectin methylesterases belong to a gene family that counts a high number of members in dicotyledonous species such as *A. thaliana* and poplar (*P. trichocarpa*), with 66 and 88 sequences annotated as *PMEs*, respectively (Pelloux et al., 2007; Geisler-Lee et al., 2006). Conversely, grass species count a lower number of *PME* sequences: for example, *B. distachyon* has 35 sequences annotated as *PMEs* and rice (*O. sativa* japonica group) has 41 sequences annotated as *PMEs* (Pelloux et al., 2007; Wang et al., 2013). The lower number of *PMEs* in grasses is generally explained with the lower amount of pectin present in monocotyledonous in comparison to dicotyledonous. PMEs are synthesized in the endoplasmic reticulum and they act *in muro*; for this reason they must be secreted into to cell wall and to do that, enzymes should possess a signal peptide (SP) and/or a transmembrane domain (TM). Analysis of PMEs sequences in *A. thaliana* and *O. sativa* japonica group (Senechal et al., 2014) reveals that most sequences (53% and 46%, respectively) possess a signal peptide. Many sequences possess also a transmembrane domain (38% and 37%, respectively); only a minor part possess both a SP and a TM (3% and 7%, respectively). The 6% of *Arabidopsis* PMEs and the 10% of *Oryza* PMEs are classified as soluble isoforms as they possess neither a SP nor a TM domain. The functional role of the soluble isoforms is to be determined, even if a biochemical characterization of them suggest that they could act in defence mechanism against pathogens (Dedeurwaerder et al., 2009). Up to now, a 3D crystallographic structure for plant PMEs has been resolved only for carrot (Johansson et al., 2002) and tomato (D'Avino et al., 2003; Di Matteo et al., 2005), whereas the purification and the characterization of the activity was performed for tomato (Lee and McMillan, 1968), papaya (Fayyaz et al., 1994), apple (Castaldo et al., 2005), kiwi (Giovane et al., 1996), grapefruit and mandarin orange (Rillo et al., 1994).

PMEs activity is dependent on different factors, such as changes in pH (Catoire et al., 1998; Jolie et al., 2009; Dixit et al., 2013), cations concentration (Jolie et al., 2010), or the presence of free carboxyl groups near the active site. In fact, seems that PMEs are more active on a partially demethylesterified pectin (Fries et al., 2007). Another important factor is the presence of the pectin methylesterase inhibitors (PMEI; pfam04043), proteinaceous inhibitors that forms a 1:1 stoichiometric complex with PMEs (Di Matteo et al., 2005), implying the inhibition of PME activity by a non-covalent binding.

The mode of action of PMEs could be different. Three mechanisms have been described:

1- single-chain mechanism, where PMEs act by removing contiguous methylesters within a single homogalacturonan chain;
2- multiple-attack mechanism, where PMEs act by removing few methylesters within different homogalacturonan chains;
3- multiple-chain mechanism, where PMEs catalyses a number of reactions before dissociate from the substrate.

A linear PMEs activity lead to the formation of the egg-box structure that confers to the cell wall an increase strengthening, whereas a random PMEs activity lead to a cell wall loosening.

1.6 PAEs and PMEs in plant defence

Acetylation of the cell wall polysaccharides is involved in plant–pathogen interaction. In fact, it was demonstrated that in *Arabidopsis* and *Brachypodium* a lower acetylation degree is associated with an increased resistance against *B. cinerea* and *Bipolaris sorokiniana* (Pogorelko et al., 2013).

Methyl esterification (DM) is another important determinant in plant-pathogen interaction, as a higher DM has been associated with an increased resistance against different pathogenetic organisms in different plant species. In fact, it was demonstrated that a higher DM increased resistance to the bacteria *Pectobacterium carotovorum* in wild potato plants (McMillan et al., 1993) and in *pme3* mutants of *A. thaliana* (Raiola et al., 2011). *Arabidopsis pme* mutants (*ppme1*, *pme17*, *pme31*, *pme39*, and *pme44*) with an increased DM are more resistant to *Pseudomonas syringae* pv. *maculicola* ES4326 (*Pma* ES4326) (Bethke et al., 2014). The over-expression of *PMEI* genes enhanced plant resistance both in dicotyledonous plants against *B. cinerea* (Lionetti et al., 2007) and in monocotyledonous plants against *B. sorokiniana*, *Fusarium graminearum* and *C. purpurea* (Volpi et al., 2011; 2013).

Conversely, it was demonstrated that an over-expression of a *PME* gene in strawberry plants (*Fragaria vesca*) increased the resistance against the fungal pathogen *B. cinerea* (Osorio et al., 2008). This result has been explained with the formation of specific oligogalacturonides (OGs) able to induce the plant defence response.

A PME also participate to *Arabidopsis*-nematode (*Heterodera schachtii*) interaction, by facilitating the parasitic organism through a direct contact with the cellulose binding protein (CBP) synthesized from *Heterodera* (Hewezi et al., 2008).

Not only the different DM, but also a random distribution rather than a blockwise distribution of methyl groups was associated with an increased resistance against *Puccinia graminis* in wheat plants (Whietölter et al., 2003). Also Bonnin et al. (2002) found that a blockwise distribution of methyl groups favoured PGs activity of *Fusarium moniliforme*.

Microarray data for *PME* genes expression in *Arabidopsis* are available at www.genevestigator.com (Lionetti et al., 2012) and they were collected from infection experiments performed with pathogens having different lifestyles. Results showed that each pathogens alter the expression profile of different *PMEs*, with a higher number of genes induced by hemibiotrophic and necrotrophic organisms than by biotrophs.

Finally, PMEs could be correlated to an increased resistance both with a direct reinforcement of the cell wall and with an indirect role through the formation of eliciting OGs. In any case, PMEs are valid candidates as resistance factors.

1.7 *Fusarium graminearum*

One of the principal fungal disease in wheat is the Fusarium Head Blight (FHB) disease, caused by different *Fusarium* species, with *F. graminearum* being one of the most widespread causal agent of FHB (Parry et al., 1995). The first symptoms of FHB occur shortly after flowering, leading to the bleaching of spikelets around the infection site; in a short time bleached spikelets are visible throughout the whole spike. Later in the fungal progression, within the infected spikes black spherical structures became visible, being the sexual reproductive elements of the pathogen. Grains became rough and turn in colour from pink to brown. *F. graminearum* infection lead to a decreasing grains yield and quality (McMullen et al., 1997) mainly due to the production of mycotoxins, fungal molecules harmful for human and animal health. The major mycotoxin produced by *F. graminearum* is the deoxynivalenol (DON), also called vomitoxin because of its effects on the digestive apparatus.

Generally two different types of FHB resistance are indicated: type I resistance, that is the resistance against the initial entry of the pathogen and type II resistance, that is the resistance against the spread of the pathogen within plant tissues (Schroeder and

Christensen, 1963). Type II resistance is better studied and employed because is controlled by resistance genes. Molecular mapping of quantitative trait loci (QTL) conferring partial resistance has been largely reported and allowed to identify a high numbers of QTLs (Buerstmayr et al., 2009). Between all of them, the two most effective QTLs are *Fusarium head blight 1* (*Fhb1*) and *Qfhs.ifa*, located on 3BS and 5A chromosomes, respectively (Anderson et al., 2001; Buerstmayr et al., 2002; 2003). For the first time these QTLs were identified in Chinese Spring cv. Sumai3, becoming the most used source of FHB resistance. *Fhb1* confers type II resistance, whereas *Qfhs.ifa* confers both type I and type II resistance, albeit a less extent.

The genetic determinants are still unknown, even if significant efforts were conducted in order to isolate *Fhb1* and *Qfhs.ifa* genes (Liu et al., 2006; 2008). Several studies have been conducted, trying to reveal the relationship existing between the presence of *Fhb1* QTL and *F. graminearum* resistance. For instance, Zhuang et al. (2013) identified one gene named *WFhb1_c1* that was both functionally associated with and physically located within *Fhb1* and it was found to be weakly similar to an *Arabidopsis* gene encoding a PMEI. Expression analysis conducted on *WFhb1_c1* gene revealed that a lower expression level of this gene was associated with more severe disease. They also found the down-regulation of the expression of the pectin methylesterase inhibitor gene in Sumai3 plants lacking *Fhb1* and they associated this evidence with the QTL. Lionetti et al. (2015) concentrated their studies on *PME* genes localized on the short arm of chromosome group 2 in the same bin position of the major FHB QTLs, thus suggesting a possible involvement of these *PMEs* in *F. graminearum* resistance. They found a down-regulation of *PMEs* in resistant cultivar compare to the up-regulation observed in the susceptible one.

2. OBJECTIVES

The aim of this present work was to identify and characterize the wheat (*Triticum aestivum*) *PME* gene family and to evaluate their involvement in wheat resistance against *F. graminearum*.

We have pursed this objectives by searching the wheat genome and by evaluating the expression behaviour of *PME* genes in different bread wheat tissues and following *F. graminearum* infection in a susceptible and a tolerant bread wheat cultivar.

We attempted also to verify *in planta* by RNAi and TILLING the role of specific *PMEs* in wheat resistance against *F. graminearum*.

CHAPTER I

Wheat *PMEs in silico* identification and structural analysis

The results presented in this chapter has been submitted to *Plant Physiology and Biochemistry*.

Abstract

Pectin methyl esterase (*PME*) genes code for enzymes that are involved in structural modifications of the plant cell wall during plant growth and development. They are also involved in plant-pathogen interaction. *PME* genes belong to a multigene family and in this study we report the first comprehensive analysis of the *PME* gene family in bread wheat (*Triticum aestivum* L.). Like in other species, the members of the *TaPME* family are dispersed throughout the genome and their encoded products retain the typical structural features of PMEs. qRT-PCR analysis showed variation in the expression pattern of *TaPME* genes in different tissues and revealed that these genes are mainly expressed in flowering spikes. In our attempt to identify putative *TaPME* genes involved in wheat defense, we revealed a strong variation in the expression of the *TaPME* following *Fusarium graminearum* infection, the causal agent of Fusarium head blight (FHB). Particularly interesting was the finding that the expression profile of some *PME* genes was markedly different between the FHB-resistant wheat cultivar Sumai3 and the FHB-susceptible cultivar Bobwhite, suggesting a possible involvement of these *PME* genes in FHB resistance. Moreover, the expression analysis of the *TaPME* genes during *F. graminearum* progression within the spike revealed those genes that responded more promptly to pathogen invasion.

Keywords: *Triticum aestivum*; Cell wall; Pectin methyl esterase (PME); Wheat-pathogen interactions; Gene family; Gene expression

1. Introduction

The plant cell wall represents a main barrier to the entry of the pathogens and its reinforcement can limit the colonization of host tissue (Cantu et al., 2008). The primary plant cell wall is a complex and dynamic structure composed mainly by the polysaccharides cellulose, hemicelluloses and pectins. Pectins are complex polysaccharides (Mohnen, 2008) represented mainly by homogalacturonan (HG), synthesized in a highly methyl esterified form in the Golgi apparatus and de-methylesterified in muro by pectin methyl esterases (PME; EC3.1.1.11). PME belong to the class 8 of the carbohydrate esterase (CAZY: http://www.afmb.cnrs-mrs.fr/CAZY/; Coutinho et al., 2003) and catalyse the de-methylesterification of the C6 linked methyl ester group of HG. As result of PME activity the distribution of free carboxyl groups on HG can be contiguous (or blockwise) or non-contiguous (or random) (Willats et al., 2001). The presence of consecutive negative charges on carboxyl groups can favor the interaction with Ca^{2+} ions forming the so called egg-box (Grant et al., 1973) that contribute to cell wall strengthening.

PME can be divided into two groups: group 1 (or type II) and group 2 (or type I) sharing a catalytic PME domain (pfam01095) at the C-terminus and in most cases a signal peptide (SP) and/or a transmembrane domain (TM) at the N-terminus that allows their secretion. PME belonging to group 2 possess also a domain (pro-region) at the N-terminal region that share a high similarity with pectin methyl esterase inhibitor (PMEI domain; pfam04043). The pro-region is removed by a subtilisin-like protease before secretion into the cell wall by acting on a processing motif (PM) that in most cases has the sequence RRLL or RKLL (Pelloux et al., 2007).

PME are encoded by gene families whose members are involved in various physiological processes, including hypocotyls elongation, fruit ripening and maturation, cellular adhesion and seed germination. PME activity and pectin methylesterification have been also related to plant defense (Pelloux et al., 2007).

Despite the limited amount of pectin in cereal cell wall (Vogel, 2008), PME activity and pectin methylesterification affects wheat resistance. In particular, wheat resistance to stem rust (*Puccinia graminis* f. sp. *tritici*) has been associated with a more random distribution of methyl ester in the homogalacturonans, whereas a more blockwise distribution of the methyl esters was associated with susceptibility (Wiethölter et al., 2003). A more direct evidence has been reported by analysing transgenic wheats expressing a kiwi pectin methyl esterase inhibitor (AcPMEI). These plants that

contained a reduced PME activity and an higher level of pectin methylesterification compared to non transgenic plants, were more resistant to the fungal pathogen *Bipolaris sorokiniana* and *Fusarium graminearum* (Volpi et al., 2003).

To further define the contribution of PME activity and pectin methylesterification in the wheat defence response, the aim of the present work was the characterization of the wheat (*Triticum aestivum L.*) *PME* gene family. In particular, we focus our attention on the expression profiles of the *TaPME* members in different wheat tissues and following *F. graminearum* infection, the causal agent of the worldwide devastating disease Fusarium Head Blight (FHB). For this latter aspect, we compared the expression pattern between a tolerant and a susceptible bread wheat cultivar at the inoculation point and during fungal progression within the spike.

2. Materials and methods

2.1 Plant material and growth conditions

Bread wheat cultivars Bobwhite and Sumai3, susceptible and resistant to FHB caused by *Fusarium graminearum*, respectively, were grown in a growth chamber at 18-23°C, 16-8h photoperiod and at a light intensity of 300 mE m^{-2} s^{-1}.

2.2 Databases searches and sequences analysis

Brachypodium distachyon PME sequences were used as query sequences to perform blast searches against the International Wheat Genome Sequencing Consortium (IWGSC) database (https://urgi.versailles.inra.fr/blast/blast.php; The International Wheat Genome Sequencing Consortium, 2014).

The complete nucleotide sequence of *TaPME13-5A* or *TaPME45-5A* were obtained by PCR amplification from nulli-tetrasomic lines (NT) of *T. aestivum* cv. Chinese Spring. Primers were developed from the completed coding region of the homoeologous *TaPME13-5D* or *TaPME45-5D* and have the following sequences: (TaPME13-5A forward) 5′-CTTGTTGCAGCAGCAACAACAACAG-3′ and (TaPME13-5A reverse) 5′-ACCCGGCCGCTGCCCCCTCCCAT-3′; (TaPME45-5A forward) 5′-GCCGCGCATCGTTTGATTCGTTTCT-3′ and (TaPME45-5A reverse) 5′-GGCCATGGTGTCGATGATTATA-3′. PCR reactions were performed in a reaction volume of 50 μl with 10 ng of genomic DNA, 2.5 U of FastStart High Fidelity PCR system (Roche Diagnostics, Monza, Italy), 1× Taq PCR buffer, 50 ng of each of the two primers, and 100 μM each deoxyribonucleotide. Amplification conditions were: 1 cycle at 95°C for 2 min; 30 cycles at 95°C for 45 sec, 60°C for 45 sec, and 72°C for 2 min; 1 cycle at 72°C for 5 min.

Chromosomal assignment of *TaPME* genes were obtained from the International Wheat Genome Sequencing Consortium database.

Exonic and intronic regions were identified into wheat *PME* gene sequences using both GENSCAN tool (http://genes.mit.edu/GENSCAN.html; Burge and Karlin, 1997; Burge, 1998) and *B. distachyon* sequences as reference. The genomic sequences and the coding regions were used as inputs in the Gene Structure Display Server (GSDS) software (http://gsds.cbi.pku.edu.cn/; Hu et al., 2015) in order to generate the intron-exon structure of wheat *PME*s.

Sequence analyses were performed using the DNAMAN software (Lynnon Biosoft, Quebec, Canada) that uses ClustalW algorithm for multiple sequence alignment (Thompson et al., 1994). The parameters for sequence alignment were a protein gap open penalty of 10 and a protein gap extension penalty of 5.

Deduced protein sequences were used to perform a blast research against the Conserved Domain Database (CDD) of the NCBI database (http://www.ncbi.nlm.nih.gov/Structure/cdd/wrpsb.cgi; Marchler-Bauer et al., 2015).

SignalP (http://www.cbs.dtu.dk/services/SignalP/; Petersen et al., 2011) was used to search for signal peptides whereas WoLF PSORT (http://wolfpsort.org/; Horton et al., 2007) and Plant-mPLoc (http://www.csbio.sjtu.edu.cn/bioinf/plant-multi/; Chou and Shen, 2010) were employed in order to predicted the subcellular localizations of PME proteins.

In silico expression of *TaPME* genes was performed in the EST database at NCBI (http://www.ncbi.nlm.nih.gov/nucest/; Boquski et al., 1993).

2.3 Tissue samples and plants infection

Roots (Zadoks Z7), second leaf (Zadoks Z13) and flag leaf (Zadoks Z47) were collected from bread wheat cv. Bobwhite. Three samples for each tissues were collected, frozen in liquid nitrogen and stored at -80°C until use.

The infection experiments were performed by using the point inoculation method. Twenty µL of a suspension of *F. graminearum* conidia (25 conidia/µL) were injected into the two central opposite wheat flowering spikelets. Mock samples were inoculated with water. Infected and control spikelets were collected at 24 and 48 hours after inoculation (hpi). Two opposite spikelets below and upper the inoculation site (central opposite spikelets) were collected at 48 hpi.

After sampling, plant material was immediately frozen in liquid nitrogen and stored at -80°C until use. For each biological replicate, two inoculated spikelets per time point were collected and for each biological replicate, three technical replicates were conducted.

2.4 Real-time quantitative PCR (real-time qPCR)

Total RNA was extracted from plant material using RNeasy plant mini kit (Qiagen, Milan, Italy) and the first strand cDNA was obtained using QuantiTect Reverse Transcription kit (Qiagen). Specific primer pairs were developed for group of *TaPME* sequences sharing high sequence identity (at least 95%) (Table S1) and primer pairs specificity was verified both in silico with BLAST tool and by nucleotide sequence of PCR amplicons. qRT-PCR reactions were carried out in a reaction volume of 15 µL and included 7.5 µL of a 2x master mix (iQ SYBR Green Supermix, Bio-Rad Laboratories, Monza, Italy), 100 ng of cDNA, 0.5 µL (10 µM) of each forward and reverse primers and volume was adjusted with water. The Bio-Rad iCycler iQ instrument was employed. The PCR reaction conditions were: 1 cycle at 55°C for 2 min; 1 cycle at 95°C for 15 min; 40 cycles at 95°C for 30 sec, 60°C for 30 sec and 72°C for 30 sec; 1 cycle at 77°C for 2 min.

A primer pair specific for the homologs *TaPr-1-1*, *TaPr-1-2* and *TaPr-1-3* (herein named *PR1.1*) was included in the analysis as control of gene induction, whereas the *actin* gene was used as housekeeping gene (Moscetti et al., 2013). The Ct values of target genes and reference gene were used for further relative expression analysis by using the $2^{-\Delta\Delta Ct}$ method (Livak and Schmittgen, 2001; Yuan et al., 2006). In each experiment two biological replicates and three technical replicates were performed.

Quantification of *F. graminearum* biomass was performed by a qPCR analysis for the *TRI6* gene by using the primer pair Tri6_10F and Tri6_4R (Horevaj et al., 2011). Infected spikelets at 48 hpi from both cultivars Bobwhite and Sumai3 were collected and used for total DNA extraction employing DNeasy plant mini kit (Qiagen) following the manufacturer's instructions. qPCR was carried out by following the same conditions as previously described, using the *actin* gene as housekeeping gene. Relative DNA quantification was performed with the $2^{-\Delta\Delta Ct}$ method (Livak and Schmittgen, 2001; Yuan et al., 2006) taking as reference sample the one with the lowest amount of fungal biomass. In each experiment two biological replicates and three technical replicates were conducted.

Student's t-test and the analysis of variance (ANOVA) were used to obtain the statistical significance of the difference between samples and the reference sample.

3. Results

3.1 Members of the PME family are dispersed throughout the wheat genome

Predicted wheat *PME* sequences were identified by searching the bread wheat genome at the IWGSC database, using *B. distachyon PME* sequences as queries. In total 40 complete and 4 partial wheat *PME* sequences were identified. These *PME* genes were named on the basis of the corresponding *B. distachyon* gene used for their identification. Moreover, to distinguish the homoeologous genes on the A, B and D genomes of bread wheat, the specific chromosomal assignment was included at the end of each name (*e.g. TaPME53-4DS* or *TaPME53-4AL*, where 4 specify the chromosome, D or A specify the genome and S or L specify the assignment to Short or Long chromosome arm, when available).

Two of the four partial sequences, that is *TaPME13-5A* and *TaPME45-5A* localized on chromosome 5A, were completed by using a strategy based on PCR amplification of genomic DNA of nulli-tetrasomic (NT) lines of *T. aestivum* cv. Chinese Spring. On the basis of the high sequence conservation between the A and D wheat genomes, we developed primer pairs from the completed coding region of the homoeologous *TaPME13-5D* or *TaPME45-5D* and we use them to amplify the genomic DNA of N5DT5B line of homoeologous group 5. We obtained a single amplicon from each PCR reaction and their nucleotide sequencing confirmed the identity with the two partial sequences deposited on the database, thus providing the complete sequence of *TaPME13-5A* and *TaPME45-5A*. The remaining two partial genes were *TaPME58-2AL* (1758 bp) and *TaPME58-2DL* (604 bp) homoeologous of *TaPME58-2BL* that was present as a complete gene in the database.

The 42 complete *PME* sequences were subjected to GENSCAN analysis to identify exons and introns composition. In general, group I *PMEs* showed an higher number of introns than *PMEs* of group II. In fact, most *PMEs* belonging to group I have three or four introns, whereas most *PMEs* belonging to group II have a single intron. However, five genes do not contain introns. Specifically, *TaPME51-2AL*, *TaPME51-2BL* and *TaPME51-2DL* of group I and *TaPME21-1BS*, *TaPME21-4DL*, *TaPME21-4AS* and *TaPME21-2DL* of group II. In general, coding regions sharing an high sequence identity shared also a similar exon-intron structure (Fig. 1).

The intron-exon distribution was confirmed experimentally for three *PME* genes, *TaPME13-5A*, *TaPME21-2DS* and *TaPME28-2BL*, by comparing their genomic and

corresponding cDNA full length sequences of the bread wheat cv. Sumai3 (Fig. S1, Fig. S2 and Fig. S3).

Among the predicted TaPMEs, 20 belong to group I, encoding only a PME domain and 24 to group II (including also the two incomplete *PME* genes), encoding both PMEI and PME domains. The length of the PMEI domains were in the range of 100-150 residues, whereas that of the PME domains were in the range of 200-460 residues. Only TaPME2.2-3B and TaPME21-1BS have a shorter PME domain of 50 and 80 residues, respectively (Table 1).

Further, we analyzed the structural features of the 42 complete TaPMEs deduced proteins (Tab. 1).

The pre-region or signal peptide was present in 28 TaPMEs, while in the remaining 14 PME sequences, indifferently whether belonging to PME group I or PME group II, no signal peptide was predicted (Tab. 1). Similarly, the transmembrane region was present only in 32 TaPMEs (Tab. 1).

Concerning the subcellular localization, PSORT predicted that the PME proteins are mainly localized outside the cell or in the plasma membrane. However, all PMEs were predicted in the cell wall by using Plant-mPLoc (Tab. 1).

Sequence analysis of all TaPMEs showed that the five conserved functional motifs of the PME domain (Markovic and Janecek, 2004) were present in 33 genes, whereas in the remaining 9 were missing between one and three motifs. Also the number of cysteine residues in the PMEI domain showed variation. Only 10 PMEs contained the four conserved cysteines, the remaining ones contained between 1 and 6 cysteines. These analysis showed also that most of the PMEs of group II contained the two basic motifs, BM1 and BM2, for the processing and the release of the PME domain from the pro-region. BM1 and BM2 showed the consensus RRLL and RKLL, respectively (Tab. 1).

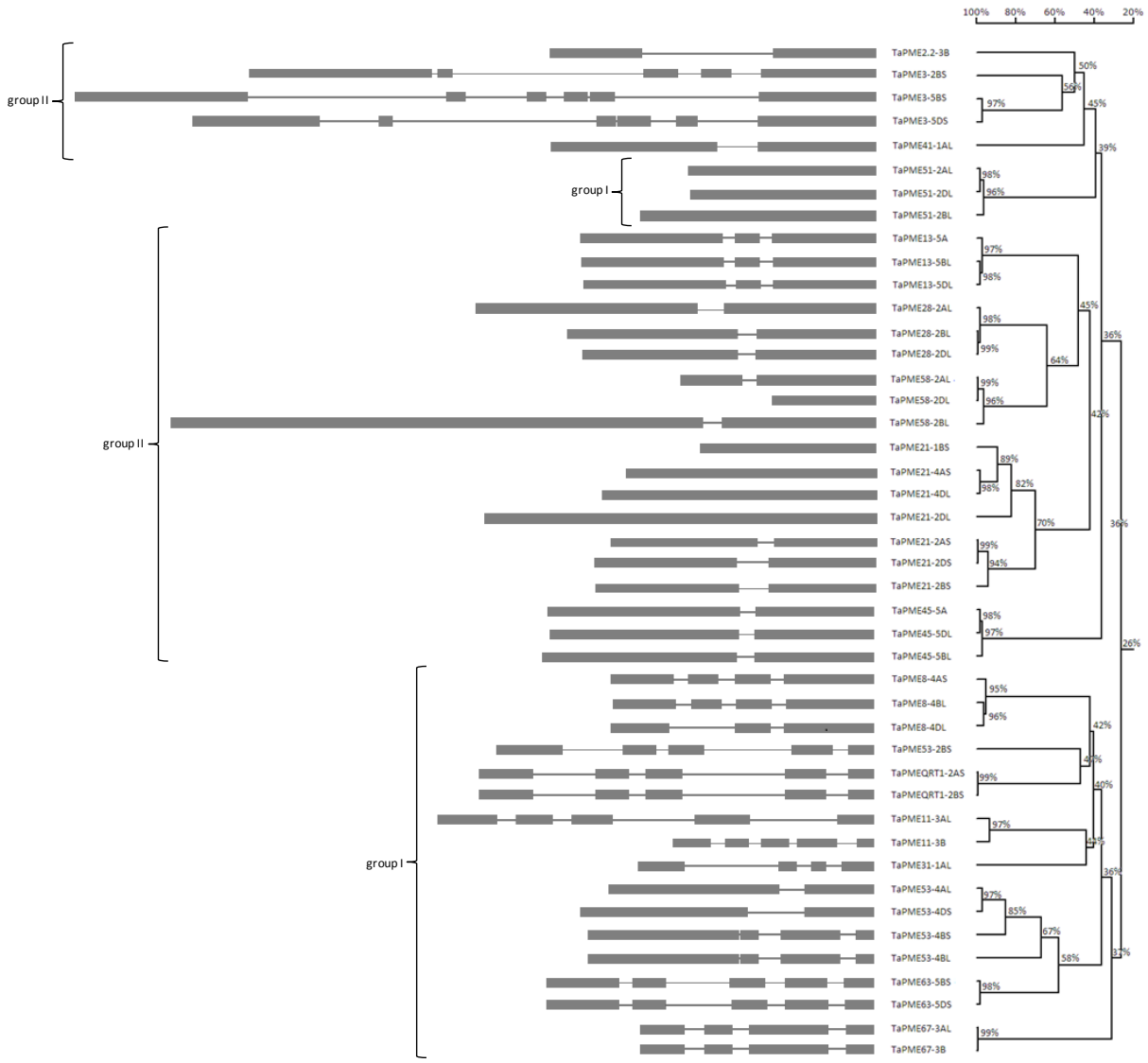

Figure 1. Dendrogram (right) showing the amino acid sequence identity (%) between the wheat PME proteins. The exon-intron structure (left) was obtained using both GENSCAN and GSDS tools. The distinction between PMEs of group I or group II is also indicated.

Table 1. Main features of TaPME protein.

TaPME	Group	Mature protein			Subcellular localization						Binding motifs for cleveage	Conserved motifs	
		Protein (aa)	PMEI (aa)	PME (aa)	sp	tm	PSort	Plant mPLoc	BM1	BM2	Position BM1-BM2	PMEI cys	PME
TaPME8-4AS	I	420		327	-	+	pl, pe	cw					5
TaPME8-4BL	I	417		324	-	+	pl, er, pe, g	cw					5
TaPME8-4DL	I	354		260	-	+	ex, pe	pl, cw					4
TaPME11-3AL	I	339		291	+	+	ex, pe	cw					3
TaPME11-3B	I	335		257	+	+	ex, pe	cw					3
TaPME31-1AL	I	214		212	-	-	pe, cy, ch	cw					5
TaPME51-2AL	I	461		311	+	+	ex, pe	cw					4
TaPME51-2BL	I	461		311	+	+	ex, pe	cw					5
TaPME51-2DL	I	447		303	+	+	ex, pe	cw					5
TaPME53-2BS	I	388		343	+	+	er, pe, pl	cw					5
TaPME53-4AL	I	464		303	+	+	ex, v, pe	cw					5
TaPME53-4BS	I	476		298	+	-	ex, pe	cw					4
TaPME53-4BL	I	476		298	+	-	ex, v	cw					4
TaPME53-4DS	I	462		303	+	-	ex, v, pe	cw					5
TaPME63-5BS	I	413		309	+	+	ex, pe	cw					5
TaPME63-5DS	I	413		309	+	+	ex, pe	cw					5
TaPME67-3AL	I	368		344	+	-	ex, pe	cw					2
TaPME67-3B	I	343		318	+	-	ex, pe	cw					3
TaPMEQRT1-2AS	I	389		361	+	+	ex, pe	cw					5
TaPMEQRT1-2BS	I	364		335	+	+	ex, pe	cw					5
TaPME2.2-3B	II	442	51	298	-	-	n, pe	cw	RDVL	RALL	98-118	1	5
TaPME3-2BS	II	731	151	477	+	+	ex, n, pe	cw		RRLL	261	5	5
TaPME3-5BS	II	734	152	461	+	+	ex, n	cw		RRLL	246	6	5
TaPME3-5DS	II	643	109	464	-	-	cy, pe, m	cw		RRLL	153	3	5
TaPME13-5A§,$	II	608	146	296	-	+	pl, ch, g, pe	cw	RRLL	RRVL	247-279	5	5
TaPME13-5BL	II	608	146	296	-	+	pl, ch, g, pe	cw	RRLL	RRVL	247-279	5	5
TaPME13-5DL	II	608	145	296	-	+	pl, ch,	cw	RRLL	RRVL	247-279	5	5

							g, pe						
TaPME21-1BS	II	449	81	267	-	-	cy, pe	cw	RRLL	RRLL	95-112	1	5
TaPME21-2AS	II	562	152	298	+	+	pl, er, g	cw	RRLL	RRLL	208-226	4	5
TaPME21-2BS	II	560	152	298	+	+	pl, er, g	cw	RRLL	RRLL	206-224	4	5
TaPME21-2DL$	II	560	145	298	+	+	pl, er, g	cw		RRLL	224	4	5
TaPME21-2DS	II	561	152	298	+	+	pl, er, g	cw	RRLL	RRLL	207-225	4	5
TaPME21-4AS	II	567	150	300	+	+	pl, er, g	cw	RRLL	RRLL	210-227	4	5
TaPME21-4DL	II	588	150	319	+	+	pl, er, g, pe	cw	RRLL	RRLL	210-227	4	5
TaPME28-2AL	II	563	148	296	+	+	ex, v, pe, n	cw	RRLL	RKLL	220-239	4	5
TaPME28-2BL$	II	563	148	296	+	+	ex, v, pe, n	cw	RRLL	RKLL	220-239	4	5
TaPME28-2DL	II	563	150	296	+	+	ex, v, pe, n	cw	RRLL	RKLL	220-239	4	5
TaPME41-1AL	II	556	106	297	+	-	ex	cw		RRMAL	224	3	5
TaPME45-5A§	II	606	152	296	-	+	pl, ch, g, er	cw		RRIL	277	5	4
TaPME45-5BL	II	609	150	290	-	+	pl, ch, g, er	cw		RRIL	280	5	5
TaPME45-5DL	II	601	153	295	-	+	pl, ch, g, er	cw		RRIL	272	5	5
TaPME58-2AL*	II	nd	nd	nd	nd	nd	n	cw	RRKL	RRLL	nd	nd	5
TaPME58-2BL	II	1077	141	297	-	+	ex	cw	RRKL	RRLL	734-752	4	5
TaPME58-2DL*	II	nd	nd	nd	nd		pe, cy	cw	nd	nd	nd	nd	3

SP: Signal peptide. **TM:** Transmembrane domain. **Subcellular localization:** ch: chloroplast; cw: cell wall; cy: cytosol; er: endoplasmic reticulum; ex: extracellular/cell wall; g: Golgi apparatus; m: mitochondria; n: nuclear; pl: plasma membrane; v: vacuolar membrane; pe: peroxisome. **BM1-BM2:** binding motif 1-binding motif 2 (RRLL-RKLL) for the pro-region removal and for releasing of the active protein. **PMEI:cys:** number of the conserved cysteins found in the PMEI domain. **PME:** number of the conserved motifs (GxYxE, QAVAL, QDTL, DFIFG, LGRPW) found in the PME domain. * indicates partial TaPME sequences. § indicates *TaPME* genes sequenced in this work. $, indicates *TaPME* genes whose intron-exon distribution was confirmed experimentally in this work.

Amino acid sequence identity showed that the TaPME family clustered in two main groups, one containing only PMEs of group I and the other is composed of all PMEs of group II plus the homoeologous genes of *TaPME51* belonging to group I (Fig. 1). Analysis of the sub-clusters clearly highlighted that the *PME* gene family underwent rearrangement into the hexaploid wheat genome. Indeed, except *TaPME13*, *TaPME21-2*, *TaPME28*, *TaPME45*, *TaPME51* and *TaPME58* having each homoeologous gene on corresponding chromosomal arm on the A, B and D genomes, all the other homoeologous genes of the family showed only a partial conservation of their chromosomal localization (Fig. 1). This resulted in the spreading of all *PME* sequences over the wheat genome except on homoeologous group 6 and 7 chromosomes.

3.2 *PME* genes are differentially expressed in wheat tissues

In order to verify the expression level of the *TaPME* genes, we performed in silico searches of Expressed Sequence Tags (ESTs) at NCBI database. Only a limited number of ESTs corresponding to some *PME* genes were present and most of them were from the spike (Tab. S2). To obtain a more complete representation of *PME* gene expression, we performed a real-time quantitative retro-transcription PCR (qRT-PCR) on different tissues of the bread wheat cv. Bobwhite.

To simplify the qRT-PCR analysis, we developed primers pairs at conserved positions of *TaPME* genes sharing a nucleotide sequence identity higher than 95% in the coding region. In total, we developed 14 different primer pairs each amplifying a group of genes typically corresponding to the homoeologous genes (Tab. S1). We analysed the expression level in seedling roots, second leaf fully expanded, flag leaf and flowering spikes (Fig. 2). For each *PME* gene we identified the tissue where it was less expressed (i.e. higher Ct value) and we compared to it the expression level in the other tissues. In seedling roots all *PME* genes were expressed except *TaPME58* and *TaPME63*. The lowest expression level in seedling roots was found for *TaPME3*, *TaPME13*, *TaPME21-2*, *TaPME21-1/2/4*, *TaPME51*, *TaPME53* and *TaPMEQRT1*, whereas the remaining *PME* genes showed between 2 and 25 fold higher expression (Fig. 2). In the second leaf and in the flag leaf all genes were expressed except *TaPME21*, *TaPME45*, *TaPME53* and *TaPME58*. In the second leaf, *TaPME8* and *TaPME11* showed the lowest level of expression, whereas the other *PMEs* were between 5 and 30 fold more expressed. In the flag leaf, *TaPME8*, *TaPME13*, *TaPME28*, *TaPME58*, *TaPME63* and *TaPME67* showed the lowest level of expression, whereas *TaPME3*, *TaPME11* and *TaPME51* were 35, 5

and 25 fold more expressed, respectively (Fig. 2). Finally, in the flowering spike all *PMEs* were expressed, showing values between 7 (*TaPME11*) and about 3300 (*TaPME53*) fold higher than *TaPME45* and *TaPMEQRT1* (Fig. 2).

All together these results indicate a variable pattern of expression of *TaPME* genes in different tissues with all genes expressed in the spike tissue at flowering time.

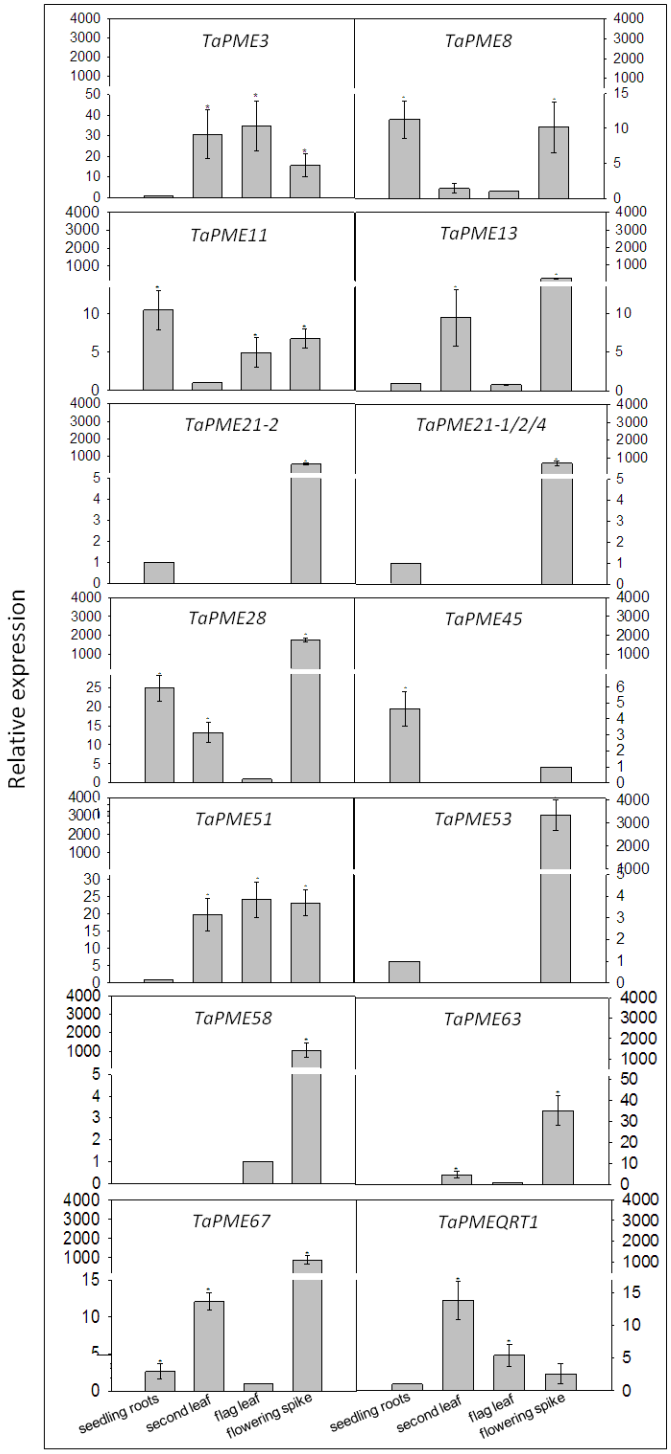

Figure 2. qRT-PCR in four different tissues of bread wheat cv. Bobwhite: seedling roots (Zadoks Z7), second leaf fully expanded (Zadoks Z13), flag leaf (Zadoks Z47) and flowering spike (Zadoks Z68). The relative expression for each *PME* gene was calculated taking as reference sample the tissue showing the lowest level of expression (higher Ct value). Bars indicated the standard deviation; *p< 0,05.

3.3 The susceptible cv. Bobwhite showed a slightly higher expression of *TaPMEs* as compared to the resistant cv. Sumai3 in flowering spikes

To reveal the possible role of *PMEs* in wheat-*F. graminearum* interaction, the temporal changes in *PME* gene expression was monitored in the bread wheat cultivars Bobwhite and Sumai3 that show a susceptible or tolerant response to *F. graminearum* infection, respectively.

Before analysing the temporal changes following pathogen infection, we verified the basal expression profiles of *TaPME* genes in flowering spikes of cv. Sumai3 and compared them to those of cv. Bobwhite. The two cultivars showed a comparable overall expression profile, although gene expression was slightly higher in most genes of cv. Bobwhite, especially the genes *TaPME53*, *TaPME63* and *TaPME67* (Fig. 3).

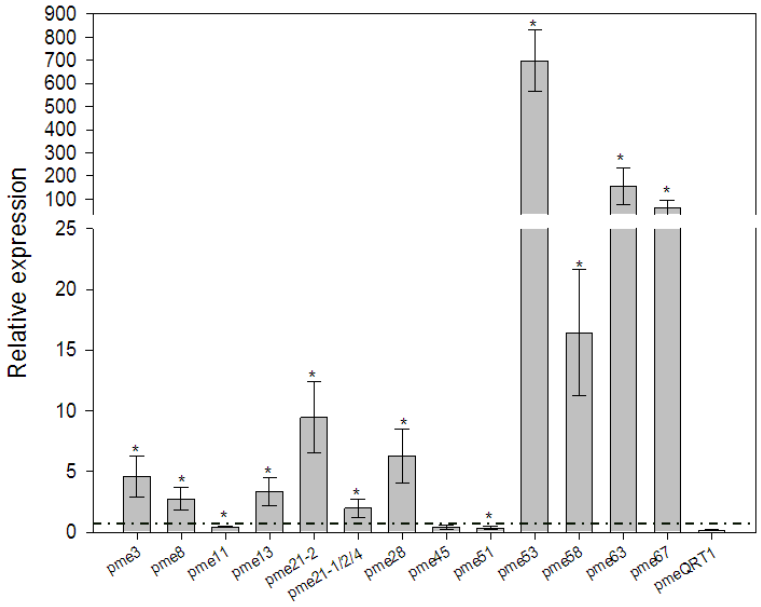

Figure 3. qRT-PCR showing the basal level of *PME* expression in cv. Bobwhite compared to cv. Sumai3. The relative expression were calculated by using cv. Sumai3 as reference sample, indicated in the graph with a dotted line. Bars indicated the standard deviation; *p< 0,05.

3.4 The opening of florets during point-inoculation of *F. graminearum* conidia causes changes in *TaPME* expression

To analyse *PME* expression during fungal progression within the spike, we infected the two central opposite spikelets by using the point inoculation method. We preferred this method of infection over the spray infection method because this method ensured the same amount of inoculum at the same inoculation site between the compared genotypes.

However, since this method requires the opening of florets to inoculate conidia, we verified the effect of this operation on the expression of *TaPME* genes.

We first verified if during the 48 hours after flowering the expression of *PMEs* varied. To this end we compared the expression of untreated spikes at anthesis (time T0) and 48 hours post anthesis (hpa). We performed this analysis by analysing the *PME* genes *TaPME3*, *TaPME13*, *TaPME21-2*, *TaPME21-1/2/4*, *TaPME28*, *TaPME58* and *TaPME63* and we did not find any significant difference in their expression (Fig. S4).

Subsequently, we compared the expression of *TaPME* genes between untreated spikes at anthesis (time T0) and spikes subjected to floret opening and inoculated with water (mock-inoculated) at 24 and 48 hpi (Fig. 4). As shown in figure 4, most of the genes underwent down-regulation in both cultivars Bobwhite and Sumai3, although *TaPME3* and *TaPME8* were clearly induced in cv. Bobwhite (Fig. 4). Also *PR1.1* was induced in both cultivars Bobwhite and Sumai3 (Fig. 4).

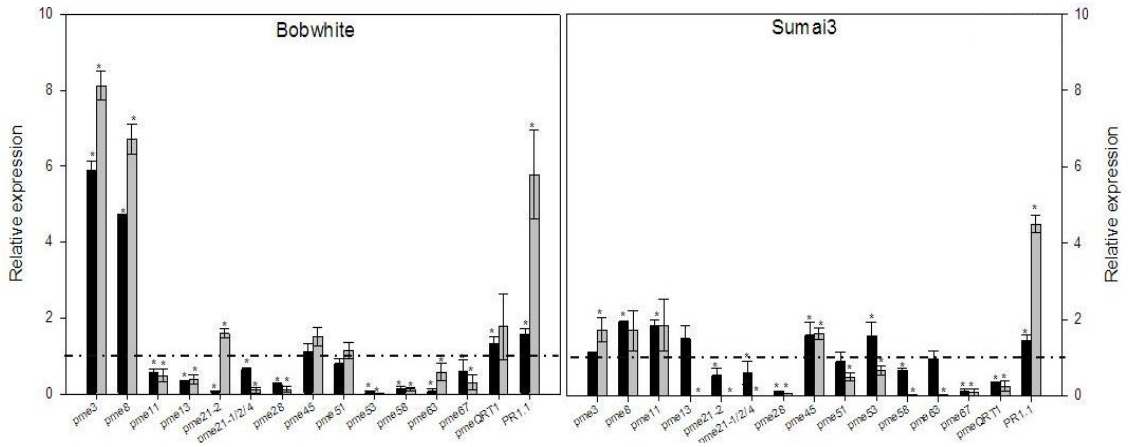

Figure 4. qRT-PCR showing *PME* genes expression in cv. Bobwhite and cv. Sumai3 following floret opening for inoculation. Relative expression in the opened florets inoculated with water (mock-inoculated) was calculated at 24 hpi (black histograms) and 48 hpi (grey histograms) taking as reference sample the untreated plants (florets not subjected to opening, time T0, indicated as dotted lines in the graphs). Bars indicated the standard deviation; *p< 0,05.

3.5 Expression of *TaPME* genes differs in susceptible and resistance plants following *F. graminearum* infection

Comparison of gene expression following *F. graminearum* infection was performed on RNA extracted from spikes of the susceptible cv. Bobwhite and the resistant cv. Sumai3 point-inoculated at anthesis with *F. graminearum* conidia. Samples were analysed at 24 and 48 hpi and included the two opposite central spikelets of a spike, that are those typically inoculated in the point-inoculation method. Mock-inoculated central spikelets at the same time point were used as control.

Pathogen infection caused a marked variation of the expression pattern of *TaPME* genes in both cultivars. Comparison between the expression pattern of cv. Bobwhite and cv. Sumai3 showed a general higher induction of *PME* genes in cv. Bobwhite. In particular, some genes were induced in cv. Bobwhite and repressed in cv. Sumai3. For example, *TaPME21* and *TaPME63* showed 8 and 5 fold induction at 48 hpi as compared to mock-inoculated samples in cv. Bobwhite, whereas the same genes at the same time showed about 0.4 and 0.2 fold down regulation in cv. Sumai3 as compared to mock-inoculated samples (Fig. 5).

In these analyses we included also the *PR1.1* gene as marker of gene induction following *F. graminearum* infection (Moscetti et al., 2013). As expected this gene is already induced at 24 hpi and increased strongly at 48 hpi (Fig. 5).

Taken all together these results indicate that during host infection *TaPME* genes undergo a differential regulation both in the susceptible and resistant genotypes. Moreover, the contribution of specific *TaPME* genes, e.g. *TaPME21-2*, *TaPME21-1/2/4*, *TaPME58*, *TaPME63* and *TaPME67*, can be different in susceptible and resistant genotypes.

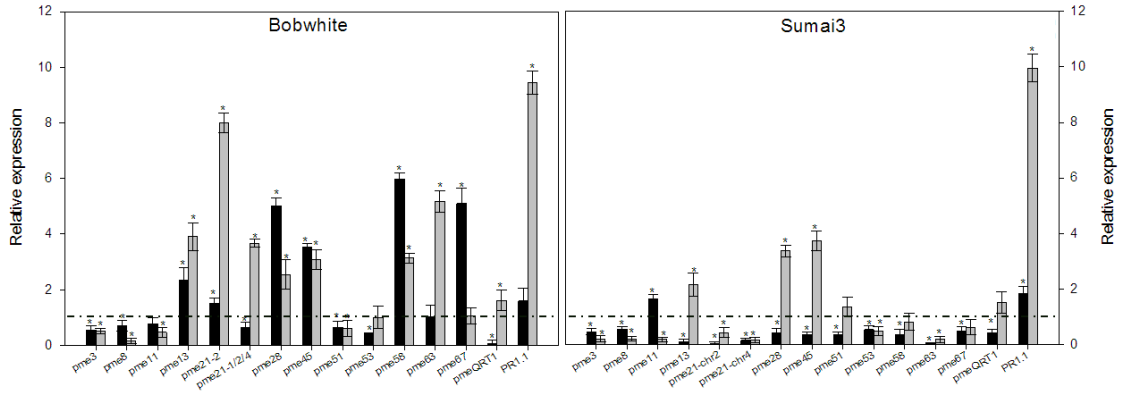

Figure 5. qRT-PCR showing *PME* genes expression in cv. Bobwhite and cv. Sumai3 following *F. graminearum* infection. Relative expression in the infected spikelets after 24 hpi (black histograms) and 48 hpi (grey histogram) was calculated taking as reference sample the mock-inoculated plants at the same time point (indicated as dotted lines in the graphs). Bars indicated the standard deviation; *p< 0,05.

3.6 Some *TaPME* genes respond promptly to fungal progression

To study the expression of *TaPME* genes during fungal progression, we analysed the two opposite spikelets just below and above the central inoculated spikelets. Comparison was made between the upper or lower spikelets of plants infected or mock-inoculated in the central spikelets. This analysis involved the *PME* genes that in the

central inoculated spikelets showed induction in cv. Bobwhite and repression or a delayed induction in cv. Sumai3 (Fig. 5). Results of these experiments showed that in the upper spikelets of cv. Bobwhite *TaPME13*, *TaPME21-2*, *TaPME21-1/2/4*, *TaPME58* and *TaPME63* were induced at 48 hpi, whereas the expression of the other *PME* genes were not significantly different from the mock-inoculated samples (Fig. 6a). In cv. Sumai3 none of the *PMEs* underwent a strong induction, however, *TaPME21-1/2/4*, *TaPME63* and *TaPME67* were slightly, although significantly, induced (Fig. 6b). In the lower spikelets of cv. Bobwhite all *PMEs* tested were significantly repressed, except *TaPME13* that showed a similar expression of the mock-inoculated sample (Fig. 6c). Similarly, the expression of all *PMEs* in cv. Sumai3 was significantly reduced (Fig. 6d).

Like to what observed in the central spikelets, *PR1.1* was induced both in the upper and lower spikelets with the induction level much higher in cv. Bobwhite compared to Sumai3 (Fig. 6).

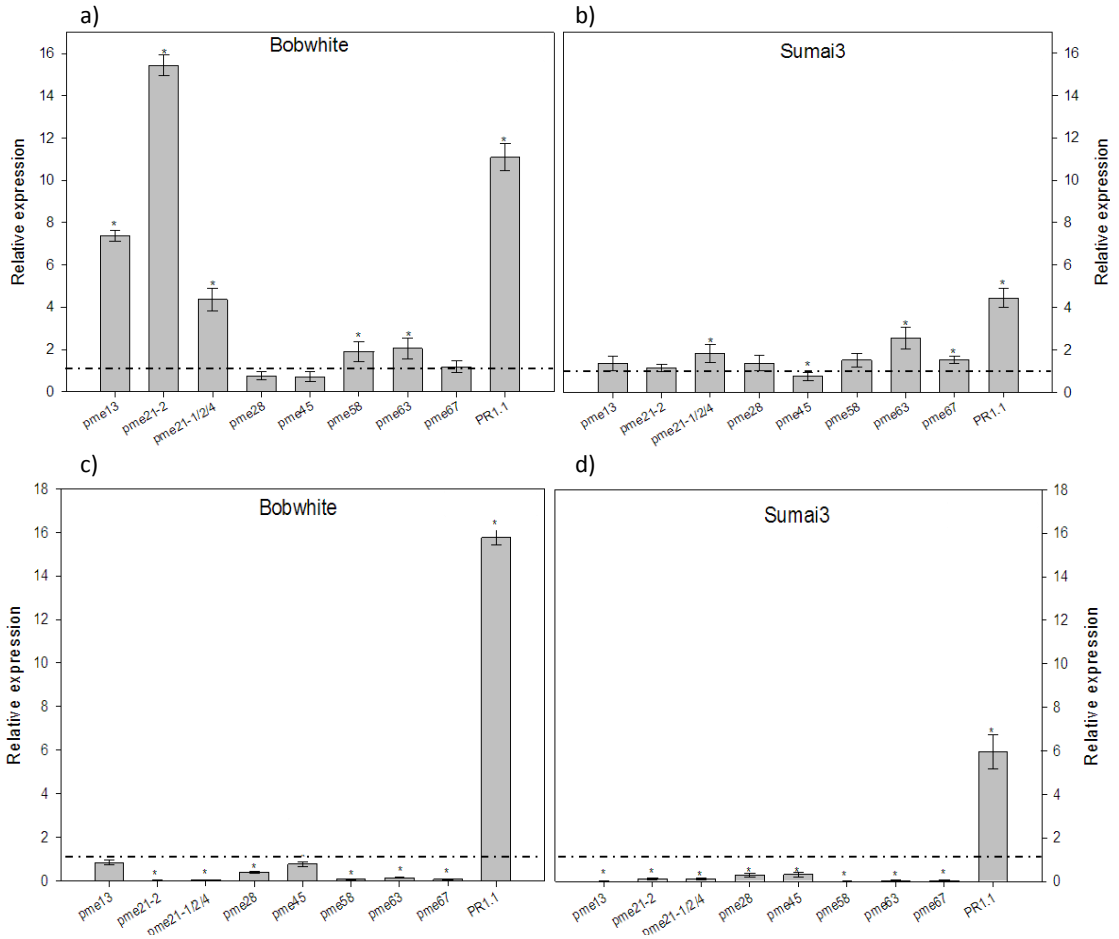

Figure 6. qRT-PCR showing *PME* genes expression in the upper and lower spikelets of cv. Bobwhite (a, c) and in the upper and lower spikelets of cv. Sumai3 (b, d) 48 hpi following *F. graminearum* infection performed in the central spikelets. Relative expression was calculated taking as reference sample the mock-inoculated plants at the same time point (indicated as dotted lines in the graphs). Bars indicated the standard deviation; *p< 0,05.

3.7 Progression of *F. graminearum* from the point-inoculated central spikelets

To correlate the expression of *TaPME* genes with fungal progression, we verified the presence of the fungal pathogen in spikelets at 48 hpi. Fungal biomass, quantified by qPCR of the *TRI6* gene (Horevaj et al., 2011), was present in the central inoculated spikelets and in the upper spikelets, whereas was absent in the lower spikelets. The central inoculated spikelets of both cultivars showed the larger amount of fungal biomass compared to the upper spikelets. In these spikelets Sumai3 contained an higher amount of fungal biomass as compared to cv. Bobwhite. Conversely, in the upper spikelets the fungal biomass of cv. Bobwhite was much higher (about 24 fold) as compared to that present in Sumai3 (Fig. 7).

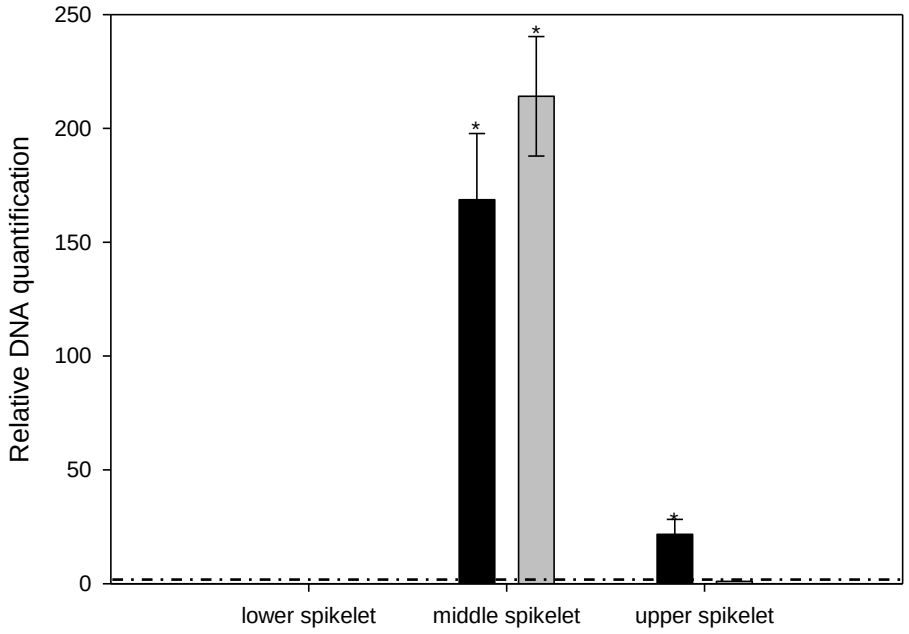

Figure 7. *F. graminearum* biomass quantification by using *TRI6* gene amplification in cv. Bobwhite (black histograms) and cv. Sumai3 (grey histograms). Relative DNA quantification was calculated taking the value of the upper spikelet of Sumai3 as reference sample (dotted line), being this the lowest value detected. Bars indicated the standard deviation; *p< 0,05.

4. Discussion

We showed that the PME family in wheat is rather large, similarly to those in other plant species (Wang et al., 2013). We identified 44 different *TaPME* genes some of which were present as triplicated homoeologous genes sharing a very high sequence identity (up to 99%). Like in other species, i.e. *Arabidopsis* and *Brachypodium*, the members of the *TaPME* family are dispersed throughout the genome and most of them contain introns. The putative encoded products of these genes retain the typical structural features of the PMEs, including the signal peptide, the transmembrane domain, the four cysteines in the PMEI domain and the conserved residues in the PME domain. However, sequence comparison between *TaPME* genes showed variation for all these features and highlighted the particular short size of the PME domain of TaPME2.2-3B and TaPME21-1BS, being of only 50 and 80 residues, respectively.

The expression profile of each *TaPME* gene vary considerably in the different tissues and some of them are not expressed in roots and leaves. However, all *TaPME* genes showed relatively high expression in flowering spikes, that is in agreement with the importance of *PMEs* in flower development (Wolf et al., 2009)

The large number of genes composing the PME families in the different plant species is probably related to the several physiological processes where this class of enzymes are involved (Pelloux et al., 2007).

Concerning the role of PMEs in plant defense, several observations indicate that they may contribute in different host-pathogen interactions (Pelloux et al., 2007; Lionetti et al., 2012). Indeed, several evidences indicate that a high degree of pectin methylesterification, that imply low PME activity, is related to increased host resistance. This outcome has been mostly associated with the reduced capacity of the polygalacturonases (PG) secreted by the pathogens to degrade the methylated pectin of the cell wall during the invasion of the host tissue. This possibility has been also suggested to explain the improved resistance of transgenic wheat plants expressing the pectin methyl esterase inhibitor AcPMEI against the fungal pathogen *Bipolaris sorokiniana*, *F. graminearum* and *Claviceps purpurea* (Volpi et al., 2011; 2013). Moreover, it has been also reported that wheat resistance can be related to the distribution of methyl ester rather than to the degree of pectin methylesterification (Wiethölter et al., 2003). This result can be related to the substrate specificities of the pathogen enzymes. For example, a blockwise distribution of pectin methylesterification is more favorable than a random one for the activity of a PG from *F. moniliforme* (Bonnin et al., 2002).

In such contest, plant PMEs that contribute to reduce or modify the pattern of pectin methyl esterification during host-pathogen interaction can be regarded as susceptibility factors, since they favor the PG activity of the pathogen and the consequent host tissue colonization. An example in this direction is represented by the *PME3* gene of *Arabidopsis*. This gene is induced following *Pectobacterium carotovorum* or *Botrytis cinerea* infection and the *pme3* mutant plants have an higher level of pectin methylesterification and are more resistant to both pathogens compared to the wild type plants (Raiola et al., 2011).

On the other end, PMEs can contribute to plant resistance. A recent report demonstrated that the increased susceptibility of some *Arabidopsis pme* mutants (e.g. *ppme1*, *pme17*, *pme31*, *pme39*, and *pme44*) to *Pseudomonas syringae* pv. *maculicola* ES4326 (*Pma* ES4326) was related to the lack of expression of these genes (Bethke et al., 2014). Similarly, an improved resistance response against *B. cinerea* have been obtained by over-expressing the fruit-specific *PME* gene, *FaPE1*, in wild strawberry (Osorio et al., 2008). This result has been explained with the capacity of the transgenic plants to release oligogalacturonides (OGA) with reduced esterification capable to induce defense responses (Osorio et al., 2008).

To complicate further the role of PME and pectin methylesterification in plant defense is the observation that the contribution of PME in plant defense can vary between plant pathosystems. For example, the same *Arabidopsis pme* mutants contributing to immunity against *Pma* ES4326 showed the same response of wild type plants against the fungal pathogen *Alternaria brassicicola* (Bethke et al., 2014).

Although intricate, all these results indicate the importance of the activity of specific PMEs rather than the total PME activity.

In our attempt to identify putative *TaPME* genes involved in wheat defense, we revealed a strong variation in the expression of the *TaPME* following *F. graminearum* infection. Interestingly, none of them remained unaffected by pathogen challenge but showed a contrasting response of induction or down-regulation. This contrasting expression variation between *PME* genes have been also reported in microarray analysis of *Arabidopsis PME* following pathogen infections (Lionetti et al., 2012). In our analysis, we showed also that the expression profile following *F. graminearum* infection was markedly different between the susceptible and resistant cultivars. The cv. Bobwhite showed a larger number of induced *PME* genes that showed also a stronger variation in the level of induction as compared to what observed in the resistant cv. Sumai3. Particularly interesting was the expression profile of the genes *TaPME21-2, TaPME21-*

1/2/4, *TaPME58*, *TaPME63* and *TaPME67* that was induced in the susceptible cv. Bobwhite and repressed in the resistant cv. Sumai3. A similar result have been recently reported by analysing the *WheatPME1* gene, corresponding to *TaPME21-2* reported in this work, in response to *F. graminearum* infection. This gene was induced in the susceptible *T. durum* cv. Saragolla and down-regulated in the resistant genotype 02-5B-318. Moreover, this gene have been also located in the same bin position of quantitative traits loci (QTLs) for FHB (Lionetti et al., 2015).

All these *PME* genes deserve a more in-depth analysis to clarify their contribution in the wheat-*F. graminearum* interaction.

The parallel expression analysis of *PME* genes in the upper and lower spikelets from the inoculation point revealed an acropetal movement of the pathogen in the first 48 hpi. This is in agreement with what reported in the interaction *B. distachyon-F. graminearum* (Pasquet et al., 2014).

The analysis of *PME* expression in the upper spikelets from the central inoculated spikelets revealed those genes that responded more promptly to the pathogen invasion. *TaPME13*, *TaPME21-2*, *TaPME21-1/2/4* were clearly induced in the upper spikelets of the susceptible cv. Bobwhite and their induction coincided with the presence of the pathogens, as revealed by the analysis of the *TRI6* gene. The limited presence of the pathogen in the upper spikelets of the resistant cv. Sumai3 affected poorly the expression profiles of its *PME* genes.

The parallel analysis of *PME* expression in the lower spikelets highlighted that modulation of *PME* expression by the pathogen occurred only when the pathogen colonized the host tissues. Indeed, the analysis of the *TRI6* gene proved the absence of the pathogen in the lower spikelets, whereas the analysis of *PME* expression showed a general down-regulation. Most probably this down-regulation of *PME* genes was the result of the stress signals following the manual opening of the central spikelets to perform the point inoculation. In fact, we have shown that the manual opening of the spikelets caused a general down-regulation of *PME* genes in both cvs. Bobwhite and Sumai3.

In conclusion, this study provides the first comprehensive analysis of the *PME* gene family in wheat. The structural analysis of these genes showed that wheat, like other plant species, contains a large PME family whose members are dispersed throughout the genome and retain the typical structural features of the PMEs. Moreover, the expression data highlighted the possible involvement of specific *TaPMEs* in wheat defense against pathogens.

Author contributions

A. Zega: performed the experiments, analyzed the data and wrote the first draft of the paper. R. D'Ovidio: conceived the project, performed the critical revision of the data and wrote the final version of the paper.

Acknowledgments

Research supported by the Italian Ministry of University and Research (PRIN 2010–2011, Grant Number 2010T7247Z_002) to R. D'Ovidio. We would like to thank the International Wheat Genome Sequencing Consortium for the access to the sequence data.

5. Supplementary material

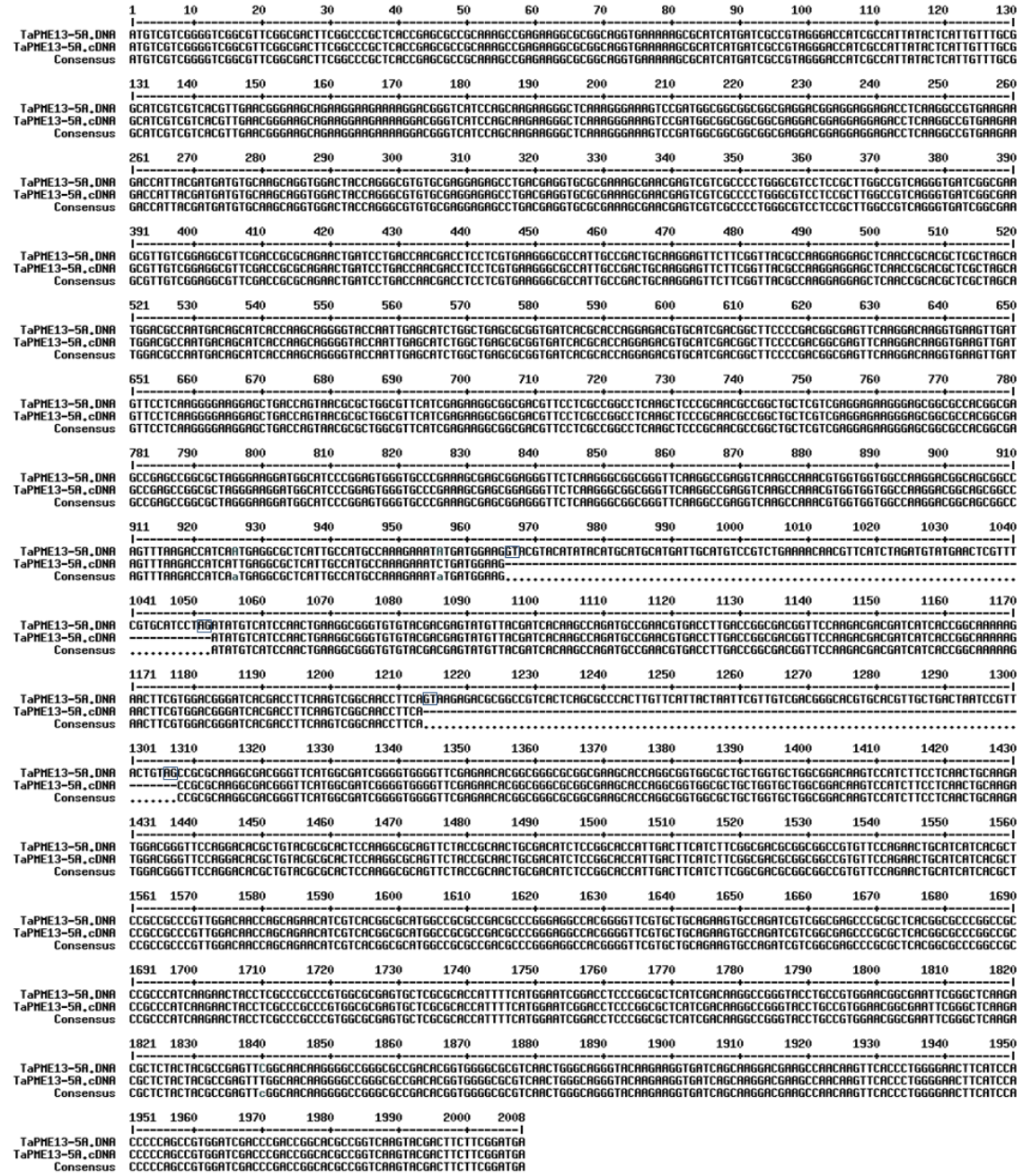

Figure S1. Multiple alignment of the *TaPME13-5A* genomic sequence from the nulli-tetrasomic lines of cv. Chinese Spring and the *TaPME13-5A* coding sequence from Sumai3 cDNA isolated from a flowering spike. The acceptor and donor splicing sites of introns are highlighted in a grey box and single nucleotide polymorphisms (SNPs) between the two sequences are indicated as black/grey letters.

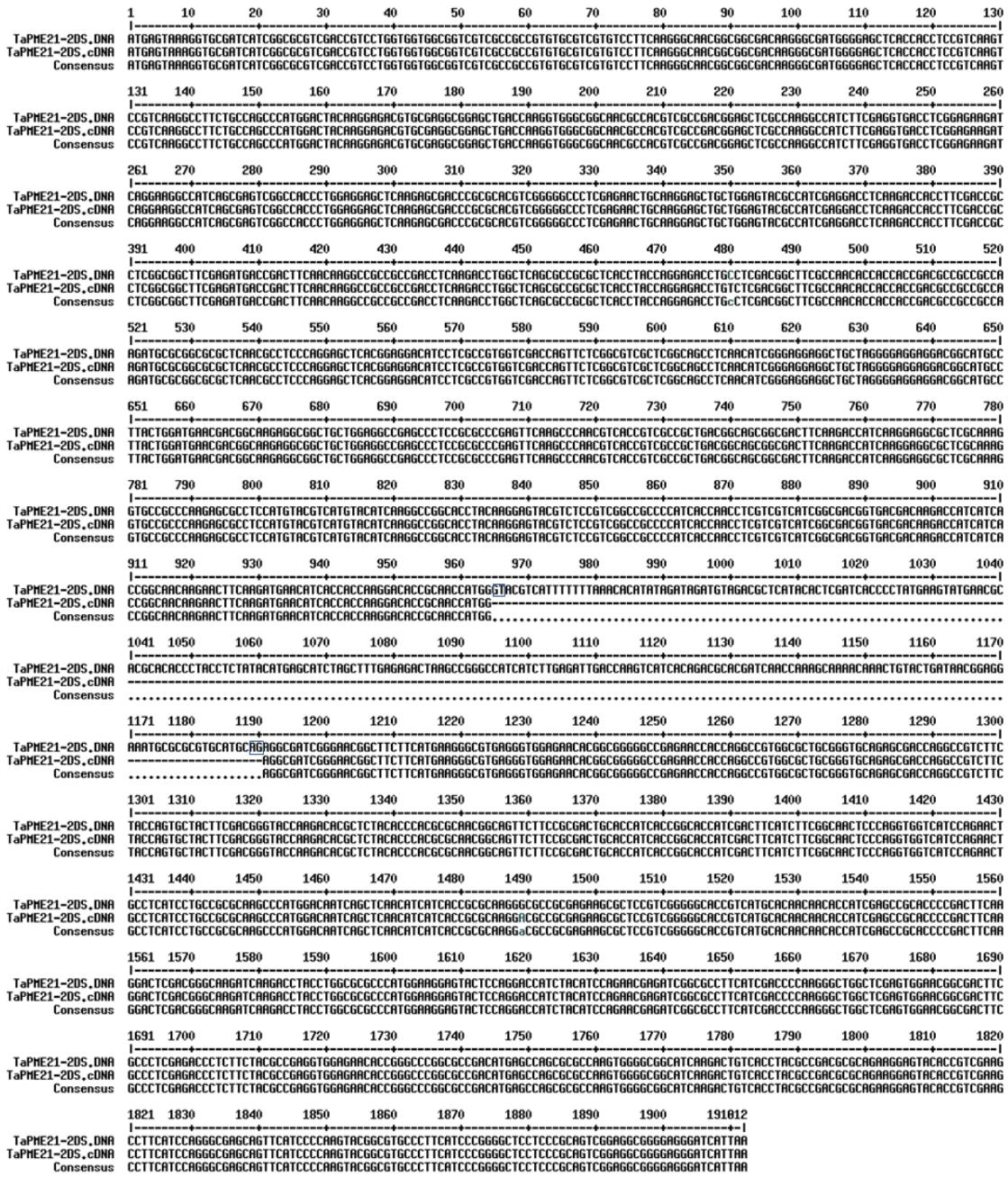

Figure S2. Multiple alignment of the *TaPME21-2DS* genomic sequence retrieved from the IWGSC database and the *TaPME21-2DS* coding sequence from Sumai3 cDNA isolated from a flowering spike. The acceptor and donor splicing sites of the single intron are highlighted in a grey box and SNPs between the two sequences are indicated as black/grey letters.

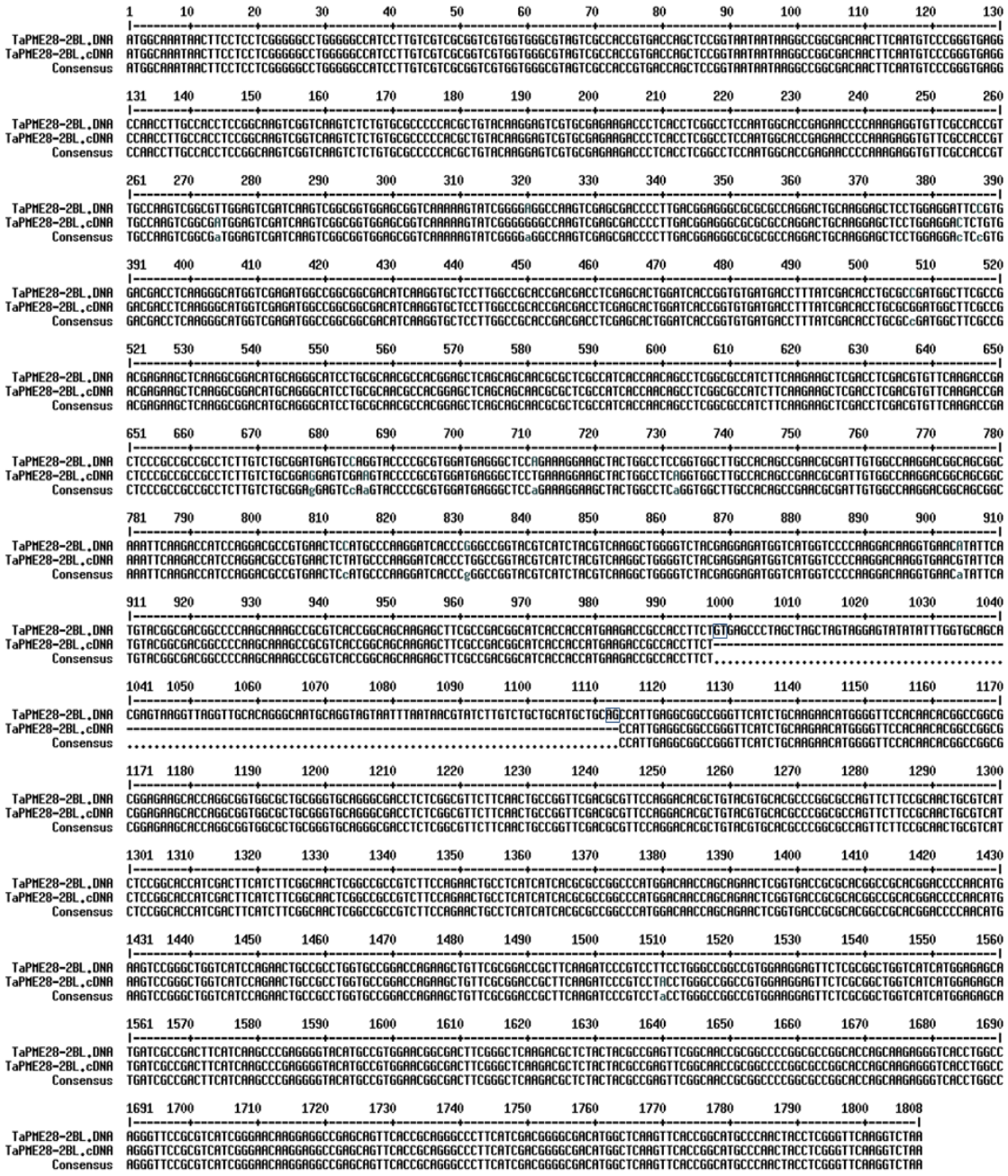

Figure S3. Multiple alignment of the *TaPME28-2BL* genomic sequence retrieved from the IWGSC database and the *TaPME28-2BL* coding sequence from Sumai3 cDNA isolated from a flowering spike. The acceptor and donor splicing sites of the single intron are highlighted in a grey box and SNPs between the two sequences are indicated as black/grey letters.

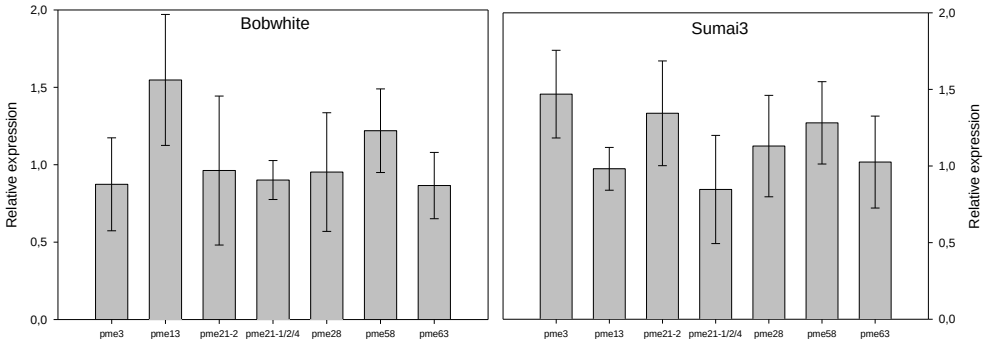

Figure S4. qRT-PCR showing *PME* genes expression in cv. Bobwhite (left graph) and cv. Sumai3 (right graph) 48 hours after flowering. Relative expression was calculated taking as reference sample the untreated plants at the anthesis (time T0). Bars indicated the standard deviation.

Table S1.
Primer pairs used for the real-time qRT-PCR and amplicons length reported as the number of base pair (bp) amplified.

Gene	Primers	Amplicon length (bp)
TaPME3	FP 5'-CAGCAACTTCCTGGCCCGCGA-3' RP 5'-ACGACGCTGTCGAGCTCCGA-3'	453
TaPME8	FP 5'-TACCTGCTGCATTTCTGCTCTTC3' RP 5'-GATCCACACAACGTTCCTCTTTT-3'	314
TaPME11	FP 5'-AAATGCCACCTGCACTCCACCT-3' RP 5'-CCTCTGGTTGGCGGTGTGGTT-3'	243
TaPME13	FP 5'-ATGTGCAAGCAGGTGGACTACCA-3' RP 5'-ACAACTTCACCTTGTCCTTGAACT-3'	376
TaPME21-2	FP 5'-CGCTCAACGCCTCCCAGGAGCT-3' RP 5'-CGGAGACGTACTCCTTGTAG-3'	318
TaPME21-1/2/4	FP 5'-GCCATGGACGACCTCAAGACG-3' RP 5'-ACCGTCATGTCCGGCTTGAAG3'	302
TaPME28	FP 5'-TCAAGGTGCTCCTTGGCCGC-3' RP 5'-GGCCACAATCGCGTTCGGC-3'	334
TaPME45	FP 5'-CAACCAGGTCGACCACCC-3' RP 5'-CTTGATCTGGACGCGGAC-3'	321
TaPME51	FP 5'-GCCGAATTACACTGCCGGGCA -3' RP 5'-TGCGAGCATACAAGGTGTCCTG-3'	341
TaPME53	FP 5'-TCAACCAGGCGTTGTACGCGAA -3' RP 5'-GCGATGATGGCCGGGTTCTTG-3'	283
TaPME58	FP 5'-CTGCTCCTCCACGCTGTACC-3' RP 5'-GCGCAGGTGTAGATATAGGTCATG-3'	327
TaPME63	FP 5'-GCCTTCTACAACTGCACCATT-3' RP 5'-TGTCTGTGAAGGAGTAGACC-3'	430
TaPME67	FP 5'-TGCCGAACAACCCGGAGATCCG -3' RP 5'-TTGCGGTCTTGCGCGGTGAT-3'	259
TaPMEQRT1	FP 5'-AGGGAGAAGGTGACGGTGCC-3' RP 5'-TCTCGAAGGTGATGTGGCTTGC-3'	189

FP: forward primer; **RP:** reverse primer

Table S2. ESTs corresponding to each specific *PME* gene identified in different wheat tissue as deposited in NCBI database. EST *PME* occurrence are indicated as transcripts number over the total number of transcript analyzed.

Gene EST/total EST in the pool														
	pme3	*pme8*	*pme11*	*pme13*	*pme21-2*	*pme21-1/2/4*	*pme28*	*pme45*	*pme51*	*pme53*	*pme58*	*pme63-5*	*pme67*	*pme QRT1*
callus	0/10876	0/1297	NOT FOUND	NOT FOUND	0/10876	NOT FOUND	0/10876	NOT FOUND	NOT FOUND	0/10876	0/10876	0/10876	NOT FOUND	NOT FOUND
cell culture	0/10416	0/16044			0/10416		0/10416			0/10416	0/10416	0/10416		
crown	0/13886	0/111881			0/13886		0/13886			0/13886	0/13886	0/13886		
flower	2/67783	0/7539			0/67783		0/67783			0/67783	0/67783	0/67783		
inflorescence	1/124432	0/16290			16/124432		16/124432			5/124432	4/124432	1/124432		
leaf	1/62433	0/25475			0/62433		0/62433			0/62433	0/62433	0/62433		
root	0/171181	0/32853			1/171181		1/171181			1/171181	0/171181	0/171181		
seed	3/168285	1/88540			0/168285		0/168285			0/168285	0/168285	0/168285		
sheath	0/1112	0/30839			0/1112		0/1112			0/1112	0/1112	0/1112		
stem	3/95178	0/65692			0/95178		0/95178			0/95178	0/95178	0/95178		

6. Figures and tables

Figure 1. Dendrogram (right) showing the amino acid sequence identity (%) between the wheat PME proteins. The exon-intron structure (left) was obtained using both GENSCAN and GSDS tools. The distinction between PMEs of group I or group II is also indicated.

Figure 2. qRT-PCR in four different tissues of bread wheat cv. Bobwhite: seedling roots (Zadoks Z7), second leaf fully expanded (Zadoks Z13), flag leaf (Zadoks Z47) and flowering spike (Zadoks Z68). The relative expression for each *PME* gene was calculated taking as reference sample the tissue showing the lowest level of expression (higher Ct value). Bars indicated the standard deviation; *p< 0,05.

Figure 3. qRT-PCR showing the basal level of *PME* expression in cv. Bobwhite compared to cv. Sumai3. The relative expression were calculated by using cv. Sumai3 as reference sample, indicated in the graph with a dotted line. Bars indicated the standard deviation; *p< 0,05.

Figure 4. qRT-PCR showing *PME* genes expression in cv. Bobwhite and cv. Sumai3 following floret opening for inoculation. Relative expression in the opened florets inoculated with water (mock-inoculated) was calculated at 24 hpi (black histograms) and 48 hpi (grey histograms) taking as reference sample the untreated plants (florets not subjected to opening, time T0, indicated as dotted lines in the graphs). Bars indicated the standard deviation; *p< 0,05.

Figure 5. qRT-PCR showing *PME* genes expression in cv. Bobwhite and cv. Sumai3 following *F. graminearum* infection. Relative expression in the infected spikelets after 24 hpi (black histograms) and 48 hpi (grey histogram) was calculated taking as reference sample the mock-inoculated plants at the same time point (indicated as dotted lines in the graphs). Bars indicated the standard deviation; *p< 0,05.

Figure 6. qRT-PCR showing *PME* genes expression in the upper and lower spikelets of cv. Bobwhite (a, c) and in the upper and lower spikelets of cv. Sumai3 (b, d) 48 hpi following *F. graminearum* infection performed in the central spikelets. Relative expression was calculated taking as reference sample the mock-inoculated plants at the same time point (indicated as dotted lines in the graphs). Bars indicated the standard deviation; *p< 0,05.

Figure 7. *F. graminearum* biomass quantification by using *TRI6* gene amplification in cv. Bobwhite (black histograms) and cv. Sumai3 (grey histograms). Relative DNA quantification was calculated taking the value of the upper spikelet of Sumai3 as reference sample (dotted line), being this the lowest value detected. Bars indicated the standard deviation; *p< 0,05.

Table 1. Main features of TaPME protein.

Figure S1. Multiple alignment of the *TaPME13-5A* genomic sequence from the nulli-tetrasomic lines of cv. Chinese Spring and the *TaPME13-5A* coding sequence from Sumai3 cDNA isolated from a flowering spike. The acceptor and donor splicing sites of introns are highlighted in a grey box and single nucleotide polymorphisms (SNPs) between the two sequences are indicated as black/grey letters.

Figure S2. Multiple alignment of the *TaPME21-2DS* genomic sequence retrieved from the IWGSC database and the *TaPME21-2DS* coding sequence from Sumai3 cDNA isolated from a flowering spike. The acceptor and donor splicing sites of the single intron are highlighted in a grey box and SNPs between the two sequences are indicated as black/grey letters.

Figure S3. Multiple alignment of the *TaPME28-2BL* genomic sequence retrieved from the IWGSC database and the *TaPME28-2BL* coding sequence from Sumai3 cDNA isolated from a flowering spike. The acceptor and donor splicing sites of the single intron are highlighted in a grey box and SNPs between the two sequences are indicated as black/grey letters.

Figure S4. qRT-PCR showing *PME* genes expression in cv. Bobwhite (left graph) and cv. Sumai3 (right graph) 48 hours after flowering. Relative expression was calculated taking as reference sample the untreated plants at the anthesis (time T0). Bars indicated the standard deviation.

Table S1. Primer pairs used for the real-time qRT-PCR and amplicons length reported as the number of base pair (bp) amplified.

Table S2. ESTs corresponding to each specific *PME* gene identified in different wheat tissue as deposited in NCBI database. EST *PME* occurrence are indicated as transcripts number over the total number of transcript analyzed.

CHAPTER II

Investigation of the role of *PMEs* in wheat-*F. graminearum* interaction by silencing specific *PME* genes

1. Introduction

The transgenic approach is used to further characterize or to discover gene functions. Among transgenic technologies, one of the method used is the RNA interference technique (RNAi). RNAi rapidly grown as a reverse genetic tool to knock-down the expression of genes, thanks also to the possibility to target multiple genes with a single RNAi transgene. This is particularly true for polyploid species as wheat, in which homoeologous genes could be silenced by a single RNAi construct (Fu et al., 2007). Although RNAi and other transgenic approaches are very useful techniques, the application of transgenic technology is not still completely accepted from the public. As an alternative, classical mutagenesis has been used since about 60 years in plant breeding and in particular the chemical mutagenesis provides an efficient tool to generate high density mutations in the genome of target plants. Moreover, classical mutagenesis allow also to target single homeologue genes in polyploid species as wheat (Parry et al., 2009). Targeting Induced Local Lesions IN Genomes (TILLING) strategy is a novel approach of reverse genetic that allow to produce mutated plants (McCallum et al., 2000). "Traditional" TILLING is time-consuming, expensive and sometimes is difficult to find the mutations of interest. A new TILLING procedure involves an *in silico* analysis, consisting in one single TILLING screening of a database bringing together mutated genotypes (Tsai et al., 2011). The database collects exonic-captured and sequenced sequences of a genome. Thanks to this new approach, researcher are able to BLAST their genes against the database, to find the mutations of interest and finally to acquire seeds of the mutated accessions. For example, Henry et al. (2014) performed an exome-capture and sequencing of mutagenised lines of rice, successfully identifying mutations with high confidence. The study was extended to tetraploid wheat, although the lack of a completely sequenced genome increased the difficulty to identify the mutations. However, the IWGSC has recently developed a chromosome-arm specific assembly of bread wheat cv. Chinese Spring in which a large proportion of protein-coding regions are represented. Jordan et al. (2015) used the exome-capture method in several wheat varieties and accessions followed by mapping to the IWGSC draft assembly to identify SNPs and insertion/deletion events.

Recent studies carried out with mutants or transgenic plants showed how pectin methylesterases are directly involved in plant defense, remodeling and controlling the methylesterification status of homogalacturonan. PME activities, the degree of homogalacturonan methylesterification and the molecular properties of

homogalacturonan, have been correlated with changes in resistance/susceptibility of plants to pathogens. For example, Bethke et al. (2014) studied the role of PMEs in *Arabidopsis* plants immunity and found that in single, double and triple *pme* mutants there was a significant increasing of *P. syringae* pv. *maculicola* growth respect to that observed in wild type plants. Thus, they correlated the increased susceptibility of mutants to the lack of expression of these genes, even if they did not found any difference in total PME activity. They explained this result with the possibility that contribution to immunity does not lie on total PME activity but in the activity of specific PMEs. In 2013, Ma et al. conducted an experiment of infection with *Fusarium oxysporum* in resistant and susceptible cultivar of banana. They found that the expression levels of one *PME* isoform, namely *MaPME1*, rapidly decreased in resistant plants and increased in susceptible plants. In parallel, they found a higher PME activity and a lower degree of methylesterification in susceptible plants compared to the resistant ones. Raiola et al. (2011) found that *Arabidopsis pme3* mutants are more resistant to pathogens because of the increased level of pectin methylesterification that impair pathogens growth. Osorio et al., (2008) over-expressed the fruit-specific *Fragaria* x *ananassa* pectin methylesterase *FaPE1* in the wild strawberry *Fragaria vesca*, modifying the pectin composition of the cultivated strawberry. They found in transgenic lines a more frequent de-esterification in blocks than in wild type plants, forming larger size of pectin with a lower level of methylesterification. An increased resistance against the fungal pathogen *B. cinerea* was found in transgenic lines compared to the wild type plants, probably because of the formation of specific oligogalacturonides able to elicit defense responses in transgenic strawberry plants.

On the basis of the results obtained in the characterization of the *PME* family in wheat and their expression behavior following *F. graminearum* infection, as reported in the first part of this work, we silenced three selected *TaPME* genes that were particularly induced following *F. graminearum* infection to verify their involvement in the wheat defence response. Moreover, we searched *pme* mutants by analyzing a durum wheat TILLING population and by analyzing *in silico* a TILLING population developed by the University of California, Davis.

2. Material and methods

2.1 RNAi constructs

The complete coding region of the genes we wanted to be silenced (*PME3*, *PME13*, *PME21* and *PME28*) was isolated from durum wheat cv. Svevo. The cDNA of Svevo flowering spike was amplified by using primer listed in Tab. 1 and with the following PCR conditions: 1 cycle at 95°C for 2 min; 30 cycles at 95°C for 45 sec, 60°C for 45 sec and 72°C for 2 min; a final step at 72°C for 5 min. Each PCR reaction was performed in a final volume of 25 µL, with 10 ng of cDNA, 2.5 U of FastStart High Fidelity PCR system (Roche Diagnostics), 1× Taq PCR buffer, 50 ng of each of the two primers, and 100 µM each deoxyribonucleotide.

In order to separate and to visualize PCR amplification products 1.2% agarose gel was prepared in 1x TBE (Tris, Boric Acid, EDTA) with 0.5 µg/mL ethidium bromide. DNA samples to load were prepared by adding an adequate volume of 6x loading dye (Fermentas, Milan, Italy) and as molecular weight markers GeneRuler 1 kb DNA Ladder (Fermentas) was used. Agarose gel running was performed at 70-75 V for 30-45 min and the amplified DNA was observed by an UV transilluminator. Then, the PCR amplification products were purified from the agarose gel by using the Wizard SV Gel and PCR Clean-Up System (Promega) and following the manufacturer's procedure. The DNA concentration was estimated by spectrophotometer.

The amplified and gel purified coding regions of *PME3*, *PME13*, *PME21* and *PME28* genes were used as template for the amplification of the sense and the antisense strands. During this amplification, the restriction sites used for the cloning in pAHC17 vector were added to sense and antisense strands (primer in Tab. 1): *Sal*I-*Bam*HI sites and *Cla*I site were added to the 5′ and to the 3′ of the sense strand, respectively; *Xho*I site and *Xba*I-*Bam*HI sites were added to the 5′ and to the 3′ of the antisense strand, respectively. Each PCR reaction was performed with 10 ng of the template, 2.5 U of FastStart High Fidelity PCR system, 1× Taq PCR buffer, 50 ng of each of the two primer, and 100 µM each deoxyribonucleotide. Amplification conditions were the following: 1 cycle at 94°C for 2 min; 30 cycles at 94°C for 40 sec, 60°C for 40 sec and 72°C for 30 sec; a final step at 72°C for 2 min.

Table 1. Primers used for the amplification of the complete coding region (CDS) of *PME3*, *PME13*, *PME21* and *PME28* genes and primers used for the sense and the antisense strands amplification for the RNAi constructs.

Gene	CDS (FP-RP)	SS (FP-RP)	AS (FP-RP)
PME3	FP 5′-ATGTCCGCCAACTGCTCC-3′ RP 5′-TCACAACCCGCCGGAGAAC-3′	FP 5′-AATAGTCGACGGATCCCAGCAACTTCCTGGCCCGCGA-3′ RP 5′-AATAATCGATACGACGCTGTCGAGCTCCGA-3′	FP 5′-AATATCTAGAGGATCCCAGCAACTTCCTGGCCCGCGA-3′ RP 5′-AATACTCGAGACGACGCTGTCGAGCTCCGA-3′
PME13	FP 5′-ATGTCGTCGGGGTCGGCGTT-3′ RP 5′-TCATCCGAAGAAGTCGTACTTGACC-3′	FP 5′-AATAGTCGACGGATCCGGGCTCAAAGGGAAAGTCCGA-3′ RP 5′-AATAATCGATGCTGTCATTGGCGTCCATGCTA-3′	FP 5′-AATATCTAGAGGATCCGGGCTCAAAGGGAAAGTCCGA-3′ RP 5′-AATACTCGAGGCTGTCATTGGCGTCCATGCTA-3′
PME21	FP 5′-ATGAGTAAAGGTGCGATCATCGG-3′ RP 5′-TTAATGATCCCTCCCCGCCT-3′	FP 5′-AATAGTCGACGGATCCGCCATGGAAGGAGTACTCT-3′ RP 5′-AATAATCGATGTACTCCTTTTGTGCGTCA-3′	FP 5′-AATATCTAGAGGATCC GCCATGGAAGGAGTACTCT-3′ RP 5′-AATACTCGAG GTACTCCTTTTGTGCGTCA-3′
PME28	FP 5′-ATGGCAAATAACTTCCTCCTCGGG-3′ RP 5′-TTAGACCTTGAACCCGAGGTAG-3′	FP 5′-AATAGTCGACGGATCCAAGTCGGTCAAGTCTCTGTGCGC-3′ RP 5′-AATAATCGATGTCGTCGGTGCGGCCAAGGA-3′	FP 5′-AATATCTAGAGGATCCAAGTCGGTCAAGTCTCTGTGCGC-3′ RP 5′-AATACTCGAGGTCGTCGGTGCGGCCAAGGA-3′

FP: forward primer; **RP:** reverse primer; **SS:** sense strand; **AS:** antisense strand; GTCGAC sequence is *Sal*I restriction site; GGATCC sequence is *Bam*HI restriction site; ATCGAT sequence is *Cla*I restriction site; TCTAGA sequence is *Xba*I restriction site; CTCGAG sequence is *Xho*I restriction site.

DNA separation, visualization, gel purification and quantification was performed as previously described.

The sense and the antisense strands added with the restriction sites, were ligated into an intermediate pre-existing vector containing the intron sequence (Sestili et al., 2010) by two subsequently cloning events. The first one consisted in the sense strand ligation by using *Sal*I and *Cla*I sites; the second cloning event, consisted in the antisense strand ligation by using *Xba*I and *Xho*I sites. The sense-intron-antisense cassette was then moved in the pAHC17 expression vector by the enzymatic digestion of *Bam*HI sites flanking the RNAi cassette and a consecutive ligation into pAHC17 vector, preventively digested with *Bam*HI restriction enzyme.

Restriction enzymes and T4 Ligase for the ligation reaction were purchased from Promega and they were used with the provided buffers, following the manufacturer's instruction. Following each ligation reaction, a bacterial transformation with *Escherichia coli* DH5α strain and a maxi-preparation of plasmids were performed (see paragraph 2.3.3, Chapter II).

RNAi constructs were controlled by sequencing (Eurofins Genomics Service, Germany) and they were the following:

- *pAHC17_Ubi1_PME3*

In order to obtained transgenic wheat plants silenced for the pectin methylesterase 3 (*PME3*) expressed in all plant tissues, the sense-intron-antisense cassette of *PME3* gene silencing was ligated in the pAHC17 expression vector (Fig. 1) under the control of *Ubi*1 promoter from maize, containing nophaline synthase (NOS) terminator (Christensen and Quail, 1996).

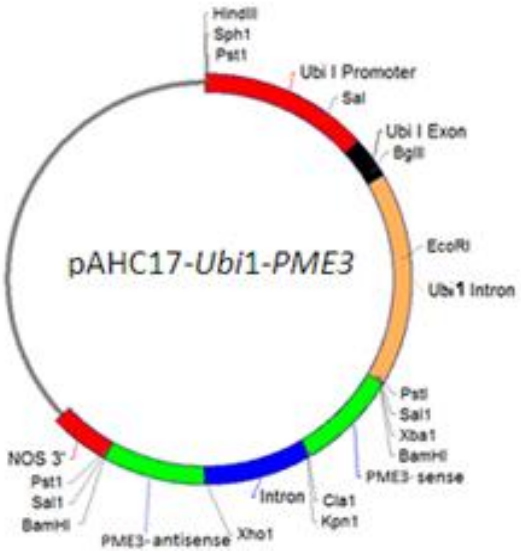

Figure 1. pAHC17-*Ubi*1-*PME3* expression vector, containing the sense and antisense strands (green boxes), the intron sequence (blue box) for *PME3* gene silencing. The cassette is under the control of *Ubi*1 promoter and with the NOS terminator. Restriction sites are indicated along the construct.

PME3 sense and antisense strands are 453 bp in length and pAHC17-*Ubi*1-*PME3* construct is 5983 bp long.

- *pAHC17_Lem1_PME3*, *pAHC17_Lem1_PME13* and *pAHC17_Lem1_PME28*

In order to obtained transgenic wheat plants silenced for the pectin methylesterase 3, 13 and 28 genes (*PME3*, *PME13* and *PME28*) only in the floral tissues, the sense-intron-antisense cassettes of *PME3*, *PME13* and *PME28* genes silencing were ligated in the pAHC17 expression vector (Fig. 2) under the control of *Lem*1 promoter from barley, containing the NOS terminator.

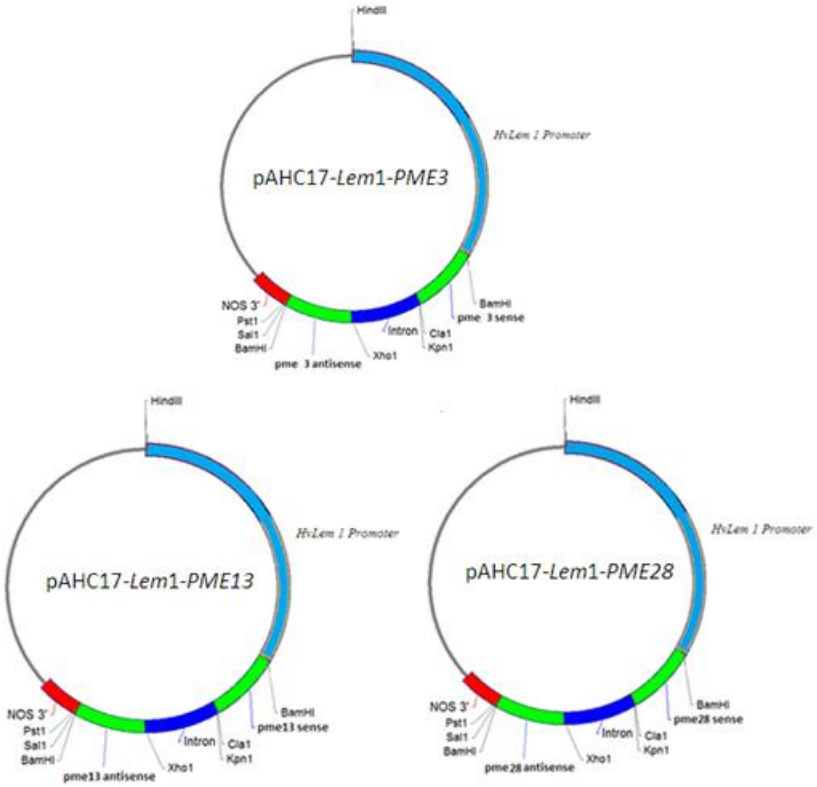

Figure 2. pAHC17-*Lem*1-*PME3*, pAHC17-*Lem*1-*PME13* and pAHC17-*Lem*1-*PME28* expression vectors, containing the sense and antisense strands (green boxes), the intron sequence (blue box) for *PME3*, *PME13* and *PME28* genes silencing. The cassettes are under the control of *Lem*1 promoter and with the NOS terminator. Restriction sites are indicated along the construct.

PME3 sense and antisense strands are, as before, 453 bp in length and pAHC17-*Lem*1-*PME3* construct is 5443 bp long. The sense and the antisense strands for *PME13* gene silencing are 346 bp long and the relevant RNAi construct is 5739 bp. Finally, the sense and the antisense strands for *PME28* gene silencing are 309 bp in length and the relevant RNAi construct is 5665 bp long.

- *pAHC17_promPME21_PME21* RNAi construct

In order to obtained transgenic wheat plants silenced for the pectin methylesterase 21 gene (*PME21*) only in the floral tissues, the sense-intron-antisense cassettes of *PME21* gene silencing was ligated in the pAHC17 expression vector (Fig. 3) under the control of *Lem*1 promoter from barley, containing the NOS terminator.

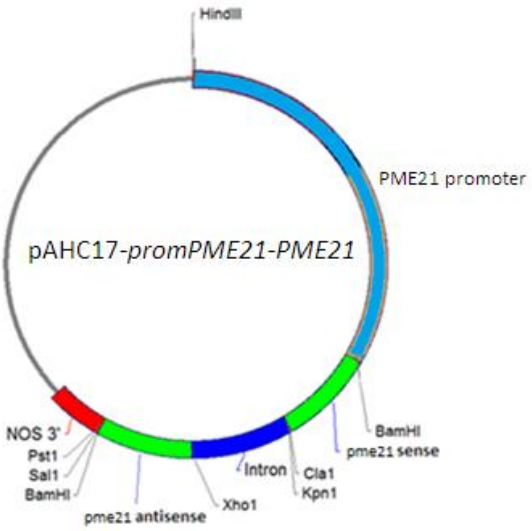

Figure 3. pAHC17-*promPME21-PME21* expression vectors, containing the sense and antisense strands (green boxes), the intron sequence (blue box) for *PME21*gene silencing. The cassette is under the control of the cognate promoter of *PME21*and with the NOS terminator. Restriction sites are indicated along the construct.

The cognate promoter PME21 was isolated from the gDNA of durum wheat cv. Svevo, adding by PCR (primers in Tab. 2) the *Hind*III-*Bam*HI sites flanking the promoter sequence used for the cloning in the pAHC17 vector.

Table 2. Primers used for the amplification of *PME21* promoter. The sequence length is also reported.

sequence	FP-RP	Sequence length
Prom_PME21	FP 5′-AATAAAGCTTCGACCATCTATTTTCGTCGTGC-3′ FP 5′- AATAGGATCCGGATCCTCTAGAGTTCTT -3′	849 bp

FP: forward primer; **RP:** reverse primer; AAGCTT sequence is *Hind*III restriction site; GGATCC sequence is *Bam*HI restriction site.

PME21 promoter is 849 bp in length and the sense and antisense strands are 216 bp each. In total the pAHC17-promPME21-*PME21* construct is 4786 bp long.

- *pUBI::BAR*

pUBI::BAR construct carries the *BAR* gene (Fig. 4), which confers resistance to the bialaphos herbicide, allowing the selection of herbicide-resistant transgenic calli and

shoots during the regeneration and growth of transformed embryos. The *BAR* gene is under control of the constitutive *Ubi*1 promoter and NOS terminator. The pUBI:BAR construct is 5505 bp in length.

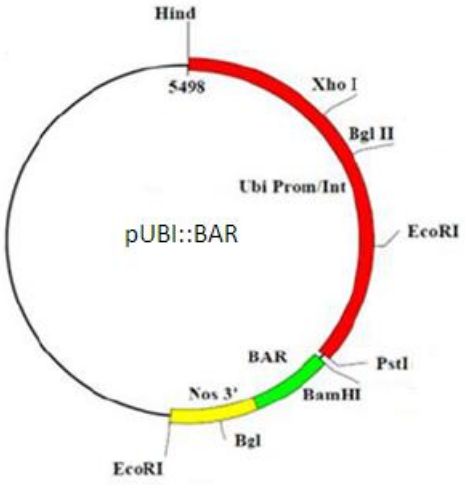

Figure 4. pUBI::BAR construct map. The pUBI::BAR plasmid contains *Ubi*1 promoter from maize driving the constitutive expression of *BAR* gene which confers resistance to the Bialaphos herbicide.

The RNAi constructs for wheat embryos-derived calli bombardment were multiplied into *E. coli* DH5α strain for a high-scale synthesis of plasmids. Plasmids were extracted by following the protocol described in the paragraph 2.4 and the concentration was calculated spectrophotometrically.

Plasmids concentration used for the bombardment was the following:

pAHC17*_Ubi1_PME3*: 1.8 µg/µL

pAHC17*_Lem1_PME3*: 3 µg/µL

pAHC17*_Lem1_PME13*: 2 µg/µL

pAHC17*_Lem1_PME28*: 3 µg/µL

pAHC17_promPME21*_PME21*: 2.5 µg/µL

pUBI::BAR: 2 µg/µL

2.2 Preparation of heterologous expression vectors for *PME* genes

The heterologous expression of PME13, PME21 and PME28 recombinant proteins was performed at the University of Marseille, France. To perform the heterologous

expression of *PME13*, *PME21* and *PME28* gene the pPICZαA expression vector was used (Fig. 5).

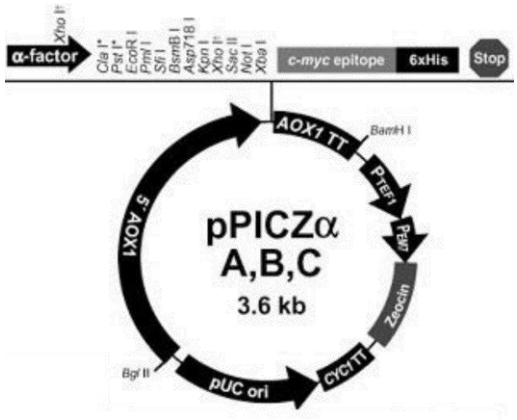

Figure 5. Map of the pPICZαA expression vector for the heterologous expression of *PME13*, *PME21* and *PME28* genes.

The vector pPICZαA contains the promoter sequence of *AOX*1 gene for methanol induced expression of the gene of interest, the α-factor secretion signal of *Saccharomyces cerevisiae* that allows the secretion of the recombinant protein and the zeocin resistance gene for selection in *Pichia* cells.

For the heterologous expression of *PME13*, *PME21* and *PME28* genes in *P. pastoris* X33 competent cells, only the nucleotide sequence corresponding to the mature part of the protein, that is the PME domain, was amplified by using the complete coding region amplified from durum wheat cv. Svevo as template. The PME domains within *PME* gene sequences were identified with SignalP on-line tool (http://www.cbs.dtu.dk/services/SignalP/; Petersen et al., 2011). The PME domain was amplified by using the primer listed in Tab. 3, adding the restriction sites *Eco*RI and *Xba*I at the 5′ and 3′ ends, respectively, for the cloning in the pPICZαA vector.

Table 3. Primer used for the amplification of the PME domain of *PME13*, *PME21* and *PME28*.

PME domain	FP-RP	Product size
PME13	FP 5′-AATAGAATCCAACGTGGTGGTGGCCAAG-3′ RP 5′- AATATCTAGATCATCCGAAGAAGTCGTACTTG-3′	948 bp
PME21	FP 5′-AATAGAATCCAACGTCACCGTGGCCGCCGA-3′ RP 5′-AATATCTAGATTAATGATCCCTCCCTGCCTCC-3′	969 bp
PME28	FP 5′-AATAGAATCCAACGCGATTGTGGCCAAG-3′ RP 5′-AATATCTAGATTAGACCTTGAACCCGAGG-3′	942 bp

FP: forward primer; **RP:** reverse primer; GAATCC sequence is EcoRI restriction site; TCTAGA sequence is *Xba*I restriction site.

Each PCR reaction was performed in a final volume of 20 µL, with 10 ng of DNA, 2.5 U of FastStart High Fidelity PCR system (Roche Diagnostics), 1× Taq PCR buffer, 50 ng of each of the two primers, and 100 µM each deoxyribonucleotide. The following PCR conditions were used: 1 cycle at 95°C for 2 min; 30 cycles at 95°C for 45 sec, 62°C for 45 sec and 72°C for 1 min; a final step at 72°C for 5 min.

The amplified sequences corresponding to the PME domain of *PME13*, *PME21* and *PME28* genes were separated and visualized through 1.2% agarose gel, prepared in 1x TBE (Tris, Boric Acid, EDTA) with 0.5 µg/mL ethidium bromide. DNA samples to load were prepared by adding an adequate volume of 6x loading dye (Fermentas) and as molecular weight markers GeneRuler 100 bp (Fermentas) was used. Agarose gel running was performed at 70-75 V for 30-45 min and the amplified DNA was observed by an UV transilluminator. Then, the PCR amplification products were purified from the agarose gel by using the Wizard SV Gel and PCR Clean-Up System (Promega) and following the manufacturer's procedure. The DNA concentration was estimated by a spectrophotometer.

The amplified and gel purified fragments were ligated into the pPICZαA vector previously digested with *Eco*RI and *Xba*I restriction enzymes.

Restriction enzymes and T4 Ligase for the ligation reaction were purchased from Promega and they were used with the provided buffers, following the manufacturer's instruction. Following ligation reactions, a bacterial transformation with *Escherichia coli* DH5α strain and a maxi-preparation of plasmids were performed (see paragraphs 2.3.3 and 2.4, Chapter II).

The heterologous expression vectors were controlled by sequencing (Eurofins Genomics Service).

The pPICZαA-PMEdomain-PME13, pPICZαA-PMEdomain-PME21 and pPICZαA-PMEdomain-PME28 vectors were digested with *Pme*I restriction enzyme in order to linearize the vectors. The linearized vectors were purified with the Wizard SV Gel and PCR Clean-Up System kit (Promega) and subsequently concentrated by precipitation as following: at the purified linearized vectors 70 µL of 3 M potassium acetate pH 5.2 and 175 µL of 100% ethanol were added. Samples were incubated 30 min at -80°C and then they were centrifugated 30 min at 4°C, 13000 rotations per minute (rpm). The supernatant was removed and pellet was washed with 1 mL of 70% ethanol and then centrifugated for 5 min at 4°C, 13000 rpm. The supernatant was removed and the pellet was well dried and finally resuspend in 20 µL of water.

The concentration of vectors employed in the heterologous expression was estimated spectrofotometrically.

2.3 Microbiological techniques

Escherichia coli DH5α and *Pichia pastoris* X33 (Invitrogen) were used for cloning procedures and heterologous expression of recombinant proteins, respectively.

2.3.1 Media and antibiotics

E. coli DH5α strain was grown in Luria Bertani (LB) medium prepared according to Sambrook et al. (1989). For the solid medium, 15 g/L of bactoagar (Sigma-Aldrich, Milan, Italy) were added to the liquid LB medium. The selection of bacterial cells both in the liquid and in the solid medium was carried out by using the antibiotic ampicillin at the concentration of 100 µg/mL.

For the expression of recombinant proteins in *P. pastoris* X33, different media were used:

YPD: 1% (g/v) yeast extract, 1% (g/v) peptone, 2% (g/v) glucose

YPDS: 1% (g/v) yeast extract, 1% (g/v) peptone, 2% (g/v) sorbitol 1M, 2% (g/v) glucose

BMGY: 1% (g/v) yeast extract, 2% (g/v) peptone, 100mM potassium phosphate pH 6.0, 1.34% (g/v) YNB, 4.10-5% D-Biotine, 1% (v/v) glycerol

BMMY: similar composition of BMGY, but 0,5% (v/v) methanol replace glycerol

MM: 1.34% (g/v) YNB, 4.10-5% D-biotine and 0,5% (v/v) methanol

MD: 1.34% (g/v) YNB, 4.10-5% D-biotine and 2% (g/v) glucose.

For the solid media, 20 g/L of agar were added. The selective media for *P. pastoris* were prepared adding the antibiotic zeocin at the concentration of 25 µg/mL.

2.3.2 Competent cells preparation

E. coli DH5α bacterial cells were induced to the competence for the transformation by employing the following protocol: a single colony of *E. coli* was inoculated in 2 mL of LB medium and it was left to grow overnight at 37°C, 180 rpm. The day after, 500 µL of the pre-culture were inoculated in 50 mL of liquid LB medium and it was left to grow at 37°C, 180 rpm, until an absorbance between 0.45 and 0.6 was reached. The cell culture was centrifugated for 15 min at 4°C, 2300 rpm and the supernatant was discarded. Then, 16.7 mL of RF1 buffer (Tab. 4) were added and the pellet was carefully resuspended. The cell suspension was kept in ice for 30-60 min and then it was centrifugated again as above and the supernatant was discarded. The pellet was resuspended in 2 mL of RF2 buffer (Tab. 4) and it was kept in ice for 15 min. Finally, 100 µL aliquots of competent cells were prepared, immediately frozen in liquid nitrogen and stored at -80°C.

Table 4. RF1 and RF2 buffers composition.

100 mL RF1 buffer (bring to pH 5.8, filter sterilized)	**100 mL RF2 buffer** (bring to pH 6.8, filter sterilized)
1.2 g RbCl	2 mL MOPS
0.99 g $MnCl_2$	0.12 g RbCl
3 mL K-acetate 1 M pH 7.5	1.1 g $CaCl_2$
0.15 g $CaCl_2$	11.9 mL glycerol
11.9 mL glycerol	-

P. pastoris X33 competent cells were prepared as following: one single fresh colony was inoculated in 2 mL of YPD media overnight at 30°C, 180 rpm. The day after, the culture was refreshed by inoculating 100 µL in 2 mL of fresh YPD media and it was incubated all day long at 30°C, 180 rpm. In the evening, 1 mL of that culture was inoculated in two 1 L flasks, each one containing 250 mL of YPD media. The culture was incubated overnight at 30°C, 180 rpm. The following day, when the cultures reached a O.D. between 1.3 and 1.5, cells were harvested by centrifugation for 10 min at

4°C, 2000 rpm and pellets were resuspended in 100 mL of YPD media added with 0.2 M HEPES buffer pH8. Then, 2.5 mL of 1 M DTT were added and cultures were gently mixed and incubated 15 min at 30°C. Subsequently, the volume of the two cultures was bring to 500 mL with cold sterile water and the cultures were centrifugated as previously. The pellets were resuspended in 250 mL of cold sterile water and centrifugated again. The pellets were then resuspended in 20 mL of cold 1 M sorbitol and centrifugated again as previously described. Finally, the pellets were resuspended in 850 µL of cold 1 M sorbitol, immediately used or otherwise frozen in liquid nitrogen and stored at -80°C until use.

2.3.3 Transformation protocols

In order to multiply the plasmid copies, *E. coli* DH5α competent cells transformation was performed with the thermal shock method, as following: 10 µL of the plasmid were mixed with 50 µL of competent cells and incubated 30 min in ice, 90 sec at 42°C, 2 min at room temperature and then 1 mL of LB medium was added and the transformed cells were let to grow for at least 1 h at 37°C. Following the incubation, samples were centrifuged 5 min at 4000 rpm and the supernatant was discarded, keeping about 100 µL of the supernatant to resuspend the pellet that finally was plated onto LB agar plates, supplied with ampicillin as selective agent. Plates were incubated overnight at 37°C.

The expression of recombinant proteins was performed by transforming *P. pastoris* X33 competent cells with the electroporation system, as following: 5 µg of the linearized vector contained in 10 µL were added to 80 µL of competent cells and the yeast suspension was then transferred to 2 mm electroporation cuvettes hold on ice. Then the cells were transformed by electroporation with a GenePulserII (BioRad) set to 200 W, 1.8 kV, 25 µF. Immediately 1 mL of ice-cold 1 M sorbitol was added to the cuvette. The cuvette contents was transferred to a sterile 15 mL tube and incubate for 1 to 2 hours at 30°C without shaking. Transformed cells were spread on YPDS plates containing increasing concentration of zeocin (100 and 500 µg/mL). Plates were incubated from 3–10 days at 30°C until colonies form.

2.4 Selection of positive transformed colonies

E. coli DH5α colonies were picked up and inoculated in 13 mL tube containing 1.5 mL of LB medium plus ampicillin and shaken overnight at 37°C, 250 rpm. The day after,

the 1.5 mL of bacterial cultures were transferred into 2 mL tubes and the bacterial pellet was recovered by centrifugation for 1 min at the maximum speed. Plasmid DNA was extracted with the following protocol: the bacterial pellet was resuspended in 1 mL of TE (1 M Tris-HCl pH8, 1 mM EDTA), centrifugated as above and resuspended again in 150 µL of SET (50 mM Tris-HCl pH 8, 50 mM EDTA pH8, 20% sucrose) using a vortex. 350 µL of lysis buffer (0.2 M NaOH, 1% SDS) were added, mixed by inverting the tube. Then, 250 µL of 3 M sodium acetate pH 5.2 were added and samples were kept on ice for 20 min, allowing SDS and chromosomal DNA precipitation that were pelleted down by centrifugation for 20 min at the maximum speed. The supernatant was collected and plasmid DNA was precipitated by adding an equal volume of cold isopropanol and by centrifugation for 10 min at the maximum speed. DNA pellet was washed with 70% ethanol, well dried and finally resuspended in 20 µL of water. An RNase treatment was performed, by using 2 µL of 1 mg/mL RNase for 20 min at 37°C. The extracted plasmid DNA was controlled by DNA sequencing.

The positive colonies checked by sequencing were grown in 100 mL of LB in order to have a high amount of plasmid DNA. The plasmid DNA was extracted from the bacterial culture with the PureLink HiPure Plasmid Filter Purification (Invitrogen) by following the manufacturer's instructions.

Transformed *P. pastoris* X33 cells were selected on increasing concentration of zeocin and only the colonies grown on the highest concentration of the antibiotic (500 µg/mL) were choose, since indicative of multi-copy recombinants. The selected colonies were grown on MM (methanol as carbon source) and MD (sucrose as carbon source) plates for the selection of the colonies where the recombination event occurred at the right locus. In fact, the DNA insertion downstream the *AOX*1 promoter determines a deletion of *AOX*1 gene and thus the Mut colonies are not able to grow on a medium containing only methanol as carbon source.

Thus, the colonies grew on MD plates but not onto MM plates were selected for the heterologous expression of recombinant PME proteins.

2.5 Expression of recombinant PME proteins

The positive *P. pastoris* X33 colonies were inoculated in 5 mL of YPD media in order to start the induction of the heterologous expression of PME13, PME21 and PME28 protein. The cultures were grown for 7 hours at 30°C, 200 rpm and then 500 µL of the

starter cultures were inoculated in 50 mL of BMGY media and incubated overnight at 30°C, 200 rpm. The following day, as the O. D. was between 2 and 6 the cultures were centrifuged for 10 min at room temperature, 6000 rpm. The pellets were resuspended in 10 mL of BMMY media and the cultures were incubated for 3-4 days at 20°C, 180 rpm. Each day, 1% methanol (v/v) was added to induce the expression from the alcohol oxidase promoter. At the end of the induction experiment the cultures were centrifugated for 20 min at 4°C, 8000 rpm and the supernatant was filtered with 0.22 µm filter and stored at -20°C until SDS-PAGE was performed.

2.5.1 SDS-PAGE

Supernatants recovered from the inducted cultures were running in a SDS-PAGE in order to verify the presence of recombinant proteins. The protein gels were prepared as described by Laemmli (1970), using separating gels containing 15% polyacrylamide and stacking gels with 3.75% polyacrylamide. The composition of running buffer was 0.2 M glycine, 0.02 M Tris pH 8.8 and 0.1% SDS. Samples were denaturating by addition of a 4x concentrated SDS-sample buffer containing dithiothreitol (DTT) as reducing agent and boiled for 5 min at 95°C.

Gels were stained in 0.25% Comassie Brilliant Blue, 45% methanol and 10% acetic acid and they were destained in 45 ethanol and 10% acetic acid.

2.6 Transgenic wheat plants production

2.6.1 Media for wheat plants culture

Murashige & Skoog (MS) modified media was used for wheat cultures (Sears and Deckard, 1982) added with MS salt, maltose, thiamine-HCl, L-asparagine at pH 5.85. Phytagel was used as gelling agent. After autoclaving for 20 min at 121°C, the medium was added with 2,4-D at the final concentration of 4 mL per liter and, after cooling, it was poured in 100 mm x 15 mm size Petri dishes. The bombardment medium, instead, was poured in 60 mm x 15 mm Petri dishes.
The exact media composition is described in Tab. 5.

Table 5. Media composition for wheat cultures.

Dissection medium	- Murashige & Skoog salt mixture 4.3 g/L - Maltose 40 g/L - Thiamine-HCl (25 mg/500 mL) 10 mL/L - L-asparagine 0.15 g/L - 0.25% v/v phytagel - 2,4-D (0.5 mg/mL) 2 mL/500mL
Recovery medium	- Murashige & Skoog salt mixture 4.3 g/L - Maltose 40 g/L - Thiamine-HCl (25 mg/500 mL) 10 mL/L - L-asparagine 0.15 g/L - 0.25% v/v phytagel - 2,4-D (0.5 mg/mL) 2 mL/500mL
Bombardment medium	- Murashige & Skoog salt mixture 4.3 g/L - Maltose 40 g/L - Thiamine-HCl (25 mg/500 mL) 10 mL/L - L-asparagine 0.15 g/L - 2,4-D (0,5 mg/mL) 2 mL/500mL - Sucrose 171.5 g/L
Regeneration medium	- Murashige & Skoog salt mixture 4.3 g/L - Maltose 40 g/L - Thiamine-HCl (25 mg/500 mL) 10 mL/L - L-asparagine 0.15 g/L - 2,4-D (0,5 mg/mL) 2 mL/500mL - Bialaphos (1 mg/mL) 1.5 mL/500mL
Rooting medium	- Murashige & Skoog salt mixture 2.15 g/L - Maltose 20 g/L - Thiamine-HCl (25 mg/500 mL) 5 mL/L - L-asparagine 0.075 g/L - Bialaphos (1 mg/mL) 1.5 mL/500mL
Early germination medium	- Murashige & Skoog salt mixture 4.3 g/L - Maltose 40 g/L - Thiamine-HCl (25 mg/500 mL) 10 mL/L - L-asparagine 0.15 g/L - Bialaphos (1 mg/mL) 1.5 mL/500mL

2.6.2 Embryo isolation

Seeds from 10 to 18 days after anthesis were collected from durum wheat cv. Svevo and bread wheat cv. Bobwhite plants (Zadoks stage 72) grown in the field. The seeds were surface sterilized once for 5 min with 2% sodium hypochlorite, once for 5 min with 70% ethanol and finally washed twice for 1 min each with sterilized water. Immature embryos were removed from seeds by using a stereomicroscope in sterile conditions and then placed with the scutella upside down and kept in the dark for 5 days at 23°C, in order to induce callus formation.

2.6.3 Gold nanoparticles DNA coating, bombardment and plant regeneration

In order to perform a bombardment experiment for the genetic transformation, gold nanoparticles coating with the plasmidic DNA was required.

Thirty mg of gold nanoparticles (0.6 µm, Bio-Rad) were resuspended in 500 µL of 100% ethanol and 35 µL aliquots were made in 1.5 mL Eppendorf tubes, spinned and the supernatant discarded. The micropojectiles were washed with 200 µL of cold sterile water, spinned again and the supernatant discarded. Then, plasmidic DNA (pAHC17-*Ubi*1-PME3, pAHC17-*Lem*1-PME13, pAHC17-*Lem*1-PME28, pAHC17-*Lem*1-PME3 or pAHC17-promPME21-PME21) of the silencing vectors and the pUBI::BAR marker plasmid, carrying the *BAR* gene resistance for the bialaphos herbicide, were added to the pellet for the co-bombardment, using a 3:1 ratio.

The following *formulae* were used:

RNAi plasmid (µL): RNAi construct bp/marker bp x 15 µg x (1/RNAi plasmid concentration) x 3

Marker plasmid (µL): 15 µg x (1/marker plasmid concentration).

24.45 µL of pAHC17-*Ubi*1-PME3 (44 µg), 22.23 µL of pAHC17-*Lem*1-PME13 (44.5 µg), 13.65 µL of pAHC17-*Lem*1-PME28 (41 µg), 14.83 µL of pAHC17-*Lem*1-PME3 (44.5 µg), 15.7 µL of pAHC17-promPME21-PME21 (39.25 µg) and 7.5 µL of pUBI::BAR (15 µg) were used.

Subsequently to the DNA addition, 250 µL of 2.5M $CaCl_2$, 50 µL of spermidine and water to make the final volume of 530 µL were added. Samples were mixed by vortex for 15-20 min at 4°C and then briefly centrifugated at the maximum speed. The supernatant was removed and the pellet washed with 600 µL of 100% ethanol. The DNA-coated gold nanoparticles were then resuspended with 36 µL of 100% ethanol and stored in ice until use.

About 200 embryos-derived calli were transferred onto the bombardment medium (see Tab. 5 for the composition) 4 hours before the bombardment. Then, 10 µL of the DNA-coated gold nanoparticles were placed in the centre of a macrocarrier disk and bombarded into the embryos-derived calli using a Model PDS-1000/He Biolistic particle delivery system (Bio-Rad, Hercules, CA, U. S. A; Fig. 6) as described in Weeks et al. (1993). The distance from the macrocarrier and the target was 13 cm and the rupture disk strength was 1100 psi. Following the bombardment, calli were kept in the dark for 24 hours at 23°C.

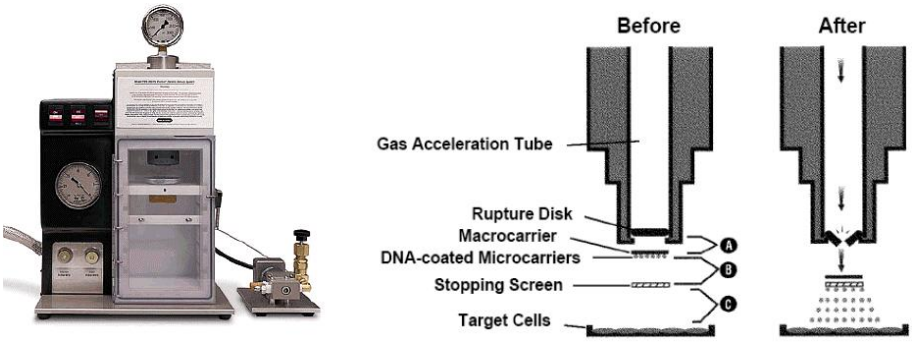

Figure 6. The Biolistic PDS-1000/He instrument (left). The biolistic bombardment process: the system uses high pressure helium and vacuum to propel DNA-coated nanoparticles placed onto a macrocarrier toward target tissue at high speed. The macrocarrier is stopped by a stopping screen, whereas nanoparticles proceed until they penetrate the cells. The launch speed depends on the helium pressure (rupture disk strength), the vacuum inside the chamber and (A) the distance between the rupture disk and the macrocarrier; (B) distance between the macrocarrier and the stopping screen; (C) distance between the stopping screen and the target cells.

The day after the bombardment, calli were transferred in the recovery medium (see Tab. 5 for the composition) for 4 weeks and sub-cultured in a fresh medium every 2 weeks. During the recovery stage, calli were kept at 23°C in the dark.

After 4 weeks, calli were transferred to the regeneration medium (see Tab. 5 for the composition) containing the bialaphos herbicide as selective agent, where they were kept for 6 weeks and sub-cultured in a fresh medium every 2 weeks. During the regeneration stage, calli were kept at 23°C with 16 hours light/8 hours dark photoperiod. Generally from the third week onward, resistant calli regenerated new shoots.

After 6 weeks, the regenerated shoots were transferred in pyrex tubes containing the rooting medium (see Tab. 5 for the composition), where they were kept for 2-3 weeks at 23°C with 16 hours light/8 hours dark photoperiod. At this stage, plants were defined resistant if they were able to form long and highly branched roots.

Once the regenerated plants had sufficient roots and leaves, they were transferred into pots in a growth chamber for 5-10 days at 23°C with 16 hours light/8 hours dark photoperiod. Plants were covered with plastic bags in order to maintain a high humidity and to allow them to acclimatize to the *ex-vitro* conditions. After 5-10 days, the T0 plants were transferred to bigger pots.

2.7 Screening of regenerated wheat plants

2.7.1 DNA extraction

The presence of the transgene was checked by PCR by using DNA extracted from the second fully expanded leaf of regenerated plants (Zadoks Z13). The following protocol was used: a small piece of T0 leaf from each regenerated plant was sampled and homogenized in liquid nitrogen with mortar and pestle. The powder thus obtained was added with 80 µL of extraction buffer (100 mM Tris-HCl pH 8.0, 50 mM EDTA pH 8.0, 500 mM NaCl) plus 32 µL of 10% SDS and it was incubated for 10 min at 65°C. Then, 26.7 µL of 5 M potassium acetate were added to the sample, it was incubated in ice for 20 min and then it was centrifugated 20 min at the maximum speed. After centrifugation the supernatant was recovered and the DNA precipitation was carried out by adding an equal volume of cold isopropanol. Following a centrifugation for 20 min at the maximum speed, supernatant was discarded and the DNA pellet was washed with 70% ethanol, well dried and then resuspended in 20 µL of water.

2.7.2 Polymerase Chain Reaction (PCR)

A Polymerase Chain Reaction (PCR) was conducted in order to verify the presence of transgene in the regenerated wheat plants. To avoid any interference with the endogenous *PME* genes, primer pairs composed by the forward specific primer for the *Ubi*1 or *Lem*1 promoter sequences and the reverse specific primer for the RNAi construct were employed (Tab. 6)

The PCR reaction was performed using 1 µL of the extracted DNA, 10 µL of the 2X GoTaq PCR Green Master Mix (Promega) and 0.5 µL of each 10 µM forward and reverse primer. The following amplification conditions were employed: 1 cycle at 94°C for 2 min; 35 cycles at 94°C for 1 min, 60°C for 40 sec, 72°C for 1 min; a final step at 72°C for 2 min.

Table 6. Primers employed for T0 plants screening for the presence of the transgene.

Construct	FP-RP	Product size
pAHC17-*Ubi*1-*PME3*	FP 5′-TCGATGCTCACCCTGTTGTTT-3′ RP 5′-AATAATCGATACGACGCTGTCGAGCTCCGA-3′	526 bp
pAHC17-*Lem*1-*PME3*	FP 5′-ACCTTAACCTGGCGCCTTAG-3′ RP 5′-AATAATCGATACGACGCTGTCGAGCTCCGA-3′	768 bp
pAHC17-*Lem*1-*PME13*	FP 5′-ACCTTAACCTGGCGCCTTAG-3′ RP 5′-AATAATCGATGCTGTCATTGGCGTCCATGCTA-3	661 bp
pAHC17-promPME21-*PME21*	FP 5′-AATAAAGCTTCGACCATCTATTTTCGTCGTGC-3′ RP 5′- AATAATCGATGTACTCCTTTTGTGCGTCA-3′	1063 bp
pAHC17-*Lem*1-*PME28*	FP 5′-ACCTTAACCTGGCGCCTTAG-3 RP 5′-AATAATCGATGTCGTCGGTGCGGCCAAGGA-3′	624 bp

FP: forward primer; **RP:** reverse primer; AAGCTT sequence is the *Hind*III restriction site; ATCGAT sequence is *Cla*I restriction site.

A PCR was also performed in order to verify the presence of *BAR* gene in the regenerated plants. The PCR reactions were conducted by using the forward specific primer for the *Ubi*1 promoter (UBI-49F) 5′-TCGATGCTCACCCTGTTGTTT-3′ and the reverse specific primer for the terminator sequence (RTNOS) 5′-CAAATGTTTGAACGATCTGC-3′. The same amplification conditions previously described for the amplification of transgenes were employed.

2.7.3 RNA extraction and retro-transcription

Total RNA was extracted from flowering spikelets of transgenic plants (Zadoks Z68) in order to verify gene silencing. RNA extraction was performed with the RNeasy Plant Mini-Kit (Qiagen) following the manufacturer's instructions, starting from 100 mg of fresh plant material immediately frozen in liquid nitrogen after sampling.

Five-hundred ng of the total extracted RNA were retro-transcript with the Retro-Transcription Kit (Qiagen) by following the manufacturer's instructions, providing also the genomic DNA (gDNA) contamination elimination.

The bounty of the neo-synthesized cDNA and the completely removal of gDNA was confirmed for each sample by a PCR amplification for *actin* gene. In fact, the amplification for *actin* gene give a 300 bp band in the case of gDNA contaminations because of the presence of an intron within the amplified sequence, whereas the exclusive presence of a 250 bp band confirmed the gDNA complete elimination, as the intron is not present.

2.7.4 RT-PCR analysis

The cDNA obtained from the RNA extracted from flowering spikelets of transgenic plants was employed in RT-PCR analysis in order to check the effective silencing of wheat *PMEs*. For each bombardment experiment, two different specific primer pairs were used (Tab. 7): the first one, amplifying a small fragment within the complete coding region of each genes and the second one, amplifying the complete coding region of each genes. In both cases, PCR reactions were performed using 1 µL of cDNA, 10 µL of the 2X GoTaq PCR Green Master Mix (Promega) and 0.5 µL of each 10 µM forward and reverse primer. For the amplification of the small fragment, the following amplification conditions were employed: 1 cycle at 94°C for 2 min; 35 cycles at 94°C for 1 min, 60°C for 40 sec, 72°C for 1 min; a final step at 72°C for 2 min. For the amplification of the complete coding region, the same amplification conditions were used, but the extension time at 72°C was 2 min instead of 1 min.

Table 7. Primers employed for RT-PCR analysis.

Construct	**Small fragment FP-RP**	**Size**	**CDS FP-RP**	**Size**
pAHC17-*Ubi*1-*PME3*	FP 5'-CAGCAACTTCCTGGCCCGCGA-3' RP 5'-ACGACGCTGTCGAGCTCCGA-3'	453 bp	FP 5′-ATGTCCGCCAACTGCTCC-3′ RP 5′-TCACAACCCGCCGGAGAAC-3′	2000 bp
pAHC17-*Lem*1-*PME3*	FP 5'-CAGCAACTTCCTGGCCCGCGA-3' RP 5'-ACGACGCTGTCGAGCTCCGA-3'	453 bp	FP 5′-ATGTCCGCCAACTGCTCC-3′ RP 5′-TCACAACCCGCCGGAGAAC-3′	2000 bp
pAHC17-*Lem*1-*PME13*	FP 5'-ATGTGCAAGCAGGTGGACTACCA-3' RP 5'-ACAACTTCACCTTGTCCTTGAACT-3'	376 bp	FP 5′-ATGTCGTCGGGGTCGGCGTT-3′ RP 5′-TCATCCGAAGAAGTCGTACTTGACC-3′	1827 bp
pAHC17-promPME21-*PME21*	FP 5'-CGCTCAACGCCTCCCAGGAGCT-3' RP 5'-CGGAGACGTACTCCTTGTAG-3'	318 bp	FP 5′-ATGAGTAAAGGTGCGATCATCGG-3′ RP 5′-TTAATGATCCCTCCCCGCCT-3′	1689 bp
pAHC17-*Lem*1-*PME28*	FP 5'-TCAAGGTGCTCCTTGGCCGC-3' RP 5'-GGCCACAATCGCGTTCGGC-3'	334 bp	FP 5′-ATGGCAAATAACTTCCTCCTCGGG-3′ RP 5′-TTAGACCTTGAACCCGAGGTAG-3′	1692 bp

FP: forward primer; **RP:** reverse primer; **CDS:** complete coding region.

2.7.5 qRT-PCR analysis in transgenic plants

Total RNA was extracted from a flowering spike of the silenced AZ4-11 and AZ5-5 lines according to the procedure described in Chapter II, paragraph 2.7.3 and cDNA synthesis was performed as described in the same paragraph. A qRT-PCR analysis was conducted in order to verify the effect of *PME13* and *PME28* genes silencing on the other endogenous *PME* genes. qRT-PCR conditions were as described in Chapter I, paragraph 2.4 and primer are listed in Chapter I, Tab. S1. The relative expression was calculated according to Livak and Schmittgen (2001). Only one biological replicate and three technical replicate were conducted because of the scarcity of plant material.

Student's t-test was used to obtain the statistical difference between samples and durum wheat cv. Svevo used as reference sample.

2.8 Infection of transgenic plants

2.8.1 Fusarium graminearum culture

F. graminearum strain 3827 was cultured in SNA medium (Urban et al., 2002) containing 0.1% KH_2PO_4, 0.1% KNO_3, 0.1% $MgSO_4$.7H2O, 0.05% KCl, 0.02% glucose, 0.02% sucrose, 2% bactoagar (Sigma) with 200 ppm biotin and 200 ppm thiamine.

Macroconidia were harvested by a gently scraping of the mycelium surface with 1 mL of sterile water and the concentration was estimated by Thoma chamber. For plant inoculation, final conidia concentration was 500 conidia/20 μL.

2.8.2 Plant growth

Transgenic wheat plants used for the infection were grown in a climatic chamber with 16-8 photoperiod at 23°C. The transgenic plants were AZ4-11 and AZ5-5 lines. The durum wheat cv. Svevo was used as non-transgenic negative control.

2.8.3 Point-inoculation infection method and symptoms detection

The point inoculation method used for the infection of transgenic wheat plants consisted in the injection of 20 μL of *F. graminearum* conidia suspension (25 conidia/μL) in the two central opposite spikelets of a spike during the anthesis stage. Following the conidia injection, plants were covered with a plastic bag in order to increase humidity and to improve pathogen growth. After 2 days plastic bags were removed and symptoms were started to detect. Symptoms were identified as the number of yellowish or brownish spikelets within the infected spikes and they were annotated until the complete desiccation of the spike was achieved.

2.8.4 Statistical analysis of infection

Symptoms were calculated as the percentage of infected spikelets within the whole spike. Data were analyzing by applying the Student's t-test.

2.9 Targeting Induced Local Lesions IN Genomes (TILLING) analysis

The Targeting Induced Local Lesions IN Genomes (TILLING) analysis was conducted by using a durum wheat cv. Svevo population treated with ethyl methanesulfonate (EMS) available at the University of Tuscia. The TILLING population is composed by the DNA extracted from about 4000 plants; the extracted DNA is collect in 96 wells plates, each well containing DNA coming from two different wheat plants. A general workflow of a TILLING analysis is show in Fig. 7.

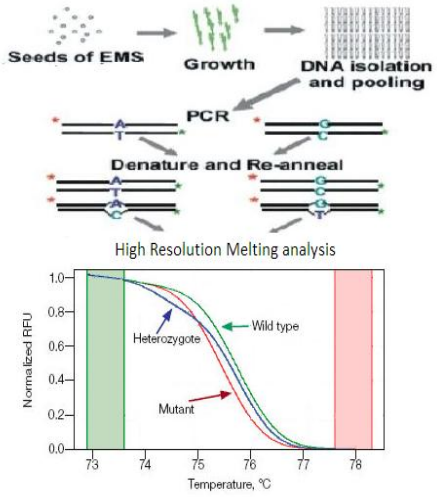

Figure 7. General workflow of TILLING analysis. Seeds treated with EMS are grow and DNA is extracted and pooled. The DNA is amplified by PCR and analyzed by HRM analysis.

The gene chosen to be analyzed by the TILLING approach was the *PME13* gene. First of all a CODDLE analysis (http://blocks.fhcrc.org/proweb/input/) of *PME13* gene sequence was conducted in order to select the mutation sites that could be generated by the EMS treatment. On the basis of this analysis, both a gene-genome specific primer pair amplifying the entire coding region of *PME13* and six different primer pairs covering the regions where the mutation sites were previously predicted with the CODDLE analysis were designed (Tab. 8).

A preliminary amplification of TILLING DNA was conducted by using the gene-genome specific specific primer pair amplifying the entire coding region of *PME13* (Tab. 8). PCR reactions were performed using 2 µL of TILLING DNA, 0.5 µL of each 10 µM forward and reverse primer and 5 µL of the G2 Colorless Maser Mix (Promega) in a final volume of 10 µL. In each reaction 10 µL of mineral oil (Sigma Aldrich) were added. The following amplification conditions were employed: 1 cycle at 95°C for 5

min; 40 cycles at 95°C for 1 min, 65°C for 1 min, 72°C for 2 min; a final step at 72°C for 5 min.

Following the preliminary amplification, the six different primer pairs (Tab. 8) were used in a second amplification where the PCR products coming from the first amplification were employed as template. PCR reactions were performed using 1 µL of the firs PCR product diluted 1:30, 0.5 µL of each 10 µM forward and reverse primer, 5 µL of the G2 Colorless Maser Mix (Promega) and 1 µL of LCGreen Plus Dye (Euroclone, Milan, Italy) in a final volume of 10 µL. In each reaction 10 µL of mineral oil (Sigma-Aldrich) were added. The following amplification conditions were employed: 1 cycle at 95°C for 2 min; 40 cycles at 94°C for 20 sec, 60°C for 20 sec, 72°C for 20 sec; a final step at 72°C for 1 min.

At the end of the amplification, the High Resolution Melting (HRM) analysis was performed in order to detect the mismatch in heteroduplex amplicons. The amplicons were send to sequencing in order to verify the real presence of mutations.

Table 8. Primer pairs used in TILLING analysis of *PME13* gene.

Name	FP-RP	Product size
PME13 CDS	FP 5'-GCAAGAAGGGCTCAAAGGGAAAGTC-3' RP 5'-CTTGCTGATCACCTTCTTGTACCCTG-3'	1728 bp
TILLING 1	FP 5'-GGCTCAAAGGGAAAGTC-3' RP 5'-TTGAACTCGCCGTCGGGGAAG-3'	440 bp
TILLING 2	FP 5'-AGAAGGCGGCGACGTTCCT-3' RP 5'-CGGACATGCAATCATGCATGC-3'	305 bp
TILLING 3	FP 5'-AAGCCAAACGTGGTGGTGGC-3' RP 5'-TGATGATCGTCGTCTTGGAA-3'	286 bp
TILLING 4	FP 5'-TGGACGGGATCACGACCTTC-3' RP 5'-GACTTGTCCGCCAGCACCA-3'	233 bp
TILLING 5	FP 5'-GTCCATCTTCCTCAACTGCAAG-3' RP 5'-GGGCGTCGGCGCGGCCAT-3'	212 bp
TILLING 6	FP 5'-ACATCGTCACGGCGCATGG-3' RP 5'-CTCGGCGTAGTAGAGCGTCT-3'	251 bp

FP: forward primer; **RP:** reverse primer. TILLING1/6 are the six primer pairs used to cover the regions within *PME13* gene where the CODDLE analysis predicted the mutation sites.

Recently, a TILLING durum wheat cv. Kronos population sequencing was available from the University of California, Davis, which produced a database (http://dubcovskylab.ucdavis.edu/) containing all the sequenced genotypes that underwent EMS treatment.

The 42 complete *PMEs* sequences (see Chapter I) were used as input in the database and trough a BLAST search mutated genotypes were found. Seeds corresponding to the mutated genotypes were ordered.

3. Results

3.1 Production and characterization of transgenic wheat plants

In order to study the role of PME in wheat defense, transgenic RNAi plants silenced for the *PME3*, *PME13*, *PME21* or *PME28* were produced. Nine different bombardment experiments, named AZ, were conducted.

In the AZ1 and AZ2 no plants were obtained. In the AZ4 and AZ6 experiments, 32 and 50 plants were transferred to the soil, respectively. In the AZ5 experiment, 47 plants were transferred to the soil. In the AZ8 and AZ9 experiments, 31 and 9 plants were transferred to the soil, respectively and finally, in the AZ10 and AZ11 experiments 4 and 2 plants were transferred to the soil, respectively.

Further details of the bombardment experiments (number of bombarded immature embryos, number of regenerated plants, number of positive plants and the transformation efficiency) are reported in Table 9.

Table 9. Bombardment experiments in durum and bread wheat; positive T0 plants were recorded by PCR.

Name	RNAi plasmid	Genotype	N° bombarded embryos	N° regenerated plants	N° positive T0 plants	Efficiency (%)
AZ1	pAHC17-*Ubi*1-*PME3*	*T. aestivum* cv. Bobwhite	840	174	0	0
AZ2	pAHC17-*Ubi*1-*PME3*	*T. aestivum* cv. Bobwhite	566	188	0	0
AZ4	pAHC17-*Lem*1-*PME13*	*T. durum* cv. Svevo	1311	162	17	1,37
AZ5	pAHC17-*Lem*1-*PME28*	*T. durum* cv. Svevo	2415	191	34	1,45
AZ6	pAHC17-*Lem*1-*PME13*	*T. durum* cv. Svevo	1242	201	22	1,77
AZ8	pAHC17-promPME21-*PME21*	*T. durum* cv. Svevo	897	115	44	4,9
AZ9	pAHC17-promPME21-*PME21*	*T. durum* cv. Svevo	1035	77	13	1,26
AZ10	pAHC17-*Lem*1-*PME3*	*T. aestivum* cv. Bobwhite	800	67	10	1,25
AZ11	pAHC17-*Lem*1-*PME3*	*T. aestivum* cv. Bobwhite	1013	260	2	0,19

The T0 plants transferred to the soil were screened by PCR for the presence of transgene at Zadoks Z13 stage, when the second leaf was fully expanded (Fig. 8). The transformation efficiency was calculated as percentage of the positive T0 plants on the total number of bombarded calli.

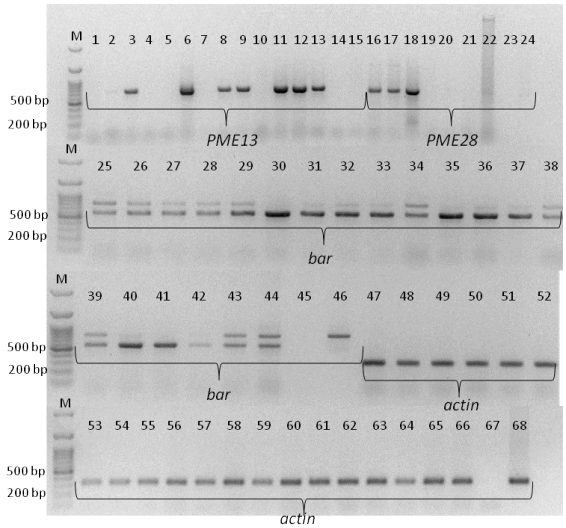

Figure 8. An example of a PCR analysis for some of the T0 wheat plants; **M:** Ladder GeneRuler DNA 100 bp; **1-13:** AZ4 plants transformed with pAHC17-*PME13* RNAi construct; **14:** H_2O; **15:** Svevo DNA; **16-22:** AZ5 plants transformed with pAHC17-*PME28* RNAi construct; **23:** H_2O; **24:** Svevo DNA; **25-44:** AZ4 and AZ5 plants amplified for pUBI::BAR construct; **45:** H_2O; **46:** Svevo DNA; **47-66:** AZ4 and AZ5 plants amplified for *actin* gene; **67:** H_2O; **68:** Svevo DNA. The amplification for *BAR* gene gave a specific band at 656 bp and a non-specific band at about 900 bp; in fact, in Svevo DNA (sample 46) only the non-specific band is detectable.

The PCR screening of T0 plants revealed the number of regenerated plants containing the transgene (Tab. 9): for AZ4 and AZ6 experiments, 17 and 22 plants were positive, respectively, for a total of 39 positive plants containing pAHC17-*Lem*1-*PME13* construct. For the AZ5 experiment, 34 plants contained the pACH17-*Lem*1-*PME28* construct. For AZ8 and AZ9 experiments, 44 and 13 plants were positive, respectively, for a total of 57 positive plants containing pAHC17-promPME21-*PME21* construct. Finally, for AZ10 and AZ11 experiments, 10 and 2 plants were positive, respectively, for a total of 12 positive plants containing pAHC17-promPME21-*PME21* construct.

The plants from AZ8, AZ9, AZ10 and AZ11 experiments were not characterized because obtained during the last year of PhD and the quite long life cycle of wheat (3 months) prevented their characterization. Only plants produced by the AZ4, AZ5 and AZ6 experiments were further characterized because produced during the first year of the PhD.

In the AZ4 experiment (17 positive T0 plants) only AZ4-11, AZ4-12 and AZ4-66 plants produced viable seeds, in the AZ6 (22 positive T0 plants) experiment only AZ6-5, AZ6-44, AZ6-70 and AZ6-89 plants gave viable seeds and, finally, in the AZ5 (34 positive

T0 plants) experiments viable seeds were obtained only from AZ5-5, AZ5-57, AZ5-60, AZ5-62, AZ5-84, AZ5-127 and AZ5-128 plants. The remaining T0 positive plants died during the acclimatization period or they did not produce a viable progeny (Tab. 10).

Table 10. Result obtained in the AZ4, AZ6 and AZ5 experiments.

Experiment	Positive T0 plants	Giving viable seeds	Died during the acclimatization period	No seeds
AZ4	17	3	5	9
AZ6	22	4	4	14
AZ5	34	7	10	17

In the table is reporting the number of positive T0 plants obtained from the AZ4, AZ6 and AZ5 experiments that gave viable seeds, as well as the number of plants that did not produce a progeny or that died during the acclimatization period.

The T1 offspring was screened again by PCR in order to distinguish the progeny that contained the transgene from that lost the construct during segregation (Tab. 11).

Table 11. T1 offspring screening.

T0 positive plants	Total number of T1 seeds	Number of positive T1 seeds
AZ4-11	12	5
AZ4-12	12	7
AZ4-66	9	6
AZ6-5	11	6
AZ6-44	6	4
AZ6-70	13	10
AZ6-89	6	4
AZ5-5	20	16
AZ5-57	12	11
AZ5-60	7	2
AZ5-62	12	10
AZ5-84	9	3
AZ5-127	7	2
AZ5-128	8	2

Seeds produced from the T0 positive plants of AZ4, AZ6 and AZ5 experiments were screened in order to distinguish seeds harboring the transgene from those which lost the construct following segregation.

The positive T1 seeds were grown in order to produce the T1 generation. One plant for each line was subsequently screened also by RT-PCR in order to verify the

effectiveness of RNAi silencing (Fig. 9). The RT-PCR analysis was performed by using two different primer pairs, one amplifying a small fragment within the *PME* sequence (Tab. S1, Chapter I) and the other one amplifying the whole CDS sequence of *PME* gene (Tab. 2, Chapter II).

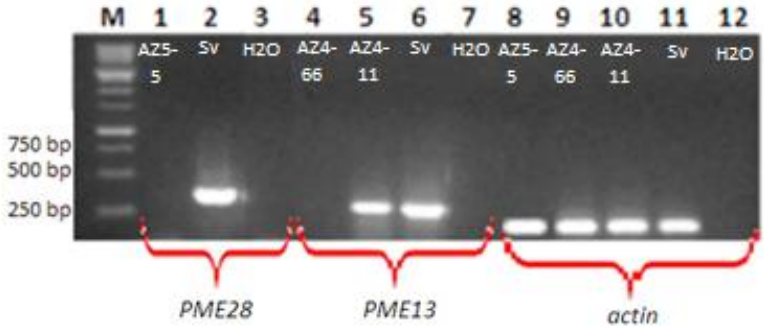

Figure 9. An example of RT-PCR analysis for some of the T1 positive wheat plants. In the figure is represented only the amplification for the small fragment. **M:** Ladder GeneRuler DNA 1kb; **1:** AZ5-5 (*PME28*) transgenic line; **2:** Svevo cDNA; **3:** H_2O; **4**: AZ4-66 (*PME13*) transgenic line; **5:** AZ4-11 (*PME13*) transgenic line; **6:** Svevo cDNA; **7:** H_2O; **8-10:** AZ5-5, AZ4-66 and AZ4-11 transgenic lines; **11:** Svevo cDNA; **12:** H_2O.

In AZ4-66 plant (*PME13* silencing) and in AZ5-5, AZ5-62 and AZ5-127 plants (*PME28* silencing) both the amplicon corresponding to the small fragment within the *PME* sequence and the whole CDS were absent, indicating a complete degradation of *PME13* and *PME28* transcripts. Conversely, in AZ4-11, AZ4-12, AZ6-5, AZ6-44, AZ6-70 and AZ6-89 plants (*PME13* silencing) and in AZ5-57, AZ5-60, AZ5-84, and AZ5-128 plants (*PME28* silencing) the complete CDS was absent, whereas the amplicon corresponding to the small fragment within *PME13* or *PME28* was present, indicating an incomplete degradation of the target transcripts (Tab. 12).

Table 12. Transgenic wheat lines screened by RT-PCR for the effective silencing of *PME13* and *PME28* genes.

T1 generation	Silenced *PME*	Small fragment	CDS
AZ4-66	*PME13*	-	-
AZ5-5	*PME28*	-	-
AZ5-62	*PME28*	-	-
AZ5-127	*PME28*	-	-
AZ4-11	*PME13*	+	-
AZ4-12	*PME13*	+	-
AZ6-5	*PME13*	+	-
AZ6-44	*PME13*	+	-
AZ6-70	*PME13*	+	-
AZ6-89	*PME13*	+	-

AZ5-57	*PME28*	+	-
AZ5-60	*PME28*	+	-
AZ5-84	*PME28*	+	-
AZ5-128	*PME28*	+	-

Table resuming the RT-PCR analysis on positive T1 plants previously screened by PCR.
+ indicated the presence of the amplified fragment and – indicated its absence.

In total 4 lines of T1 transgenic plants were found to be fully silenced and they were the AZ4-66, AZ5-5, AZ5-62 and AZ5-127 lines. AZ4-66 and AZ5-127 lines were sterile, whereas AZ5-62 line produced a very low number of viable seeds. Only AZ5-5 line produced a good amount of seeds to be further characterize. In fact, this line produced 30 seeds that were put to grow but only 17 of them actually grew; the remaining 13 seeds did not germinate. Because of the scarcity of seeds from the fully silenced plants, seeds from the T1 plants AZ4-11 and AZ6-70 lines (19 and 10 seeds, respectively) that showed the absence of the entire CDS of the *PME13* and the presence of the shorter *PME* fragment were planted in order to produce the T2 generation. All the 19 seeds from the AZ4-11 line grew, whereas only 2 seeds of AZ6-70 germinate; thus, this latter line was excluded in the subsequently infection experiment.

Seventeen seeds from AZ5-5 transgenic line and 19 seeds from AZ4-11 transgenic line were screened for the presence of the constructs pAHC17-*Lem*1-*PME28* and pAHC17-*Lem*1-*PME13*, respectively. All the screened plants resulted to be positive for the presence of the transgene and one plant for each transgenic line was sampled at the anthesis stage (Zadoks 68) in order to verify the RNAi silencing. Both the sampled plants of the AZ4-11 and AZ5-5 transgenic lines were silenced for *PME13* and *PME28* genes, respectively.
Only one plant for each line was checked for RNAi silencing in order to use a larger number of plants for the subsequent infection experiment.

3.2 Effect of the RNAi silencing of a specific *PME* gene on the expression of other *PME* genes

The same flowering spike of AZ4-11 and AZ5-5 lines was employed in a qRT-PCR analysis in order to verify the effect of *PME13* and *PME28* genes silencing on the other endogenous *PME* genes (Fig. 10).

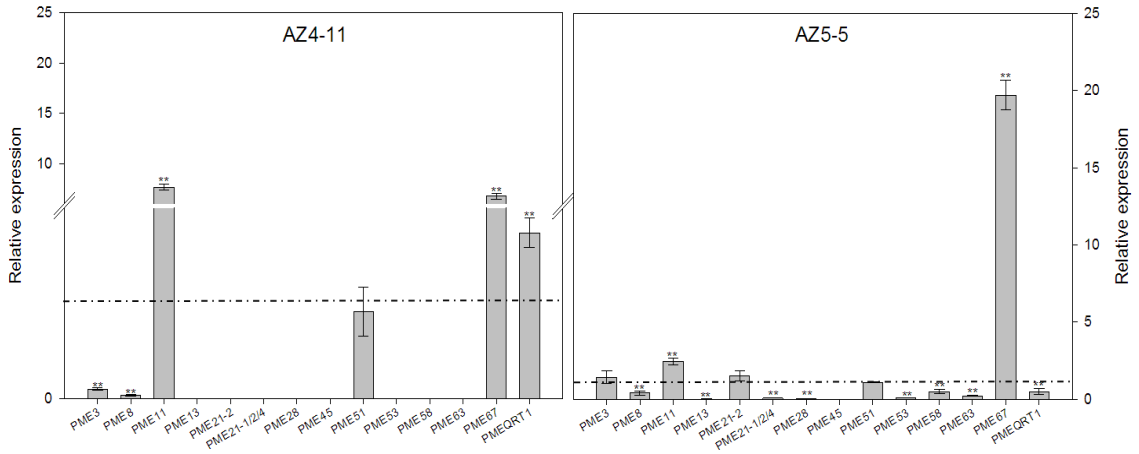

Figure 10. qRT-PCR showing the *PME* genes expression in flowering spike of AZ4-11 and AZ5-5 transgenic lines. The relative gene expression was calculated taking as reference sample the level of expression of each *PME* in durum wheat cv. Svevo (dotted line). Bars indicated the standard deviation between three technical replicate of one biological replicate; ** p< 0,05.

The qRT-PCR analysis performed on the AZ4-11 having the *PME13* gene silenced, showed silencing of several *PMEs* compared to the reference sample (Fig. 9., dotted line). In fact, in addition to *PME13*, also *PME21-2*, *PME21-1/2/4*, *PME28*, *PME45*, *PME53*, *PME58* and *PME63* were completely silenced and *PME3* and *PME8* were down-regulated as compared to cv. Svevo. Conversely, a significant induction of *PME11*, *PME67* and *PMEQRT1* genes expression was detected. Only the expression of *PME51* remained unchanged.

The qRT-PCR analysis performed on AZ5-5 transgenic plants, having the *PME28* silenced, showed the complete silencing of *PME45* and a down-regulation of *PME8*, *PME21-1/2/4*, *PME28*, *PME53*, *PME58*, *PME63* and *PMEQRT1* as compared to cv. Svevo (Fig. 9, dotted line). A slight but significant induction was found for *PME11*, whereas *PME67* was strongly induced as compared to the control. The level of expression of *PME3*, *PME51* and *PME21-2* genes remained unchanged.

3.3 Infection of transgenic plants

At the anthesis stage, 19 plants for AZ4-11 line (silenced for *PME13*) and 17 plants for AZ5-5 line (silenced for *PME28*) were infected with *F. graminearum* by using the point-inoculation method. Symptoms were annotated from the second until 10 days post infection (DPI), as the complete desiccation of spikes for all the employed plants was

achieved at this point (Fig. 11). The percentage of infection was calculated as the number of symptomatic spikelets within the total number of spikelets in the spike.

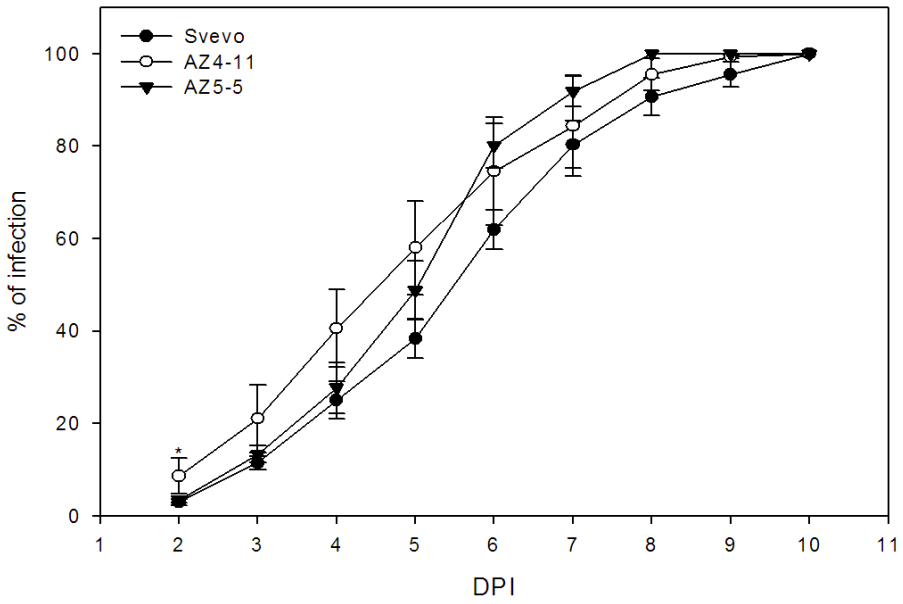

Figure 11. Time-course analysis of Fusarium head blight symptom development following *F. graminearum* infection of transgenic lines AZ4-11 and AZ5-5 and the control plants cv. Svevo. Disease symptoms are expressed as percentage of spikelets showing symptoms on the total number of spikelets per spike. * $p<0,05$.

During the 9 days of symptoms annotation the percentage of infected spikelets was always lower in Svevo plants, used as non-transgenic control, than in AZ4-11 and AZ5-5 plants. In particular, between the second and the fifth DPI the percentage of infection in AZ4-11 and AZ5-5 transgenic lines was slightly higher than in Svevo plants, however, this difference was significant only between Svevo and AZ4-11 line at 2 DPI. In this time interval, AZ4-11 line showed a higher percentage of infected spikelets than AZ5-5 line, even if no statistically significant difference was detected. Between 6 and 8 DPI the percentage of infection became slightly higher in AZ5-5 line than in AZ4-11 line with no statistical differences; in both lines the percentage of infected spikelets was higher than Svevo plants, but no a statistical significant difference was found. At 8 DPI AZ5-5 line reached the 100% of infected spikelets, whereas AZ4-11 line was completely dissected at 9 DPI. Finally, Svevo plants reached the complete desiccation of spikelets at 10 DPI.

3.4 Targeting Induced Local Lesions In Genomes (TILLING) analysis

A TILLING analysis was conducted on *PME13* sequence by using the TILLING population of cv. Svevo available at the University of Tuscia composed by about 4000 mutated genotypes. In total 1920 genotypes were analyzed by using 6 different primer pairs covering the 86% of the entire gene sequence. Only 3 missense mutations were found: 2 of them regarding he mutations of a cytosine into a thymine at the 946 and 1724 nucleotide position, respectively and the last one regarding the mutation of a guanine into an adenine at the 1436 nucleotide position. None mutations generated premature STOP codons or mutations at the splicing sites were found.

Because of these negative results, a search on the recent available TILLING database of a durum wheat cv. Kronos from the University of California, Davis, was performed. All the 42 complete *PME* gene sequences (see Chapter I) were blasted against this database in order to find genotypes carrying interesting mutations in *PME* genes (Tab. 13).

Table 13. Mutated accessions found with BLAST analysis of *PME* genes in the TILLING database of the University of California, Davis.

Gene	Accession name	Mutation
PME3-5BS	Kronos2424:C4901T	splice acceptor variant
	Kronos1434:G8067A	STOP codon
PME11-3B	Kronos774:C16912T	STOP codon
	Kronos3169:C17172T	STOP codon
	Kronos1061:G17401A	STOP codon
PME28-2AL	Kronos4502:C9667T	STOP codon
	Kronos4518:C9824T	STOP codon
	Kronos5983:G9957A	STOP codon
	Kronos2297:C10317T	splice acceptor variant
PME31-1AL	Kronos4564:G3440A	STOP codon
	Kronos3575:C4115T	STOP codon
	Kronos4539:G4133A	splice donor variant
	Kronos3964:G4293A	STOP codon
PME41-1AL	Kronos863:G14952A	STOP codon
	Kronos758:G14978A	splice donor variant
PME45-5BL	Kronos3648:C4033T	STOP codon
	Kronos1308:G5145A	STOP codon
PME51-2BL	Kronos2254:C12210T	STOP codon
	Kronos2460:C12219T	STOP codon
PME53-2BS	Kronos3196:C5667T	STOP codon
	Kronos2458:G6839A	splice acceptor variant
PME53-4AL	Kronos2086:G5311A	STOP codon
	Kronos863:C5679T	STOP codon
PME58-2BL	Kronos3481:G8142A	splice acceptor variant
PME63-5BS	Kronos2216:C1026T	splice donor variant

PMEQRT1-2BS	Kronos1405:G2206A	STOP codon
	Kronos2021:C2337T	splice acceptor variant
	Kronos2449:C3628T	splice donor variant

Mutated accession of the durum wheat cv. Kronos found through the database available from the University of California, Davis. On the left are reported *PMEs* found to be mutated in cv. Kronos genotypes. In the middle are reported mutated accessions names (e.g. Kronos4502); in the name the kind and the position of mutation is reported as well (e.g. C9667T, indicate that a cytosine at the 9667 position in the sequenced contigs is mutated in a thymine). On the right is reported the effect of the mutation.

In total 28 mutated accessions in 12 different *PME* genes were found: 18 accessions carrying mutations leading to the formation of premature STOP codons and the remaining 10 accessions carrying mutations at the splice acceptor or donor sites. Similarly, to what obtained by analyzing the TILLING population of cv. Svevo, no mutants were detected for the *PME13* gene.

Seeds corresponding to the mutated accessions were ordered directly at the University of California, Davis. Seeds corresponding to Kronos3169:C17172T, Kronos4564:G3440A, Kronos3575:C4115T and Kronos4539:G4133A were not ordered because at that moment they were unavailable.

The ordered seeds were received but they were not put to grow because they arrived the last months of the PhD and there was no enough time to further characterize these plant material.

3.5 Heterologous expression of PME recombinant proteins

In order to verify if *PME13*, *PME21* and *PME28* gene sequences used to produce the wheat RNAi plants code for functional pectin methylesterase proteins, the region encoding the predicted mature part of the protein, that correspond to the PME domain, was cloned into the pPICZαA expression vector for the heterologous expression in *P. pastoris*.

The signal peptide present in PME13, PME21 and PME28 was identified with SignalP on-line tool and excluded from the amplification of the PME domain. The PME domain was then cloned into the *Eco*RI and *Xba*I site of pPICZαA vector under the control of the methanol-inducible *AOX*1 promoter (Fig. 12).

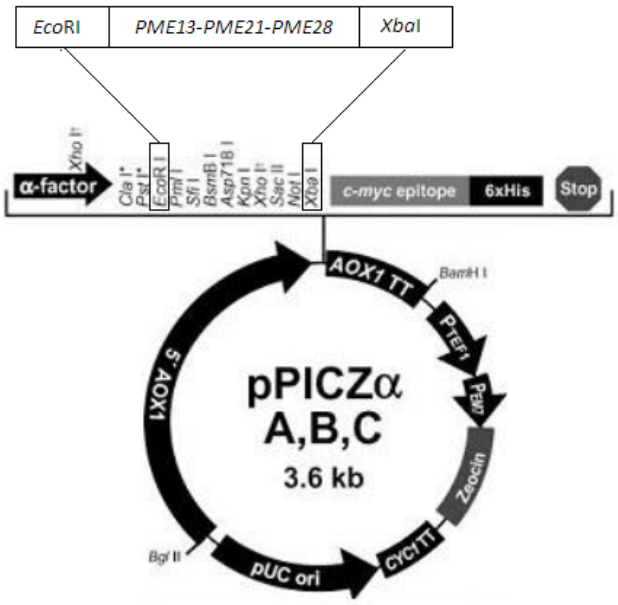

Figure 12. pPICZαA-*PME13,* pPICZαA-*PME21* and pPICZαA-*PME28* constructs used for the heterologous expression of recombinant PME proteins in *P. pastoris* X33 strain.

After yeast competent cells transformation, colonies were selected and subjected to methanol induction. The possible secretion and accumulation of the recombinant PME13, PME21 and PME28 proteins were verified by the SDS-PAGE analysis. Different induction trials were performed, however none of them expressed the recombinant PME.

4. DISCUSSION

Traditional plant breeding programs necessitate of long periods to obtain plants with novel characteristics and in many cases non-valuable agronomic traits could be co-introduced with the desired trait. Instead, a biotechnological approach could be used both to decrease the period required to obtain a new variety and to avoid the introduction of "negative genes". Recombinant DNA techniques have been developed since 80's and they allowed to obtain new potentially interesting traits in plants.

Here, we reported the genetic transformation of bread wheat cv. Bobwhite with the pAHC17-*Ubi*1-*PME3* and pAHC17-*Lem*1-*PME3* constructs, as well as the transformation of durum wheat cv. Svevo with pAHC17-*Lem*1-*PME13*, pAHC17-*Lem*1-*PME21* and pAHC17-*Lem*1-*PME28* constructs to verify their impact on wheat resistance against *F. graminearum*.

Concerning the transformation with pAHC17-*Ubi*1-*PME3* construct no plants were obtained, probably due to the high identity (at least 50%) of the small interference RNA (siRNA) with most of *PMEs* and/or to the constitutive expression of the *PME3* RNAi. Moreover, a sequence long 453 bp was used for the RNAi-forming sequence and also this aspect could lead to a high-scale silencing of *PME3* gene that was not tolerated by plants. Supporting this hypothesis, in an initially experiment Rana et al. (2014) tried to produced transgenic wheat plants silenced for *glucan synthase-like* genes (*TaGSL*), but they did not obtained regenerating wheat plants. They explained this result by sustaining that the length used for siRNA-forming sequence (230 bp) completely knocked-down those genes or, alternatively, the siRNA fragments could have negative effects also on other genes important for plant or somatic embryo development. It has also been suggested by Hirai and Kodama (2008) that RNAi could be an important impediment of transgenic plants regeneration.

Mostly, RNAi experiments are carried out by using constitutive promoters to drive transgene expression, as the *Ubiquitin* promoter from maize (Christensen et al., 1992). However, some reports clearly highlighted that, even if constitutive, these promoters did not drive the expression in all kind of cereal tissues and organs (Rooke et al., 2000; Suwannaketchanatit et al., 2006) and, in some cases, constitutive promoters could also lead to a transgene lethality. To avoid a high, constitutive silencing of *PME3*, we performed new transformation experiments by using the palea and lemma specific promoter *Lem*1 from barley (Skadsen et al., 2002). Indeed, 12 plants containing the pAHC17-*Lem*1-*PME3* RNAi construct (AZ10 and AZ11 experiments) were obtained and the plants are now growing for subsequent characterization.

We attempted also to silence *PME13* and *PME28* genes by using pAHC17-*Lem*1-*PME13* and pAHC17-*Lem*1-*PME28* constructs, obtaining 39 and 34 T0 positive plants, respectively. In these silencing experiments, we used shorter RNAi forming-sequences for both *PME13* (346 bp) and *PME28* (309 bp) since in some reports this parameter influenced the silencing result (Rana et al., 2014). Nevertheless, the exact size of double strand RNA (dsRNA) needed to trigger RNAi in plants is still not entirely clear, being very variable and ranging from below 100 to above 850 bp (Wesley et al., 2001). More experiments are necessary to identify the length of RNAi-forming sequence that could silenced only the target genes without affecting non-target sequences.

The use of tissue-specific promoters to drive RNAi silencing can have some advantages. However, this strategy has the limitation that do not allow to study the effect of that transgene in other tissues or developmental stages or the silencing in that tissue does not reveal the main physiological role. An alternative method to silence target genes, is the use of cognate promoters. Li et al. (2011) studied the effectiveness of constitutive and cognate promoters-driven RNAi transgene in the silencing of four genes in rice. By using the cognate promoters of each gene, they discovered additional informations about these genes functions in regulating rice growth and development and the researcher obtained also a gene specific silencing, without affecting the expression of the other members of the gene family under investigation. On the basis of these evidences, we produced RNAi plants for *PME21* under its own promoter to mirror its native expression domains. Also for these RNAi plants we used a short RNAi-forming sequence (216 bp). Fifty-seven positive T0 plants were obtained and the plants are now growing for subsequent characterization.

Wheat is affected by many diseases and FHB caused mainly by *F. graminearum* is one of the most important. Diverse studies have showed that different genes introduced in wheat with a transgenic approach can limit FHB symptoms (Buerstmayr et al., 2012), including the use of a pectin methylesterase inhibitor gene (PMEI; Volpi et al., 2011).

In this work, we reported an infection experiment of the transgenic lines AZ4-11 and AZ5-5 silenced for *PME13* and *PME28* genes, respectively, with the fungal pathogen *F. graminearum*. In this first experiments, no significant differences were found between the two transgenic lines and the durum wheat cv. Svevo used as non-transgenic controls. However, a slightly higher percentage of symptomatic spikelets was found in transgenic plants compared to the control, but no a statistically significant difference was detected, except between AZ4-11 line and cv. Svevo plants at 2 DPI (Fig. 10). This increased susceptibility, if confirmed in the subsequent experiments, is similar to that found in

some *Arabidopsis pme* mutants (Bethke et al. 2014), and indicate a role of PMEs in plant immunity.

The qRT-PCR analysis conducted on AZ4-11 transgenic plants, silenced for *PME13* gene, revealed the knockdown of several *PME* genes. In fact, in this plant, 8 additional *PMEs* were fully silenced and included *PME21-2*, *PME21-1/2/4*, *PME28*, *PME45*, *PME53*, *PME58* and *PME63* genes which shared at least 42% of identity with *PME13* RNAi-forming sequence. *PME3* and *PME8* genes underwent a down-regulation in AZ4-11 line compared to cv. Svevo, sharing 68% and 47% of identity, respectively, with the *PME13* RNAi-forming sequence. On the contrary, *PME11*, *PME67* and *PMEQRT1* genes were up-regulated compared to the control. In this cases the percentage of identity with the *PME13* RNAi-forming sequence was about 40%. Finally, *PME51* gene, even if it shares a higher sequence identity (57%) with the *PME13* RNAi-forming sequence compared to that one between *PME13* siRNA and the completely silenced *PMEs* (42%), it remained unaffected from the silencing.

In AZ5-5 transgenic plant, silenced for *PME28* gene, instead, we did not detect a multiple silencing of endogenous *PMEs*. Only *PME45* gene underwent a complete silencing. This gene shares 48% of identity with *PME28* siRNAi. Nevertheless, the AZ5-5 line showed a number of PME down-regulated (*PME8*, *PME13*, *PME21-2*, *PME21-1/2/4*, *PME53*, *PME58*, *PME63* and *PMEQRT1*) and two genes up-regulated (*PME11* and *PME67*). These genes share at least 26% of identity with the *PME28* RNAi-forming sequence. *PME3* and *PME51* genes remained unaffected; they share 38% and 26% of identity, respectively, with *PME28* siRNA.

In conclusion, the silencing of a single *PME* has an impact on the expression of the other *PMEs*, although this is not related to the sequence identity with *PME* RNAi-forming sequences.

Transgenic technology is not still well accepted by publics, thus an alternative method relies on classical mutagenesis. TILLING approach is a strategy that allow to identify mutated genotypes within a population treated with chemical agents as, for example, the EMS. This technology was developed in *Arabidopsis* and subsequently successfully applied to other plant species, including wheat. In wheat a 10-fold higher mutation rate respect to diploid species could be applied, as its polyploid nature allow it to be tolerant at certain level of EMS application (Uany et al., 2009). Here, we reported a TILLING screening of the wheat population available at the University of Tuscia for the *PME13* gene. About half of the whole population was analyzed, but only 3 missense mutations

were found and none concerning the formation of mutations leading to inactive PME proteins. Our results diverge from the observation of Borril et al. (2015), reporting that a high mutations density in wheat is related to the possibility to find premature stop codons and splice donor/acceptor site mutations is more than 95% in hexaploid wheat and more than 85% in tetraploid wheat, respect to the 25% found in diploid plants.

Thus, we decided to proceed with the screening of the recent available TILLING database from the University of California, Davis. All the 42 complete *PME* sequences identified through the IWGSC database (paragraph 3.1, Chapter I) were used as input in the TILLING database but only 12 of them were found to be mutated and they were: *PME3-5BS*, *PME11-3B*, *PME28-2AL*, *PME31-1AL*, *PME51-2BL*, *PME41-1AL*, *PME45-5BL*, *PME53-2BS*, *PME53-4AL*, *PME58-2BL*, *PME63-5BS* and *PMEQRT1-2BS*. According to our result, no mutation in *PME13* were found in this TILLING database screening. These mutated lines are not yet characterized but they represent a promising material to verify the involvement of PMEs in wheat-*F. graminearum* interaction.

We also attempted to express in *P. pastoris* the recombinant wheat proteins PME13, PME21 and PME28. We did not chose *E. coli* for the heterologous expression both because of the lack of post-transcriptional modifications that could lead to inactive enzymes (De-la-Peña et al., 2008) and because of the possibility of inclusion bodied formation that make more difficult the purification of recombinant proteins (Ding et al., 2002); thus we decided to use *P. pastoris* system because of the successfully expression of recombinant active PMEs (Peng et al., 2005). The sequence used for the heterologous expression did not contain the signal peptide, but only the mature part of the protein corresponding to the PME domain was present. We choose to express only the PME domain both because of the probability that the presence of the PMEI domain could provide inactive proteins and because of the possibility of an incorrect PME proteins maturation. Despite different trials, no recombinant PME proteins were obtained. Shinde et al. (1995) suggested that the pro-region of PMEs could acts as an intramolecular chaperone, allowing the correct conformational folding of the mature part of PME proteins. Thus, the expression of only the PME domain of PME13, PME21 and PME28 did not allowed probably the correct proteins folding that prevented the accumulation and/or the secretion of the recombinant proteins. The lack of information concerning the characterization *in vitro* of group II PMEs in plants suggest that these enzymes probably need organism-specific post-translational processing that is necessary

for their structural and functional integrity. In fact, only PMEs belonging to the group I, lacking the pro-region corresponding to the PMEI domain, were successfully expressed by using a heterologous system (Peng et al., 2005). One possibility to characterize *in vitro* the activity of group II PMEs could be their expression in heterologous plant system (Gaffé et al., 1997; Senechal 2015).

In conclusion, the silencing of wheat *PME* genes with the RNAi is a powerful method to study the role of these genes in wheat development and defense, even if RNA-forming sequences need to be improved in order to avoid the silencing of other genes that could be important for plant functions. Our first infection experiment of the silenced wheat plants for *PME13* and *PME28* genes with the fungal pathogen *F. graminearum* did not highlight considerable differences between the transgenic lines and the non-transgenic plants, but further analysis need to be conducted. In parallel, the availability of the TILLING wheat *PME* mutants represent a promising plant material to work on in order to unravel PMEs role in wheat-*F. graminearum* interaction.

5. Figures and tables

Figure 1. pAHC17-*Ubi*1-*PME3* expression vector, containing the sense and antisense strands (green boxes), the intron sequence (blue box) for *PME3* gene silencing. The cassette is under the control of *Ubi*1 promoter and with the NOS terminator. Restriction sites are indicated along the construct.

Figure 2. pAHC17-*Lem*1-*PME3*, pAHC17-*Lem*1-*PME13* and pAHC17-*Lem*1-*PME28* expression vectors, containing the sense and antisense strands (green boxes), the intron sequence (blue box) for *PME3, PME13* and *PME28* genes silencing. The cassettes are under the control of *Lem*1 promoter and with the NOS terminator. Restriction sites are indicated along the construct.

Figure 3. pAHC17-*promPME21-PME21* expression vectors, containing the sense and antisense strands (green boxes), the intron sequence (blue box) for *PME21*gene silencing. The cassette is under the control of the cognate promoter of *PME21*and with the NOS terminator. Restriction sites are indicated along the construct.

Figure 4. pUBI::BAR vector map. The pUBI::BAR plasmid contains *Ubi*1 promoter from maize driving the constitutive expression of *BAR* gene which confers resistance to the Bialaphos herbicide.

Figure 5. Map of the pPICZαA expression vector for the heterologous expression of *PME13, PME21* and *PME28* genes.

Figure 6. The Biolistic PDS-1000/He instrument (left). The biolistic bombardment process: the system uses high pressure helium and vacuum to propel DNA-coated nanoparticles placed onto a macrocarrier toward target tissue at high speed. The macrocarrier is stopped by a stopping screen, whereas nanoparticles proceed until they penetrate the cells. The launch speed depends on the helium pressure (rupture disk strength), the vacuum inside the chamber and (A) the distance between the rupture disk and the macrocarrier; (B) distance between the macrocarrier and the stopping screen; (C) distance between the stopping screen and the target cells.

Figure 7. General workflow of TILLING analysis. Seeds treated with EMS are grow and DNA is extracted and pooled. The DNA is amplified by PCR and analyzed by HRM analysis.

Figure 8. An example of a PCR analysis for some of the T0 wheat plants; **M:** Ladder GeneRuler DNA 100 bp; **1-13:** AZ4 plants transformed with pAHC17-*PME13* RNAi vector; **14:** H_2O; **15:** Svevo DNA; **16-22:** AZ5 plants transformed with pAHC17-*PME28* RNAi vector; **23:** H_2O; **24:** Svevo DNA; **25-44:** AZ4 and AZ5 plants amplified for pUBI::BAR construct; **45:** H_2O; **46:** Svevo DNA; **47-66:** AZ4 and AZ5 plants amplified for *actin* gene; **67:** H_2O; **68:** Svevo DNA. The amplification for *BAR* gene gave a specific band at 656 bp and a non-specific band at about 900 bp; in fact, in Svevo DNA (sample 46) only the non-specific band is detectable.

Figure 9. An example of RT-PCR analysis for some of the T1 positive wheat plants. In the figure is represented only the amplification for the small fragment. **M:** Ladder GeneRuler DNA 1kb; **1:** AZ5-5 transgenic line; **2:** Svevo cDNA; **3:** H_2O; **4**: AZ4-66 transgenic line; **5:** AZ4-11 transgenic line; **6:** Svevo cDNA; **7:** H_2O; **8-10:** AZ5-5, AZ4-66 and AZ4-11 transgenic lines; **11:** Svevo cDNA; **12:** H_2O.

Figure 10. qRT-PCR showing the *PME* genes expression in flowering spike of AZ4-11 and AZ5-5 transgenic lines. The relative gene expression was calculated taking as reference sample the level of expression of each *PME* in durum wheat cv. Svevo (dotted line). Bars indicated the standard deviation between three technical replicate of one biological replicate; ** $p < 0,05$.

Figure 11. Time-course analysis of Fusarium head blight symptom development following *F. graminearum* infection of transgenic lines AZ4-11 and AZ5-5 and the wild-type plants cv. Svevo. Disease symptoms are expressed as percentage of spikelets showing symptoms on the total number of spikelets per spike. * $p<0,05$.

Figure 12. pPICZαA-*PME13*, pPICZαA-*PME21* and pPICZαA-*PME28* constructs used for the heterologous expression of recombinant PME proteins in *P. pastoris* X33 strain.

Table 1. Primers used for the amplification of the complete coding region (CDS) of *PME3, PME13, PME21* and *PME28* genes and primers used for the sense and the antisense strands amplification for the RNAi constructs.

Table 2. Primers used for the amplification of *PME21* promoter. The sequence length is also reported.

Table 3. Primer used for the amplification of the PME domain of *PME13, PME21* and *PME28*.

Table 4. RF1 and RF2 buffers composition.

Table 5. Media composition for wheat cultures.

Table 6. Primers employed for T0 plants screening for the presence of the transgene.

Table 7. Primers employed for RT-PCR analysis.

Table 8. Primer pairs used in TILLING analysis of *PME13* gene.

Table 9. Bombardment experiments in durum and bread wheat; positive T0 plants were recorded by PCR.

Table 10. Result obtained in the AZ4, AZ6 and AZ5 experiments.

Table 11. T1 offspring screening.

Table 12. Transgenic wheat lines screened by RT-PCR for the effective silencing of *PME13* and *PME28* genes.

Table 13. Mutated accessions found with BLAST analysis of *PME* genes in the TILLING database of the University of California, Davis.

GENERAL CONCLUSIONS

This thesis reports for the first time the isolation and the structural and functional characterization of *PME* genes in wheat.

The main results obtained during this PhD project were the following:

- ✓ Forty-four wheat *PME* genes were identified with *in silico* searches, including two novel *PME* genes, *TaPME13-5A* and *TaPME45-5A*. Chromosomal assignment and structural characterization were conducted through an *in silico* analysis;
- ✓ The expression profile of *PME* genes varies notably in different tissues and some of them are not expressed in roots and leaves, whereas all *PME* genes showed relatively high expression level in flowering spikes;
- ✓ Following *F. graminearum* infection the susceptible cv. Bobwhite showed both a larger number of induced *PME* genes and a stronger variation in the level of induction compared to the resistant cv. Sumai3. The parallel analysis of *PME* expression in the upper and lower spikelets respect to the site of infection highlighted that modulation of *PME* expression by the pathogen occurred only when the pathogen colonized the host tissues;
- ✓ The silencing of *PME13* and *PME28* genes, conducted in order to verify *in planta* the role of *PME* genes in wheat defence, did not highlight significant differences between the transgenic lines AZ4-11 and AZ5-5 and the durum wheat cv. Svevo used as non-transgenic control.
- ✓ TILLING mutated genotypes in 12 different *PME* genes were identified through the database available at the University of California, Davis. This plant material represents an interesting material to further study the role of *PME* genes and pectin methylesterification in wheat defence against pathogens;
- ✓ The heterologous expression system of *P. pastoris* X33 is not suitable for the expression of the only PME domain of the recombinant proteins PME13, PME21 and PME28.

References

Anderson J. A., Stack R. W., Liu S., Waldron B. L., Fjeld A. D., Coyne C., Moreno-Sevilla P., Fetch J. M., Song Q. J., Cregan P. B., Frohberg R. C., 2001. DNA markers for *Fusarium* head blight resistance QTLs in two wheat populations. Theor. Appl. Genet. 102, 1164-1168

Bethke G., Grundman R. E., Sreekanta S., Truman W., Katagiri F., Glazebrook J., 2014. Arabidopsis pectin methylesterases contribute to immunity against *Pseudomonas syringae*. Plant Physiol. 164, 1093-1107

Bonnin E., Clavurier K., Daniel S., Kauppinen S., Mikkelsen J. D., Thibault J. F., 2008. Pectin acetylesterases from Aspergillus are able to deacetylate homogalacturonan as well as rhamnogalacturonan. Carbohydr. Polym. 74, 411–418

Bonnin E., Le Goff A., Alebeek G., Voragen A., Thibault J. F., 2003. Mode of action of *Fusarium moniliforme* endopolygalacturonase towards acetylated pectin. Carbohydr. Polym. 52, 381–388

Bonnin E., Le Goff A., Körner R., Vigouroux J., Roepstorff P., Thibault J. F., 2002. Hydrolysis of pectins with different degrees and pattern of methylation by the endopolygalacturonase of *Fusarium moniliforme*. Biochim. Biophy. Acta 1596, 83-94

Boquski M. S., Lowe T. M., Tolstoshev C. M., 1993. dbEST-- database for "expressed sequence tags". Nat. Genet. 4 (4), 332-333

Bordenave M., Goldberg R., Huet J. C., Pernollet J. C., 1995. A novel protein from mung bean hypocotyl cell walls with acetyl esterase activity. Phytochemistry 38, 315–319

Borril P., Adamski N., Uauy C., 2015. Genomics as the key to unlocking the polyploid potential in wheat. New Phytol. 208, 1008-1022

Buerstmayr H., Adam G., Lemmens M., 2012. Resistance to Head Blight caused by *Fusarium* spp. in wheat, *in*:, Indu Sharma ed., *Disease resistance in wheat*. CAB International, 255-256

Buerstmayr H., Ban T., Anderson J. A., 2009. QTL mapping and marker-assisted selection for Fusarium head blight resistance in wheat: a review. Plant Breed. 128, 1–26

Buerstmayr H., Lemmens M., Hartl L., Doldi L., Steiner B., Stierschneider M., Ruckenbauer P., 2002. Molecular mapping of QTLs for Fusarium head blight resistance in spring wheat. I. Resistance to fungal spread (type II resistance). Theor. Appl. Genet. 104, 84–91

Buerstmayr H., Steiner B., Hartl L., Griesser M., Angerer N., Lengauer D., Miedaner T., Schneider B., Lemmens M., 2003. Molecular mapping of QTLs for Fusarium head blight resistance in spring wheat. II. Resistance to fungal penetration and spread. Theor. Appl. Genet. 107, 503–508

Burge C. and Karlin S., 1997. Prediction of complete gene structures in human genomic DNA. J. Mol. Biol. 268, 78-94

Burge C., 1998. Modelling dependencies in pre-mRNA spicing signals, *In*: Salzberg S., Searls D., Kasif S. (Eds), Computational methods in molecular biology. Elsevier Science, Amsterdam, pp. 127-163

Caffal K. H., Mohnen D., 2009. The structure, function and biosynthesis of plant cell wall pectic polysaccharides. Carbohydr. Res., 344, 1879-1900

Cantu D., Vicente A. R., Labavitch J. M., Bennet A. B., Powell A. L. T., 2008. Strangers in the matrix: plant cell walls and pathogen susceptibility. Trends Plant Sci. 13 (11), 610-617

Cao J., 2012. The pectin lyases in *Arabidopsis thaliana*: evolution, selection and expression profiles. PLos One 7, e46994

Castaldo D., Quagliuolo L., Servillo L., Balestrieri C., Giovane A. X., 2005. Isolation and characterization of pectinmethylesterase from apple fruit. J. Food Sci. 54, 653-655

Catoire L., Pierron M., Morvan C., Penhoat du C. H., Goldberg R., 1998. Investigation of the action patterns of pectinmethylesterase isoforms through kinetic analyses and NMR spectroscopy. Implications in cell wall expansion. J. Biol. Chem. 273, 33150–33156

Chou K. C., Shen H. B., 2010. Plant-mPLoc: a top-down strategy to augment the power for predicting plant protein subcellular localization. PLoS One 5, e11335

Christensen A. H., Quail P. F., 1996. Ubiquitin promoter-based vectors for high-level expression of selectable and/or screenable marker genes in monocotyledonous plants. Trans. Res. 5, 213-218

Christensen A., Sharrock R., Quail P., 1992. Maize polyubiquitin genes: structure, thermal perturbation of expression and transcript splicing, and promoter activity following transfer to protoplasts by electroporation. Plant Mol. Biol. 18, 675–689

Christensen T., Nielsen J., Mikkelsen J., 1996. Isolation, characterization and immunolocalization of orange fruit acetyl esterase. Progr. Biotechnol. 14, 723–730

Coutinho P. M., Stam M., Blanc E., Henrissat B., 2003. Why there are so many carbohydrate-active enzyme-related genes in plants? Trends in Plant Sci. 8 (12), 563-565

Davidson R. M., Gowda M., Moghe G., Lin H., Vaillancourt B., Shiu S., Jiang N., Buell C. R., 2012. Comparative transcriptomics of three Poaceae species reveals patterns of gene expression evolution. Plant J. 71, 492-202

D'Avino R., Camardella L., Christensen T. M. I. E., Giovane A., Servillo L., 2003. Tomato pectin methyl esterase: modeling, fluorescence and inhibitor interaction studies-comparison with the bacterial (*Erwinia chrysanthemi*) enzyme. Proteins 53, 830-839

De-la-Peña C., Badri D. V., Vivanco J. M., 2008. Novel role for pectin methylesterase in *Arabidopsis*: a new function showing ribosome-inactivating protein (RIP) activity. Biochim. Biophys. Acta 1780, 773–783

Di Matteo A., Giovane A., Raiola A., Camardella L., Bonivento D., de Lorenzo G., Cervone F., Bellincampi D., Tsernoglou D., 2005. Structural basis for the interaction between pectin methylesterase and a specific inhibitor protein. Plant Cell 17, 849-858

Ding J. L. C., Hsu J. S. F., Wang M. M. C., Tzen J. T. C., 2002. Purification and glycosylation analysis of an acidic pectin methylesterase in jelly fig (*Ficus awkeotasang*) achenes. J. Agric. Food Chem. 50, 2920-2925

Dixit S., Upadhyay S., Singh H., Pandey B., Chandrashekar K., Verma P., 2013. Pectin methylesterase of Datura species, purification, and characterization from *Datura stramonium* and its application. Plant Signaling Behav. 8, e25681

Dedeurwaerder S., Menu-Bouaouiche L., Mareck A., Lerouge P., Guerineau F., 2009. Activity of an atypical *Arabidopsis thaliana* pectin methylesterase. Planta 229, 311–321

Fayyaz A., Asbi B. A., Ghazali H. M., Che man Y. B., Jinap S., 1994. Purification and molecular properties of papaya pectinesterase. Food Chem. 49, 373-378

Fries M., Ihrig J., Brocklehurst K., Shevchik V., Pickersgill R., 2007. Molecular basis of the activity of the phytopathogen pectin methylesterase. EMBO J. 26, 3879–3887

Fu D., Uauy C., Blechl A., Dubcovsky J., 2007. RNA interference for wheat functional gene analysis. Transgenic Res. 16, 689–701

Gaffé J., Tiznado M. E., Handa A. H., 1997. Characterization and functional expression of a ubiquitously expressed tomato pectin methylesterase. Plant Physiol. 114, 1547–1556

Geisler-Lee J., Geisler M., Coutinho P. M., 2006. Poplar carbohydrate-active enzymes. Gene identification and expression analysis. Plant Physiol. 140, 946-962

Giovane A., Laratta B., Loiudice R., Quagliuolo L., Castaldo D., Servillo L., 1996. Determination of residual pectin methylesterase activity in food products. Biotechnol. Appl. Biochem. 23, 181-184

Gou J., Miller L. M., Hou G., Yu X., Chen X., Liu C., 2012. Acetylesterase mediated deacetylation of pectin impairs cell elongation, pollen germination, and plant reproduction. Plant Cell 24, 50–65

Grant G. T., Morris E. R., Rees D. A., Smith P. J. C., Thom D., 1973. Biological interaction between polysaccharides and divalent cations: the egg-box model. FEBS Lett. 32 (1), 195-198

Hancock J. F., 2004. Plant evolution and the origin of crop species. CABI Publishing, Cambridge MA

Henrissat B., 1991. A classification of glycosyl hydrolases based on amino-acid sequence similarities. Biochem. J. 280, 309-316

Henry I. M., Nagalakshmi U., Lieberman M. C., Ngo K. J., Krasileva K. V., Vasquez-Gross H., 2014. Efficient genome-wide detection and cataloging of EMS-induced mutations using exome capture and next-generation sequencing. Plant Cell 26 (4), 1382–1397

Hewezi T., Howe P., Maier T. M., Hussey R. S., Mitchum M., G., Davis E. L., Baum T. J., 2008. Plant Cell 20, 3080-3093

Hirai S., Kodama H., 2008. RNAi vectors for manipulation of gene expression in higher plants. Open Plant Sci. J. 2, 21–30

Horevaj P., Milus E. A., Bluhm B. H., 2011. A real- time qPCR assay to quantify *Fusarium graminearum* biomass in wheat kernels. J. Appl. Microbiol. 111, 396- 406

Horton P., Park K. J., Obayashi T., Fujita N., Harada H., Adams-Collier C. J., Nakai K., 2007. WoLF PSORT: protein localization predictor. Nucleic Acids Res. 35, 585-587

Hu B., Jin J., Guo A. Y., Zhang H., Luo J., Gao G., 2015. GSDS 2.0: an upgraded gene feature visualization server. Bioinformatics 31 (8), 1296-1297

Idnurm A., Howlett B. J., 2001. Pathogeneticity genes of phytopathogenetic fungi. Mol. Plant Patol. 2 (4), 241-255

International Wheat Genome Sequencing Consortium, 2014. A chromosome-based draft sequence of the hexaploid bread wheat (*Triticum aestivum*) genome. Science 345 (6194)

Jensen J. K., Sørensen S. O., Harholt J., Geshi N., Sakuragi Y., Møller I., Zandleven J., Bernal A. J., Jensen N. B., Sørensen C., 2008. Identification of a xylogalacturonan xylosyltransferase involved in pectin biosynthesis in Arabidopsis. Plant Cell 20 (5), 1289-1302

Johansson K., El-Ahmad M., Friemann R., Jörnvall H., Markovic O., Eklund H., 2002. Crystal structure of plant pectin methylesterase. FEBS Lett. 514, 243-249

Jolie R. P., Duvetter T., Houben K., Clynen E., Sila D. N., van Loey A. M. V., van Loey A. M., Hendrickx M. E., 2009. Carrot pectin methylesterase and its inhibitor from kiwi fruit: study of activity, stability and inhibition. Innov. Food Sci. Emerg. Technol. 10, 601–609

Jolie R. P., Duvetter T., van Loey A. M. V., van Loey A. M., Hendrickx M. E., 2010. Pectin methylesterase and its proteinaceous inhibitor: a review. Carbohydr. Rese. 345, 2583–2595

Jordan K. W., Wang S. C., Lun Y. N., Gardiner L. J., MacLachlan R., Hucl P., 2015. A haplotype map of allohexaploid wheat reveals distinct patterns of selection on homoeologous genomes. Genome Biol. 16

Kauppinen S., Christgau S., Kofod L., Halkier T., Dorreich K., Daldoge H., 1995. Molecular cloning and characterization of a rhamnogalacturonan acetylesterase from *Aspergillus aculeatus*. J. Biol. Chem. 270, 27172–27178

Kubicek C. P., Starr T. L., Glass N. L., 2014. Plant cell wall-degrading enzymes and their secretion in plant-pathogenic fungi. Annu. Rev. Phytopathol. 52, 427-451

Laemmli U. K., 1970. Cleavage of structural proteins during the assembly of the head of bacteriophage T4. Nature 227, 680-685

Lee M., Macmillan J. D., 1968. Mode of action of pectic enzymes. I. Purification and certain properties of tomato pectinesterase. Biochemistry 7, 4005-4010

Li J., Jiang D., Zhou H., Li F., Yang J., Hong L., Fu X., Li Z., Liu Z., Li J., Zhuang C., 2011. Expression of RNA-interference/antisense transgenes by the cognate promoters of target genes is a better gene-silencing strategy to study gene function in rice. PLos One 6 (3): e17444

Lionetti V., Cervone F., Bellicampi D., 2012. Methyl esterification of pectin plays a role during plant-pathogen interactions and affects plant resistance to diseases. J. Plant Physiol. 169, 1623- 1630

Lionetti V., Giancaspro A., Fabri E., Giove S. L., Reem N., Zabotina O. A., Blanco A., Gadaleta A., Bellincampi D., 2015. Cell wall traits as potential resources to improve resistance of durum wheat against *Fusarium graminearum*. BMC Plant Biol. 15, 6

Lionetti V., Raiola A., Camardella L., Giovane A., Obel N., Pauly M., Favaron F., Cervone F., Bellincampi D., 2007. Overexpression of pectin methyl esterase inhibitors in Arabidopsis restricts fungal infection by *Botrytis cinerea*. Plant Physiol. 143, 1871-1880

Liu S., Zhang X., Pumphrey M. O., Stack R. W., Gill B. S., Anderson J., 2006. Complex microcolinearity among wheat, rice, and barley revealed by fine mapping of the genomic region harboring a major QTL for resistance to Fusarium head blight in wheat. Funct. Integr. Genomics 6, 83–89

Liu S., Pumphrey M. O., Gill B. S., Trick H. N., Zhang J. X., Dolezel J., Chalhoub B., Anderson J., 2008. Toward positional cloning of Fhb1, a major QTL for Fusarium head blight resistance in wheat. Cereal Res. Commun. 36, 195–201

Livak K. J., Schmittgen T. D., 2001. Analysis of relative gene expression data using real- time quantitative PCR and $2^{-\Delta\Delta Ct}$ method. METHODS 25, 402- 408

Lombard V., Bernard T., Rancurel C., Brumer H., Coutinho P. M., Henrissat B., 2010. A hierarchical classification of polysaccharide lyases for glycogenomics. Biochem. J. 432, 437–444

Loukoianov A., Yan L., Blechl A., Sanchez A., Dubcovsky J., 2005. Regulation of *VRN-1* vernalization genes in normal and transgenic wheat. Plant Physiol. 138, 2364–2373

Ma L., Jiang S., Lin G., Cai J., Ye X., Chen H., Li M., Li H., Takàc T., Samaj J., Xu C., 2013. Wound-induced pectin methylesterases enhance banana (*Musa* spp. AAA) susceptibility to *Fusarium oxysporum* f. sp. *cubense*. J. Exp. Bot. DOI: 10.1093/jxb/ert088

Marchler-Bauer A., Derbyshire M. K., Gonzales N. R., Lu S., Chitsaz F., Geer L. Y., Geer R. C., He J., Gwadz M., Hurwitz D. I., Lanczycki C. J., Lu F., Marchler G. H., Song J. S., Thanki N., Wang Z., Yamashita R. A., Zhang D., Zheng C., Bryant S. H., 2015. CDD: NCBI's conserved domain database. Nucleic Acids Res. 43, 226-226

Markovic, O. and Janecek, S., 2004. Pectin methylesterases: sequence-structural features and phylogenetic relationships. Carbohydr. Res. 339, 2281-2295

Martinez-Perez E., Shaw P., Moore G., 2001. The *Ph1* locus is needed to ensure specific somatic and meiotic centromere association. Nature 411, 204-207

McCallum C. M., Comai L., Greene E. A., Henikoff S., 2000. Targeting induced local lesions in genomes (TILLING) for plant functional genomics. Plant Physiol. 123, 439-442

McMillan G. P., Hedley D., Fyffe L., Pérombelon M. C. M., 1993. Potato resistance to soft-rot erwinias is related to cell wall pectin esterification. Physiol. Mol. Plant Pathol. 42, 279–289

McMullen M., Jones R., Gallenberg D., 1997. Scab of wheat and barley: a re-emerging disease of devastating impact. Plant Dis. 81 (12), 1340- 1348

Mendgen, K., Hahn M., 2002. Plant infection and establishment of fungal biotrophy. Trends Plant Sci. 7, 352–356

Mohnen D., 2008. Pectin structure and biosynthesis. Curr. Opin. Plant Biol. 11, 266-277

Moreira L. R. and Filho E. X., 2008. An overview of manna structure and mannan-degrading enzyme system. Appl. Microbiol. Biotechnol. 79, 165-178

Moscetti I., Tundo S., Janni M., Sella L., Gazzetti K., Tauzin A., Giardina T., Masci S., Favaron F., D'Ovidio R., 2013. Constitutive expression of the xylanase inhibitor TAXI-III delays Fusarium Head Blight symptoms in durum wheat transgenic plants. Mol. Plant Microbe Interact. 26 (12), 1464-1472

Oeser B., Heidrich P. M., Muller U., Tudzynski P., Tenberge K. B., 2002. Polygalacturonase is a pathogenicity factor in the Claviceps purpurea/rye interaction. Fungal Genet. Biol. 36 (3), 176-186

Oosterveld A., Beldman G., Searle-van Leeuwen M. J. F., Voragen A. G. J., 2000. Effect of enzymatic deacetylation on gelatin of sugar beet pectin in the presence of calcium. Carbohydr. Polym. 43, 249-256

Orfila C., Degan F. D., Jørgensen B., Scheller H. V., Ray P. M., Ulvskov P., 2012. Expression of mung bean pectin acetyl esterase in potato tubers: effect on Acetylation of cell wall polymers and tuber mechanical properties. Planta 236, 185-196

Osorio S., Castillejo C., Quesada M. A., Medina-Escobar N., Brownsey G. J., Suau R., Hereida A., Botella M. A., Valpuesta V., 2008. Partial demethylation of oligogalacturonides by pectin methyl esterase 1 is requied for eliciting defense responses in wild strawberry (*Fragaria vesca*). Plant J. 54, 43-55

Parry D. W., Jenkinson P., McLeod L. (1995). *Fusarium* ear blight (scab) in small grain cereals. Plant Pathol. 44, 207- 238

Parry M. A. J., Madgwick P. J., Bayon C., Tearall K., Hernandez-Lopez A., Baudo M., Rakszegi M., Harmada W., Al-Yassin A., Ouabbou H., Labhilili M., Phillips A. L., 2009. Mutation discovery for crop improvement. J. Exp. Bot. 60 (10), 2817-2825

Pasquet J. C., Chaouch S., Macadré C., Balzergue S., Huguet S., Martin-Magniette M. L., Bellvert F., Deguercy X., Thareau V., Heintz D., Saindrenan P., Dufresne M., 2014. Differential gene expression and metabolomic analysis of *Brachypodium distachyon* infected by deoxynivalenol producing and non-producing strains of *Fusarium graminearum*. BMC Genomics 15, 629

Pelloux J., Rustérucci C., Mellerowicz E. J., 2007. New insight into pectin methylesterase structure and function. TRENDS Plant Sci. 12, (6), 267- 277

Peng C. C., Hsiao E. S. L., Ding J. L. C., Tzen J. T. C., 2005. Functional expression in *Pichia pastoris* of an acid pectin methylesterase from jelly fig (*Ficus awkeotsang*). J. Agr. Food Chem. 53, 5612-5616

Petersen T. N., Brunak S., von Heijne G., Nielsen H., 2011. SignalP 4.0: discriminating signal peptides from transmembrane regions. Nat. Methods 8, 785-786

Pogorelko G., Lionetti V., Fursova O., Sundaram R. M., Qi M., Whitham S. A., Bogdanove A. J., Bellincampi D., Zabotina O. A., 2013. *Arabidopsis* and *Brachypodium distachyon* transgenic plants expressing *Aspergillus nidulans* acetylesterases have decreased degree of polysaccharide acetylation and increased resistance to pathogens. Plant Physiol. 162, 9–23

Raiola A., Lionetti V., Elmaghraby I., Immerzeel P., Mellerowicz E., Salvi G., Cervone F., Bellincampi D., 2011. Pectin methylesterase is induced in *Arabidopsis* upon infection and is necessary for a successful colonization by necrotrophic pathogens. Mol. Plant Microbe Interact. 24 (4), 432-440

Rana I. A., Salomon S., Schäfer W., Becker D., 2014. Downregulation of *Glucan Synthase- Like* (*TaGSL*) genes in wheat leads to inhibition of transgenic plant regeneration. In vitro Cell. Dev. Biol.-Plant DOI 10.1007/s11627-014-9636-y

Regina A., Bird A., Topping D., Bowden S., Freeman J., Barsby T., Hashemi B. K., Li Z., Rahman S., Morell M., 2005. High-amylose wheat generated by RNA interference improves indices of large-bowel health in rats. Proc. Natl. Acad. Sci. U. S. A. 103, 3546–3551

Rillo L., Castaldo D., Giovane A., Servillo L., Balestrieri C., Quagliuolo L., 1992. Purification and properties of pectin methylesterase from mandarin orange fruit. J. Agric. Food. Chem. 40, 591-593

Rogers L. M., Flaishman M. A., Kolattukudy P. E., 1994. Cutinase gene disruption in *Fusarium solani* f. sp. pisi decreases its virulence on pea. Plant Cell 6 (7), 935-945

Rooke L., Byrne D., Salgueiro S., 2000. Marker gene expression driven by the maize ubiquitin promoter in transgenic wheat. Ann. Appl. Biol. 136, 167–172

Sambrook J., Fritsch E. F., Maniatis T., 1989. Molecular Cloning-A Laboratory Manual, 2nd ed. Cold Spring Harbor Laboratory Press, Cold Spring Harbor, NY, U.S.A.

Sarka E., Krulis Z., Ruzek L., Koebarova A., Bubnik Z., Ruzkova M., 2011. Application of wheat B-starch in biodegradable plastic materials. Czech J. Food Sci. 29 (3), 232-242

Schroeder H. W., Christensen J. J., 1963. Factors affecting the resistance of wheat to scrab caused by *Gibberella zeae*. Phytopathology 53, 813- 818

Sears R. G. and Deckard E. L., 1982. Tissue culture variability in wheat: callus induction and plant regeneration. Crop Sci. 22, 546-550

Sénéchal F., L'Enfant M., Domon J. M., Rosiau E., Crépeau M. J., Surcouf O., Esquivel-Rodriguez J., Marcelo P., Mareck A., Guérineau F., Kim H. R., Mravec J., Bonnin E., Jamet E., Kihara D., Lerouge P., Ralet M. C., Pelloux J., Rayon C., 2015. Tuning of pectin methylesterification: pectin methylesterase inhibitor 7 modulated the processive activity of co-expressed pectin methylesterase 3 in a pH-dependent manner. J. Biol. Chem. 290 (38), 23320-23335

Sestili F., Janni M., Doherty A., Botticella E., D'Ovidio R., Masci S., Jones H. D., Lafiandra D., 2010. Increasing the amylose content of durum wheat through silencing of the *SbeIIa* genes. BMC Plant Biol. 10, 144

Shevchik V., Hugouvieux-Cotte-Pattat N., 1997. Identification of a bacterial pectin acetyl esterase in *Erwinia chrysanthemi* 3937. Mol. Microbiol. 24, 1285–1301

Shewry P. R., 2009. Wheat. J. Exp. Bot. 60 (6), 1537-1553

Shieh M. T., Brown R. L., Whitehead M. P., Cary J. W., Cotty P. J., Cleveland T. E., Dean R. A., 1997. Molecular genetic evidence for the involvement of a specific polygalacturonase, P2c, in the invasion and spread of *Aspergillus flavus* in cotton bolls. Appl. Environ. Microbiol. 63 (9), 3548-3552

Shinde U. et al., 1995. Propeptide mediated protein folding: intramolecular chaperones. In *Intramolecular chaperones and Protein Folding* (Shinde U. and Inouye M. eds), 1-9. Molecular Biology Intelligence Unit, RG Landes Company, Springer, Heidelberg, Germany

Skadsen R. W., Sathish P., Federico M. L., Abebe T., Fu J., Kaeppler H. F., 2002. Cloning of the promoter for a novel barley gene, Lem1, and its organ-specific promotion of Gfp expression in lemma and palea. Plant Mol. Biol. 49 (5), 545-555

Skamnioti P., Gurr S. J., 2007. *Magnaporthe grisea* cutinase2 mediates appressorium differientiation and host penetration and is required for full virulence. Plant Cell 19, 2674-2689

Suwannaketchanatit C., Chaisuk P., Piluek J., Peyachoknakul S. Huehne P. S., 2006. Evaluation of constitutive promoters for gene expression in Dendrobium protocorms and flowers. Kasetsart J (Nat. Sci). 40, 934–943

ten Have A., Mulder W., Visser J., van Kan J. A., 1998. The endopolygalacturonase gene Bcpg1 is required for full virulence of Botrytis cinerea. Mol. Plant Microbe Interact. 11 (10), 1009-1016

The Arabidopsis Genome initiative, 2000. Analysis of the genome sequence of the flowering plant *Arabidopsis thaliana*. Nature 480, 796- 815

The International Wheat Genome Sequencing Consortium (IWGSC), 2014. A chromosome-based draft sequence of the hexaploid bread wheat (*Triticum aestivum*) genome. Science 345 (6194)

Thompson J. D., Higgins D. G., Gibson T. J., 1994. Clustal W: improving the sensitivity of progressive multiple sequence alignment through sequence weighting, position-specific gap penalties and weight matrix choice. Nucleic Acids Res. 22, 4673–4680

Tsai H., Howell T., Nitcher R., Missirian V., Watson B., Ngo K. J., Lieberman M., Fass J., Uauy C., Tran R. K., 2011. Discovery of rare mutations in populations: TILLING by sequencing. Plant Physiol. 156, 1257–1268

Turquois T., Rinaudo M., Taravel F., Heyraud A., 1999. Extraction of highly gelling pectic substances from sugar beet pulp and potato pulp: influence of extrinsic parameters on their gelling properties. Food Hydrocolloid 13, 255–262

Tyler L., Bragg J. N., Wu J., Yang X., Tuskan G. A., Vogel J. P., 2010. Annotation and comparative analysis of the glycoside hydrolase genes in *Brachypodium distachyon*. BMC Genomics 11, 1–21

Uany C., Paraiso F., Colasuonno P., Tran R. K., Tsai H., Berardi S., Comai L., Dubcovsky J., 2009. A modified TILLING approach to detect induced mutations in tetraploid and hexaploid wheat. BMC Plant Biol. 9, 115

Urban U., Daniels S., Mott E., Hammond-Kosack K., 2002. *Arabidopsis* is susceptible to the cereal ear blight fungal pathogens *Fusarium graminearum* and *Fusarium culmorum*. Plant J. 32, 961-973

van den Brink J., de Vries R. P., 2011. Fungal enzyme sets for plant polysaccharide degradation. Appl. Microbiol. Biotechnol. 91, 1477–1492

Volpi C., Janni M., Lionetti V., Bellincampi D., Favaron F., D'Ovidio R., 2011. The ectopic expression of a pectin methyl esterase inhibitor increases pectin methyl esterification and limits fungal diseases in wheat. Mol. Plant Microbe Interact. 24 (9), 1012-1019

Volpi C., Raiola A., Janni M., Gordon A., O'Sullivan D.M., Favaron F., D'Ovidio R., 2013. *Claviceps purpurea* expressing polygalacturonases escaping PGIP inhibition fully infects PvPGIP2 wheat transgenic plants but its infection is delayed in wheat transgenic plants with increased level of pectin methyl esterification. Plant Physiol. Biochem. 73, 294-301

Vogel J., 2008. Unique aspects of the grass cell wall. Curr. Opin. Plant Biol. 11, 301-307

Wang M., Yuan D., Gao W., Li Y., Tan J., Zhang X., 2013. A comparative genome analysis of PME and PMEI families reveals the evolution of pectin metabolism in plant cell wall. PLoS One 8 (8), e72082

Weeks J. T., Anderson O. D., Blechl A. E., 1993. Rapid production of multiple independent lines of fertile transgenic wheat (*Triticum aestivum*). Plant Physiol. 102, 1077-1084

Wesley S. V., Helliwell C. A., Smith N. A., Wang M. B., Rouse D. T., Liu Q., Gooding P. S., Singh S. P., Abbott D., Stoutjesdijk P. A., Robinson S. P., Gleave A. P., Green A. G.,Waterhouse P. M., 2001. Construct design for efficient, effective and high-throughput gene silencing in plants. Plant J. 27 (6), 581–590

Whietölter N., Graeßner B., Mierau M., Mort A. J., Moerschbacher B. M., 2003. Differences in the methyl ester distribution of homogalacturonans from near-isogenic wheat lines resistant and susceptible to the wheat stem rust fungus. Mol. Plant Microbe Interact. 16 (10), 945-952

Willats W. G., Orfila C., Limberg G., Buchholt H. C., van Alebeek G. J. W. M., Voragen A.G. J., Marcus S. E., Christensen T. M. I. E., Mikkelsen J. D., Murray B. S., Knox J. P., 2001. Modulation of the degree and pattern of methyl-esterification of pectic homogalacturonan in plant cell walls. Implications for pectin methyl esterase action, matrix properties, and cell adhesion. J. Biol. Chem. 276 (22), 19404–19413

Williamson G., 1991. Purification and characterization of pectin acetylesterase from orange peel. Phytochemistry 30, 445–449

Wolf S., Mouille G., Pelloux J., 2009. Homogalacturonan methyl-esterification and plant development. Mol. Plant 2 (5), 851-860

Wu S. C., Halley J. E., Luttig C., Fernekes L. M., Gutiérrez-Sanchez G., Darvill A. G., Albersheim P., 2006. Identification of an endo-β-1,4-D-Xylanase from *Magnaporthe grisea* by gene knockout analysis, purification, and heterologous expression. Appl. Environ. Microbiol. 72 (2), 986-993

Wubben, J. P., Mulder W., ten Have A., van Kan J. A. L., Visser J., 1999. Cloning and partial characterization of endopolygalacturonase genes from Botrytis cinerea. Appl. Environ. Microbiol. 65, 1596–1602

Yan L., Loukoianov A., Blechl A., Tranquilli G., Ramakrishna W., SanMiguel P., Bennetzen J. L., Echenique V., Dubcovsky J., 2004. The wheat *VRN2* gene is a flowering repressor down-regulated by vernalization. Science 303, 1640–1644

Yuan J. S., Reed A., Chen F., Stewart C. N., 2006. Statistical analysis of real-time PCR data. BMC Bioinformatics 7, 85

Zhao Z., Liu H., Wang C., Xu J. R., 2013. Comparative analysis of fungal genomes reveals different plant cell wall degrading capacity in fungi. BMC Genomics 14, 274

Zhuang Y., Gala A., Yen Y., 2013, Identification of functional genic components of major Fusarium head blight resistance quantitative trait loci in wheat cultivar Sumai3. Mol. Plant Microbe Interact. 26, 442–450

On- line references

http://faostat3.fao.org/browse/Q/*/E
http://www.afmb.cnrs-mrs.fr/CAZY/
https://urgi.versailles.inra.fr/blast/blast.php
http://genes.mit.edu/GENSCAN.html
http://gsds.cbi.pku.edu.cn/
http://www.ncbi.nlm.nih.gov/Structure/cdd/wrpsb.cgi

http://www.cbs.dtu.dk/services/SignalP/
http://wolfpsort.org/
http://www.csbio.sjtu.edu.cn/bioinf/plant-multi/
http://www.ncbi.nlm.nih.gov/nucest/
http://blocks.fhcrc.org/proweb/input/
http://dubcovskylab.ucdavis.edu/

Aknowledgements

First of all I would like to thanks my professor Renato D'Ovidio to give me the pleasure to do my PhD in his lab and I would like to express my gratitude to him for giving me the possibility to experience a lot of wonderful things during these three beautiful, unforgettable, years.

I would like to thanks Prof. Stefania Masci, the coordinator of my PhD course, for her availability and kindness. Thanks to her and to Prof. Domenico Lafiandra for providing their laboratory during my studies. I would like to thanks also Dr. Francesco Sestili and Dr. Ermelinda Botticella for their kind support in my works.

Thanks to the Institute de Science Moléculaire de Marseille and in particular to Prof. Thierry Giardina for allowing me to carry out a part of my PhD in his laboratory and to Dr. Mickael LaFond for supporting me in my French experiments.

My special thanks to my colleagues and friends, Anna Pucci, Raviraj Kalunke, Ilaria Moscetti, Silvio Tundo, Giulia Mandalà and Francesco Camerlengo, with which I share not only the research problems but also, and overall, a lot of exceptional and funny moments.

A very special hearty thanks to my father and my mother, for being always on my side, for having helped me to get this objective and for being the anchors of my life.

Thanks to you… which looked at me from above.

Finally, thanks to Davide, my mate in this course and in life, for being with me over these three years, in beautiful and bad times, for having bearing and supporting me. It is with you that I want to live everything that life has still in store for me.